Journal of Photochemistry & Photobiology, C: Photochemistry Reviews 55 (2023) 100585

Contents lists available at ScienceDirect

Journal of Photochemistry & Photobiology, C: Photochemistry Reviews

journal homepage: www.elsevier.com/locate/jphotochemrev

Absorption and fluorescence spectra of open-chain tetrapyrrole pigments–bilirubins, biliverdins, phycobilins, and synthetic analogues

Masahiko Taniguchi *, Jonathan S. Lindsey *

Department of Chemistry, North Carolina State University, Raleigh, NC 27695-8204, USA

ARTICLE INFO

Keywords:
Bile pigment
Bilin
Biliprotein
Luciferin
Phycobilin
Phyllobilin
Phytochrome

ABSTRACT

Open-chain tetrapyrroles are ubiquitous and abundant in living organisms (algae, animals, bacteria, and plants), including examples such as bilirubin, biliverdin, phycocyanobilin, phycoerythrobilin, and urobilin. The open-chain tetrapyrroles, collectively termed bilins, arise from biosynthesis or degradation of tetrapyrrole macrocycles. Bilins are now known to play a wide variety of biological roles encompassing light-harvesting (in phycobiliproteins), photomorphogenesis, signaling, and redox chemistry. The absorption spectra of bilins spans the ultraviolet (UV), visible, to near-infrared (NIR) regions depending on the degree of conjugation, thereby providing a wide range of colors from red/orange to blue/green. The fluorescence intensity of bilins is often quite low and hence fewer spectra are available, but can be increased substantially by structural rigidification, as evidenced by the wide use of biliproteins as fluorescent labels. The present article describes a database of absorption and fluorescence spectra of bilins from natural and synthetic origins for 220 compounds (270 absorption and 13 fluorescence spectral traces). Spectral traces of bilins published over the past ~50 years have been digitized and assembled along with information concerning solvent, photochemical properties (molar absorption coefficient and fluorescence quantum yield), and literature references. The spectral traces (xy-coordinate data files) can be viewed, downloaded, and accessed at www.photochemcad.com. The accessibility of spectral traces in digital format should facilitate identification and quantitative calculations of interest in diverse scientific areas.

1. Introduction

Open-chain tetrapyrroles are comprised of four pyrrolic rings attached via three methylene or methine units. They are also referred to as bilins, bilanes, and bile pigments because such compounds were originally isolated from mammalian bile in the form of bilirubin and biliverdin [1]. Open-chain tetrapyrroles are also commonly called linear tetrapyrroles to draw a distinction from tetrapyrrole macrocycles; however, the molecules adopt a rich set of stereochemical conformations and are rarely linear in a strict sense [2,3]. The conformations arise from the nature of the saturation of each pyrrolic ring (pyrrole, pyrroline, or pyrrolidine), the pyrrolic substituents (oxo, alkyl, vinyl, etc.), configurations of any stereocenters, and the various paths of conjugation encompassing up to four pyrrolic rings. Open-chain tetrapyrroles are ubiquitous pigments of life found in animals (amphibians, birds, fish, insects, mammals, reptiles) [1,4], plants [5], algae (cryptomonads, glaucophytes, rhodophytes) [6,7], and bacteria (cyanobacteria) [8].

The naturally occurring open-chain tetrapyrroles are derived invariably by degradation of tetrapyrrole macrocycles such as heme or chlorophylls. One notable exception is hydroxymethylbilane, which is a precursor in the biosynthesis of tetrapyrrole macrocycles. Heme is degraded to biliverdin IXα by heme oxygenase in the presence of oxygen; thereafter, biliverdin IXα is reduced to bilirubin IXα by biliverdin reductase (Scheme 1, upper panel) [9,10]. The Roman numeral suffix is legacy nomenclature from an early era of tetrapyrrole science [11]. In mammals, heme oxygenase attacks the α-position out of four possible positions; therefore, the biliverdin α isomer is predominant in nature [4,10]. In cyanobacteria and perhaps other organisms, biliverdin IXα is further reduced to form phycoerythrobilin, which is subsequently isomerized to phycocyanobilin [12,13]. A further class of open-chain tetrapyrroles is found through the breakdown process of chlorophylls at the α-position, which leads to red chlorophyll catabolite (RCC) in senescent leaves (Scheme 1, lower panel, right) [14,15]. Further metabolism of RCC occurs to form a diverse collection of phyllobilins, which now have been characterized in > 30 plant species [16,17]. Phyllobilins differ from heme-derived bilins in the presence of the fifth ring characteristic

* Corresponding authors.
E-mail addresses: mtanigu@ncsu.edu (M. Taniguchi), jlindsey@ncsu.edu (J.S. Lindsey).

https://doi.org/10.1016/j.jphotochemrev.2023.100585
Received 20 December 2022; Accepted 31 March 2023
Available online 3 April 2023

of photosynthetic tetrapyrrole macrocycles.

Open-chain tetrapyrroles are also found in marine organisms, namely krill and dinoflagellates. Such structures are derived from degradation of chlorophyll *a* at the δ-position and are referred to as luciferins (Scheme 1, lower panel, left). Dinoflagellates are known as one source of the toxic "red tides," and the brilliant blue bioluminescence that can illuminate the summer ocean at night is ascribed to the air oxidation of a dinoflagellate luciferin [18,19]. Krill luciferin, the cause of krill bioluminescence, is analogous to dinoflagellate luciferin [19,20], and is assumed to originate from dietary sources such as dinoflagellates [21]. Studies of the biosynthetic origins of dinoflagellate luciferins are under progress [22,23].

Beyond ubiquity and diversity, open-chain tetrapyrroles are abundant: the amount of heme degraded by an average human is estimated as ~375 mg per day [24], which extrapolated for a world population of 8 billion equates to 10^9 kg per year. The net production of chlorophylls is estimated to be 10^{12} kg/yr [25], which provides an upper bound on the production of phycobilins. Numerous synthetic open-chain tetrapyrroles have also been prepared as follows: (i) part of the total synthesis of naturally occurring [2,26] or synthetic [27–29] open-chain tetrapyrroles, (ii) as diverse metal complexes in fundamental studies of coordination chemistry [30,31], (iii) from ring cleavage of tetrapyrrole macrocycles via oxidation [5,30], or (iv) as precursors of synthetic tetrapyrrole macrocycles [32–40].

The physiological functions of naturally occurring open-chain tetrapyrroles often occur in the confines of protein complexes. Examples include the following: (i) light-harvesting in algae and bacteria as phycobiliproteins/phycobilisomes [13]; (ii) photomorphogenesis regulation as phytochromes in plants [41]; and (iii) coloration of bird eggshells [40–43], molluscan shells [44], fishes [45], and insects [46]. These light and color-related features are attributed to diverse photochemical and photophysical properties of open-chain tetrapyrroles, which are enabled by the wide range of absorption in a region where chlorophylls have little absorption. The region between the intense blue and intense red absorption bands of chlorophylls is referred to as the green gap. Accordingly, applications of open-chain tetrapyrroles are found in a wide variety of fields, for instance as natural food colorants [47], cosmetic patches [48,49], photosensitizers for photodynamic therapy [50,51], fluorescent markers [52], absorbers in dye-sensitized solar cells [53,54], and chromophores in genetically modified fluorescence proteins [55,56] including those in the nascent field of optogenetics [57,58].

The rich physiological features of open-chain tetrapyrroles begin in many cases with the absorption of light. Absorption and fluorescence spectral data of open-chain tetrapyrroles in the literature from four or more decades ago are largely only available in tabulated form for a

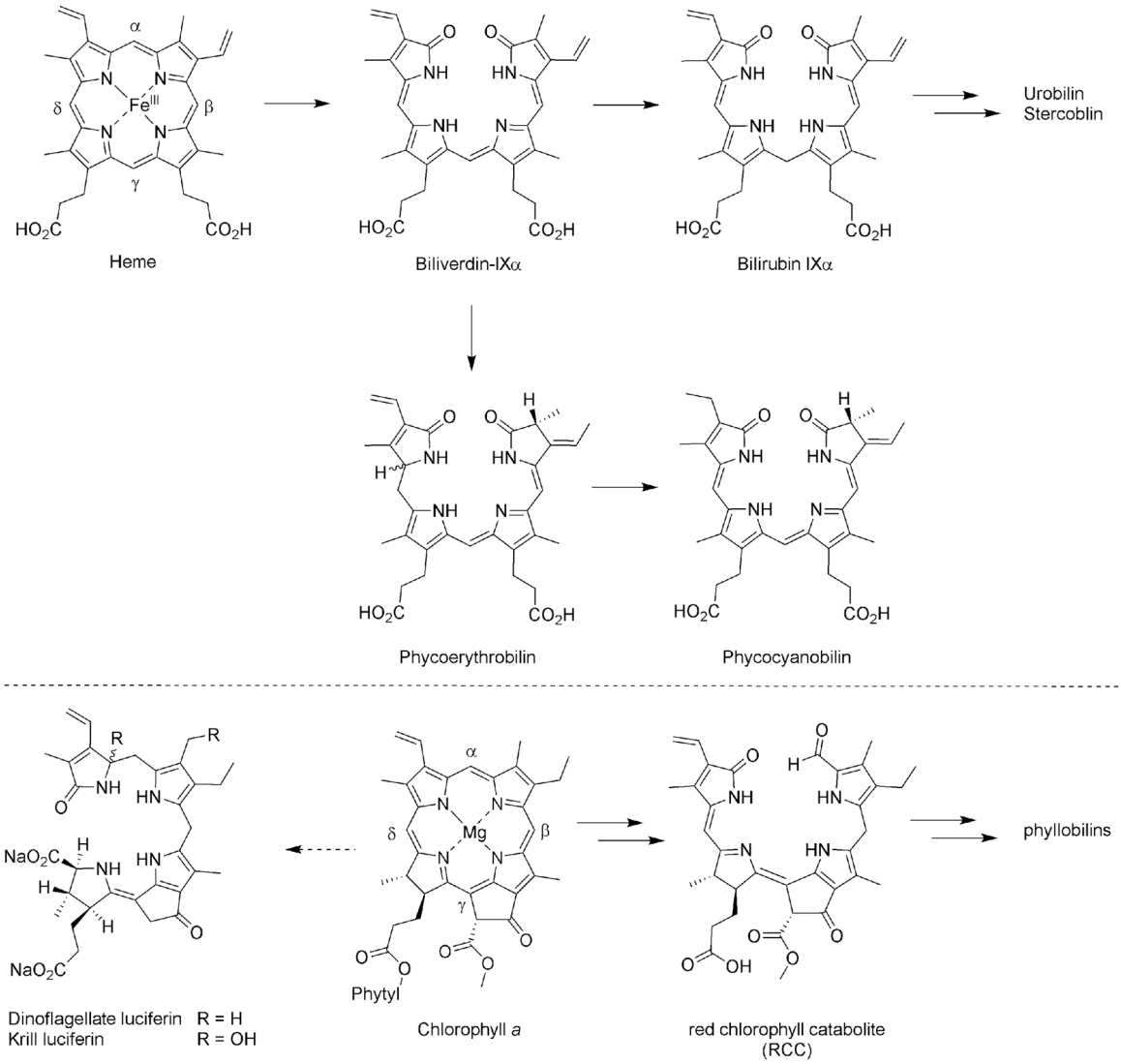

Scheme 1. Degradation pathway of heme and chlorophyll *a*.

limited number of compounds [1,27,59]. Absorption spectra of open-chain tetrapyrroles tend to exhibit broad peaks compared to other pigments (carotenoids, chlorophylls); hence, mere tabulated data (wavelength, absorption coefficient) are insufficient for understanding spectral properties. The accessibility of spectral traces is essential for structure–spectral comparisons, assessing possible color, performing multicomponent analysis, and calculating rates of excited-state energy-transfer (e.g., FRET) as well as the magnitude of oscillator strengths [60]. The scattered nature of the available specctral data has precluded a comprehensive understanding of the scope of the bilins field.

In this article, we describe a database of spectra of 220 open-chain tetrapyrroles, including 270 absorption and 13 fluorescence spectral traces. The compounds include those from natural and synthetic origins. The spectra complement those in a recently assembled database for phyllobilins [17]. The spectra were obtained from the published literature and are accompanied by photophysical data (values of the molar absorption coefficient and fluorescence quantum yield) where available. The spectral traces (xy-coordinate text format) and photophysical data can be accessed at www.photochemcad.com. Taken together, the assembled data should provide a foundation in support of research in the bilins field.

2. General overview

2.1. PhotochemCAD

PhotochemCAD is comprised of a program for performing calculations germane to the photosciences, databases of spectra along with companion photophysical parameters, and literature references. The program contains modules for calculations relevant to individual compounds (oscillator strength, transition dipole moment, natural radiative lifetime); interactions of compounds (Förster resonance energy transfer or FRET, Dexter energy transfer, energy transfer analysis); and mixtures of ≥ 2 compounds (multicomponent analysis) [60]. Additional calculational features are available to create and manipulate fictive data for comparative purposes. The databases to date include those for 300 common compounds [61], chlorophylls [62], synthetic chlorins [63], tolyporphins [64], phyllobilins [17], and flavonoids [65]. The spectra can be viewed at a website [66,67] whereas the program and spectral databases must be downloaded to carry out calculations.

The assembly of databases of spectra is essential to advance the photosciences, yet remains a painstaking endeavor given that such data typically are found rarely and irregularly across the vast print literature [68]. Tabulations of peak maxima of various compounds have value, but spectra are essential for a deep understanding and consideration of many applications in the photosciences [68–70]. For open-chain tetrapyrroles, the acquisition of absorption and fluorescence spectral traces faces challenges due to the limited commercial availability of such compounds and the impracticality of soliciting raw data – presumably mostly in print form – over a period of 50 years from research groups spread globally. Thus, we decided to assemble a database of digitized absorption and fluorescence spectral traces from the published literature.

2.2. Scope

In this article, we focused on open-chain tetrapyrroles regardless of their natural, semi-synthetic, or synthetic origin. The compounds include the free base species as well as metal complexes thereof. We generally excluded the following groups of compounds: complexes composed of two open-chain tetrapyrroles and one or more metals; synthetic oligopyrroles that contain > 4 pyrrolic species [71–73]; and double stranded or helical metal complexes of oligopyrroles [74–87]. A few representative difluoroboron complexes of open-chain oligopyrroles have been included where valuable comparisons can be made, but many such compounds [88,89] have been omitted. The present database also excludes all but three phyllobilins (which are employed for comparison purposes), as a spectral database of such compounds has recently been assembled [17]. Finally, we also have excluded the many articles concerning open-chain tetrapyrroles that include tables of absorption maxima but without absorption spectral traces.

2.3. Sources of spectra

Altogether, 270 absorption spectral traces and 13 fluorescence spectral traces were digitized from the scientific literature by using the software WebPlotDigitizer [90]. In some older literature, the spectral traces in the diagrams were hand-drawn, and the resulting absorption maxima were significantly offset from the values listed in the text. For those cases, the absorption maxima were adjusted to cohere with the values in the companion text. The process for digitization has been described in detail [62,64,65].

Nine absorption spectral traces (**1**, **21**, **214**–**220**) were drawn from our prior publications [37–40,61]. Such spectra were measured at room temperature using 1-cm path length cuvettes with an Agilent 8453 spectrometer. An absorbance maximum was maintained below A = 1.5 to avoid detector saturation.

3. Bilin structures and spectral parameters

3.1. Nomenclature and terminology

The nomenclature of compounds that are germane to bilin chemistry is shown in Chart 1, along with common motifs and their terminology. The nomenclature in the field of tetrapyrroles is a hodgepodge of legacy terms, idiosyncratic conventions, semi-systematic names, and more formal names drawn from the American Chemical Society (ACS) and the International Union of Pure and Applied Chemistry (IUPAC). For example, the α,β,γ,δ labels to denote the meso-positions of heme shown in Scheme 1 date to Hans Fischer approximately a century ago. The most recent formal review of tetrapyrrole nomenclature, now somewhat dated, was prepared by Moss [11]. Any discussion of nomenclature should be leavened by the spirit of Fox and Powell [91], authors of an authoritative text on the topic, who stated *"The only real requirement for conventional nomenclature is that it provide unambiguous and understandable names for the audience being addressed. The main goal of any systematic nomenclature is to convey the composition, and as far as possible, the structure of chemical compounds and substances. However, there are circumstances that need, even require, a unique name, that is, one and only one name for each substance."* The development of nomenclature within a family of substances in a given domain within the tetrapyrrole field is quite challenging given that many families include a variety of natural substances, each often with a unique name, along with diverse collections of non-natural, synthetic compounds [92,93].

A collection of pyrrolic monomers is shown in the top row of Chart 1, where "pyrrolic" is the all-encompassing term to describe all members. The common names used herein are shown in red font. The pyrrolidin-2-one compound is a lactam (cyclic amide), as is the pyrrolin-2-one. Given the common presence of such structures in the bilin family, the common names pyrrolidinone and pyrrolinone are used herein.

The second row shows dipyrrolic structures. The term dipyrrin has supplanted the previous term dipyrromethene [11]. The dipyrrinone is a very common motif in naturally occurring bilins. In principle, the dipyrrinone can tautomerize to give a hydroxy-dipyrrin, and although the equilibrium profoundly favors the dipyrrinone, trapped derivatives and analogues of the hydroxy-dipyrrin are described in the collection presented herein. The value of common names even for relatively small structures is seen by one of the formal names of dipyrrinone, which is (*Z*)− 5-((1*H*-pyrrol-2-yl)methylene)− 1,5-dihydro-2*H*-pyrrol-2-one.

The third row of Chart 1 shows nomenclature for bilane, which is the parent, or reference, structure of bilins. The numbering system proceeds

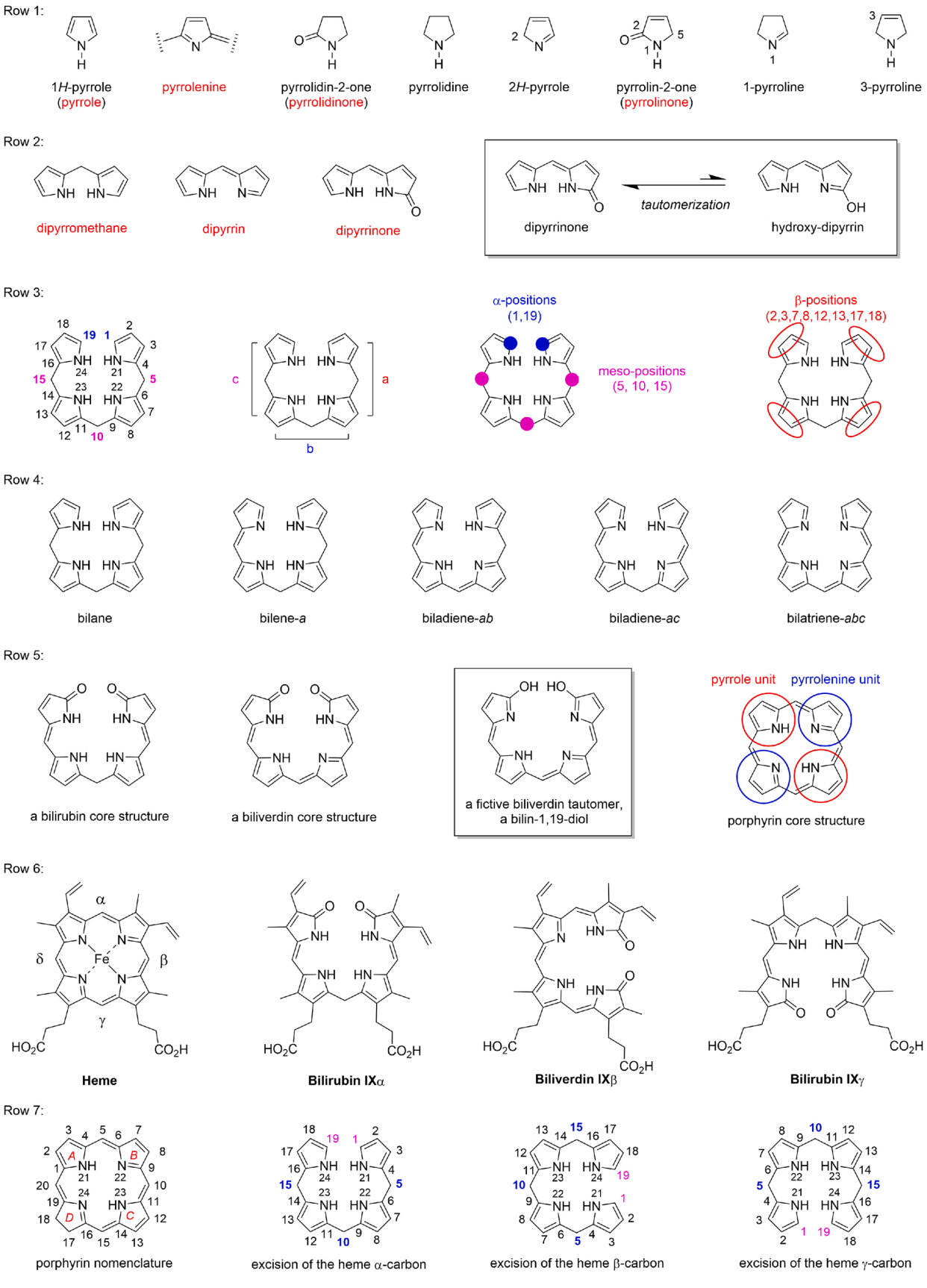

Chart 1. Nomenclature and terminology of bilin-related motifs and compounds.

from 1 to 19 encompassing all carbon atoms, with nitrogens numbered 21–24. A legitimate question concerns the skipped 20 position. Excerpting from Moss [11] with elision of figure callouts here and in the following, *'the bilane is defined without oxygen substituents, and is numbered (omitting C-20) to agree with the numbering of the unsubstituted porphyrin ring system. Unless otherwise specified it is implied that each nitrogen atom of bilane is saturated.'* The dipyrrolic units are labeled a, b, and c as shown. Other terminology drawn from the analogous tetrapyrrole field includes "meso-positions" to define the carbon bridging the pyrrolic units, and α- and β-positions as indicated.

The fourth row of Chart 1 shows the series of various dehydrogenated bilane derivatives. The progression from bilane → bilene → biladiene → bilatriene entails a $2e^-$, $2H^+$ oxidation at each step; thus, the entire transformation from bilane to bilatriene represents a $6e^-$, $6H^+$ oxidation. In this regard, the transformation resembles the conversion of a porphyrinogen to a porphyrin [94]. We note the statement by Moss [11], *'Unsubstituted oxidised bilanes may be named semisystematically on the basis of the bilane structure. The number of additional double bonds involving the carbon bridges is indicated by changing the ending '-ane' to '-ene' (1 such additional double bond, total 9 double bonds), and '-adiene' (2 such additional double bonds, total 10 double bonds). The system with one further double bond (total 11 double bonds) has already been defined as bilin and this name is used in preference to bilatriene.'* Here, we depart from Moss and use the term bilatriene rather than bilin to indicate the specific, fully unsaturated structure; as is now common in the field, we use "bilin" as a sweeping term to encompass the family of open-chain tetrapyrroles. The terms *a,b,c* to indicate the position of unsaturation can be used as a prefix or suffix; thus, for example, bilene-*a* and *a*-bilene are equivalent, with usage dependent on author's preference and dictates of language. There are multiple possible isomers in many bilin structures; for example, biladiene-*ab* and biladiene-*ac* structures are isomers, as are bilene-*a*, bilene-*b* and bilene-*c* (not shown). It should not escape the careful reader that in a substituted bilin, there is some arbitrariness as to the orientation of the bilin in numbering of carbons beginning 1–19 and use of labels *a,c*; in other words, either of the two terminal carbons could be numbered 1 versus 19. We have generally tried to be faithful to the choices employed in the published manuscripts that form the basis for this review.

The fifth row of Chart 1 shows the core structure of a bilirubin and a biliverdin. Each contains an oxo group at positions 1 and 19. A bilirubin thus is comprised of two dipyrrinones attached to the 10-methylene unit. A biliverdin is the $2e^-$, $2H^+$ oxidation product of a bilirubin. The porphyrin structure is shown to emphasize the presence of pyrrole and pyrrolenine units, which exchange via facile tautomerization. This point is germane to bilin chemistry, where similar pyrrole and pyrrolenine motifs are present, and we emphasize that a given line drawing of a bilin may represent one of several possible tautomeric forms. In this regard, we again turn to Moss, who in referring to bilindiones stated [11] *'The linear tetrapyrrole structures are formally tautomeric with the corresponding bilin-1,19-diols. However, present evidence indicates that the bislactam form predominates and most naturally occuring [sic] linear tetrapyrroles are named on the basis of the bislactam (*i.e. *−1,19-dione) tautomer.'* Accordingly, the reader should be aware of additional tautomers and resonance forms beyond the single display provided herein for a given compound. In some cases, distinct tautomers may underlie reactivity and spectra, whereas in other cases the tautomers are only an academic possibility.

The aforementioned nomenclature for bilin species has a compelling and consistent logic. A wrinkle on this otherwise clean description arises, however, because bilins typically originate from porphyrins. The sixth row of Chart 1 shows the structure of heme and three bilins derived therefrom. The seventh row shows the full numbering system of all positions corresponding to the structures in row six. Bilirubin IXα, an *ac*-biladiene, is derived by excision of the carbon at the 5-position of heme (the heme α-carbon). The numbering system of heme does not carry over to the bilin species; the 4- and 6-positions flanking the excised carbon in heme now are numbered 19- and 1-, respectively, in the resulting bilirubin IXα. Similarly, biliverdin IXβ, an *abc*-bilatriene, is derived by excision of the carbon at the 10-position of heme (the heme β-carbon); the 9- and 11-positions flanking the excised carbon in heme now are numbered 19- and 1-, respectively, in the resulting biliverdin. So it goes also for bilirubin IXγ, an *ac*-biladiene derived by excision of the carbon at the 15-position of heme (the heme γ-carbon), whereupon the 14- and 16-positions flanking the excised carbon in heme now are numbered 19- and 1-, respectively, in the resulting bilirubin. The centrality of the heme–bilin legacy cannot be overstated. Here we close with Moss [11], in referring to bilirubin and biliverdin structures, *"In the recommended nomenclature the Roman numeral and Greek letter (that in the Fischer system refer in a formal way to the substitution pattern and to the position of cleavage of the corresponding porphyrin respectively) have been dropped. Thus biliverdin was formerly biliverdin IXα. Because the vast majority of references are to this common substitution pattern, it has become common practice to drop the IXα designation."* Thus, the α–δ labels showing the site of excision are dropped in naming bilins derived from heme. The numbering system also is not carried over. For those whose world is porphyrincentric, the disjoint in nomenclature from porphyrin to bilin, despite the shared legacy, is often discombobulating.

3.2. Structures

The structures of 220 open-chain tetrapyrroles and related compounds are displayed in Chart 2. Common names are also provided where available.

3.3. Tabulated spectral parameters

The absorption spectral data (absorption maxima, relative intensities, solvents, molar absorption coefficients, and literature citations) of open-chain tetrapyrroles are listed in Table 1 [18–20,95–199]. The compounds are categorized in the following 10 groups: (1) bilirubins and related compounds (**1–19**), (2) biliverdins/bilindiones and related compounds (**20–81**), (3) extended bilindiones (**82–98**), (4) urobilins and related compounds (**99-101**), (5) phycocyanobilin and related compounds (**102–131**), (6) biladiene derivatives (**132–163**), (7) boron difluoride complexes (**164–170**), (8) bilins derived from synthetic tetraarylporphyrins (**171–203**), (9) chlorophyll catabolites (**204–213**), and (10) Knoevenagel enones (**214–220**). In Table 1, the position of the absorption maxima are as stated in the given reference even though the spectra may show slight deviations therefrom.

4. Absorption spectra by compound class

The absorption spectral traces of open-chain tetrapyrroles are displayed in Fig. 1. Each panel displays normalized spectra. The reader is referred to Table 1 for listings of molar absorption coefficients, where available. The absorption spectral range of open-chain tetrapyrroles is mainly dictated by the degree of conjugation encompassing the pyrrolic units. For comparison purposes, the absorption spectra of pyrrole-containing compounds in diverse conjugation levels are shown in Fig. 2. The absorption maxima of each pyrrolic compound is as follows: pyrrole (**221**, λ_{max} = 206 nm, in hexane) [61]; dihydrodipyrrin **222** (λ_{max} = 225 and 330 nm, in diethyl ether) [200]; xanthobilirubic acid, a dipyrrinone (**223**, λ_{max} = 411 nm, in DMSO) [103]; dipyrrin **224** (λ_{max} = 446 nm, solvent unspecified) [201]; and tripyrrinone **225** (λ_{max} = 326 and 569 nm, in ethanol) [202]. The spectra are compared with that of bilindione **24**, which exhibits a relatively sharp band in the near-UV region as well as a weaker but broad absorption band extending into the NIR region. The progressive increase in position of wavelength maximum with the extent of conjugation provides a systematic Aufbau approach for understanding the spectra of members of the bilin family. A similar Aufbau approach has been taken to understand the spectra of chlorins [63].

Other major factors that influence absorption spectral properties of

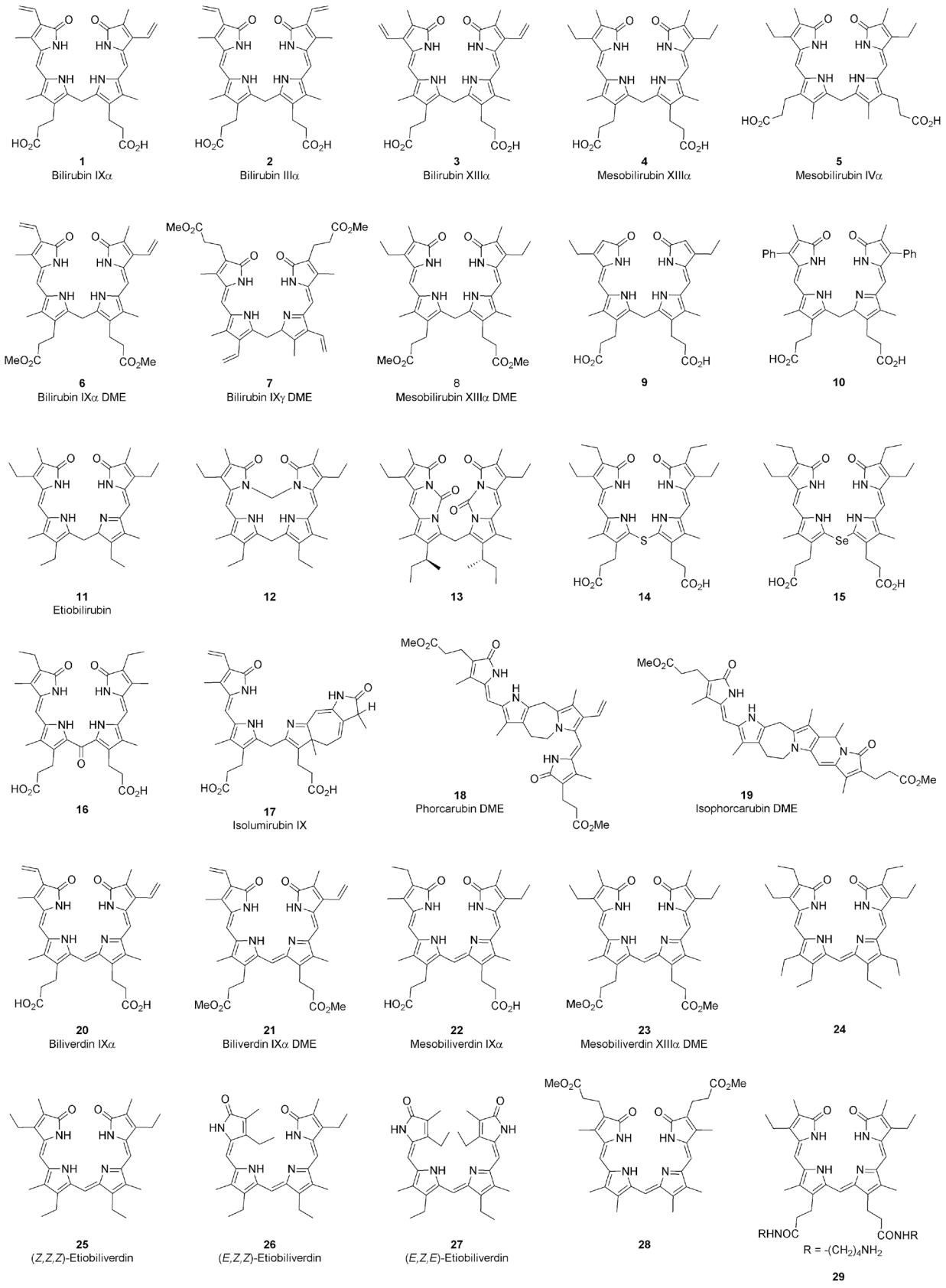

Chart 2. The structures of open-chain tetrapyrroles.

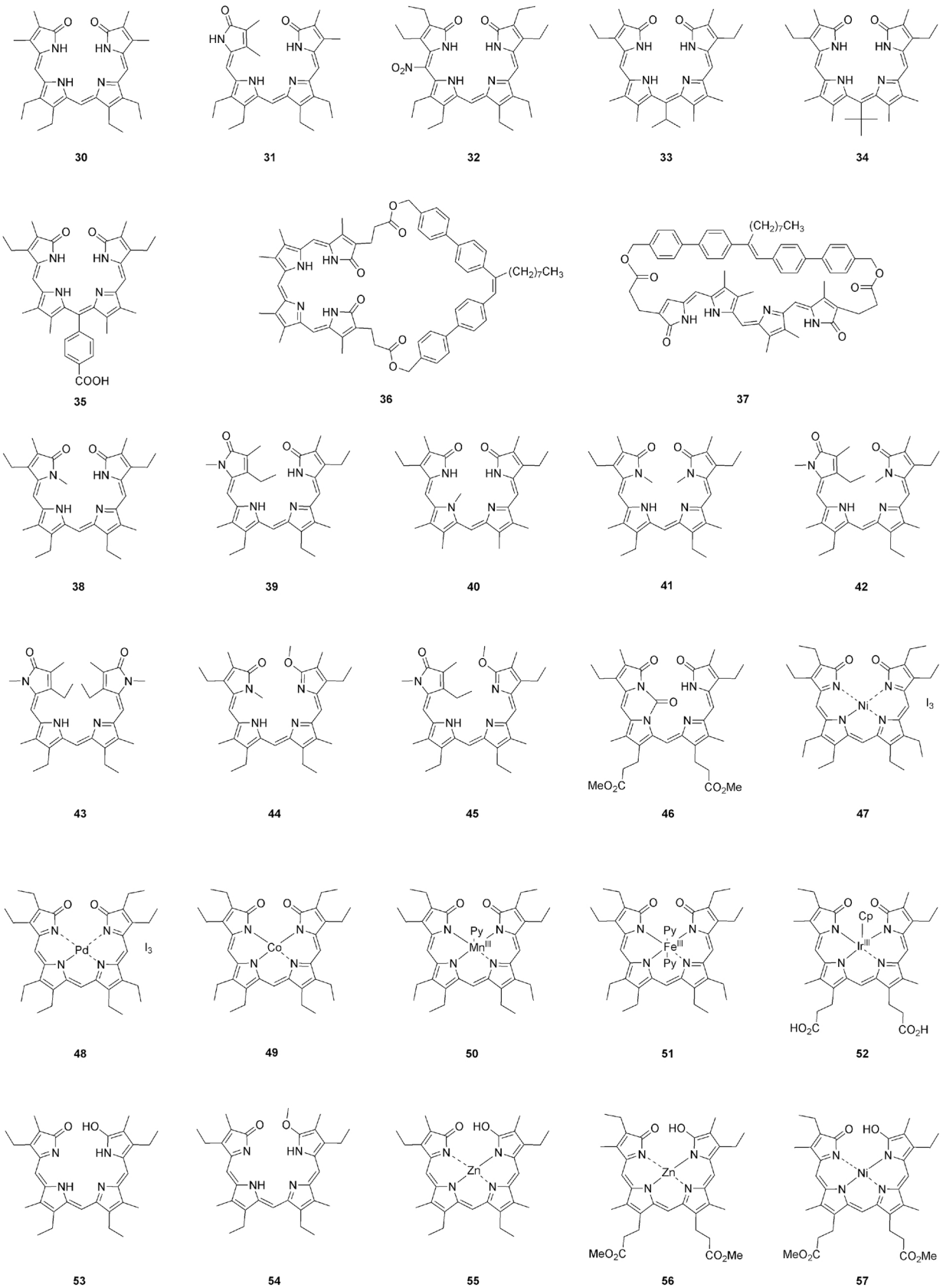

Chart 2. (*continued*).

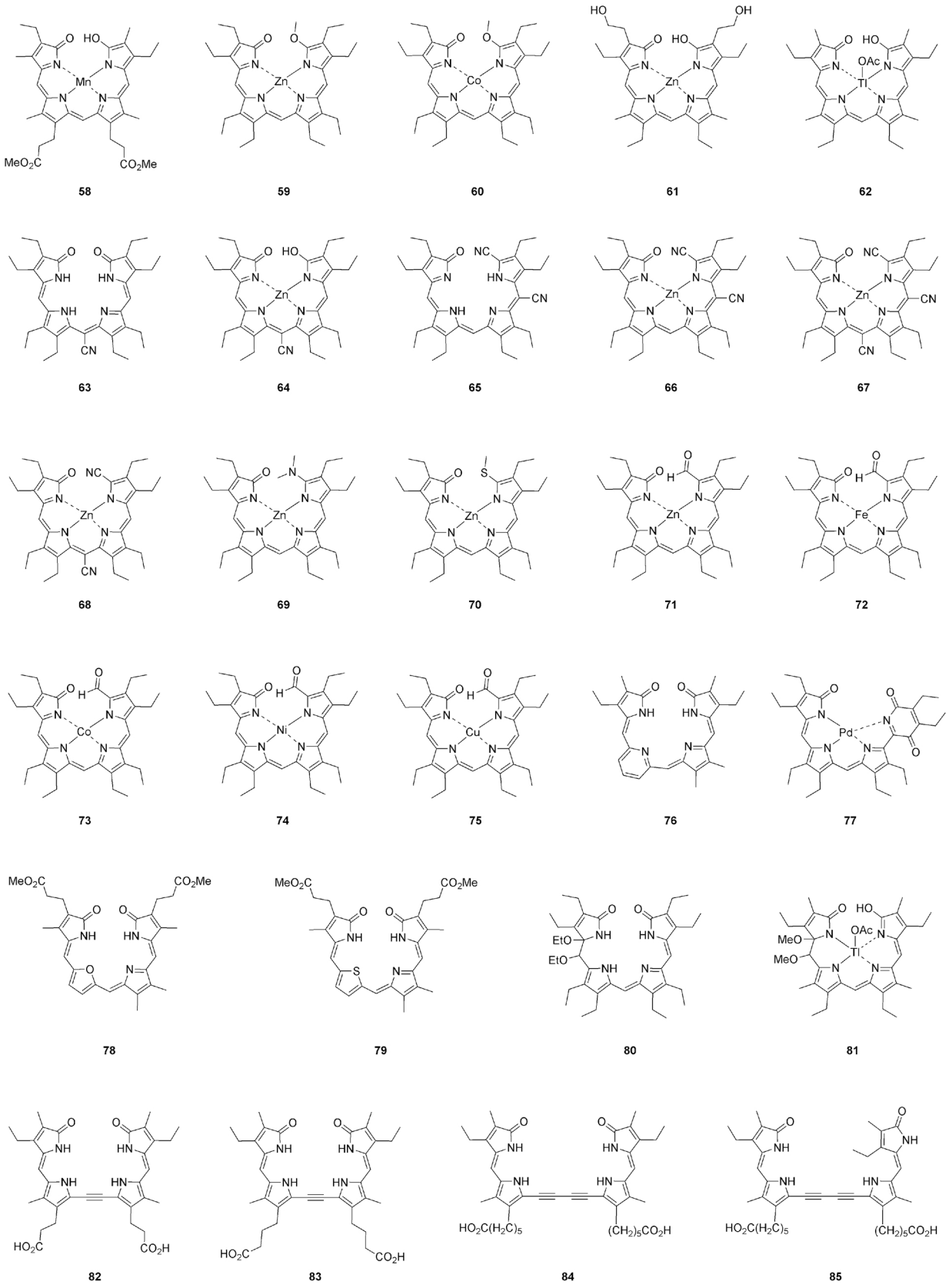

Chart 2. (*continued*).

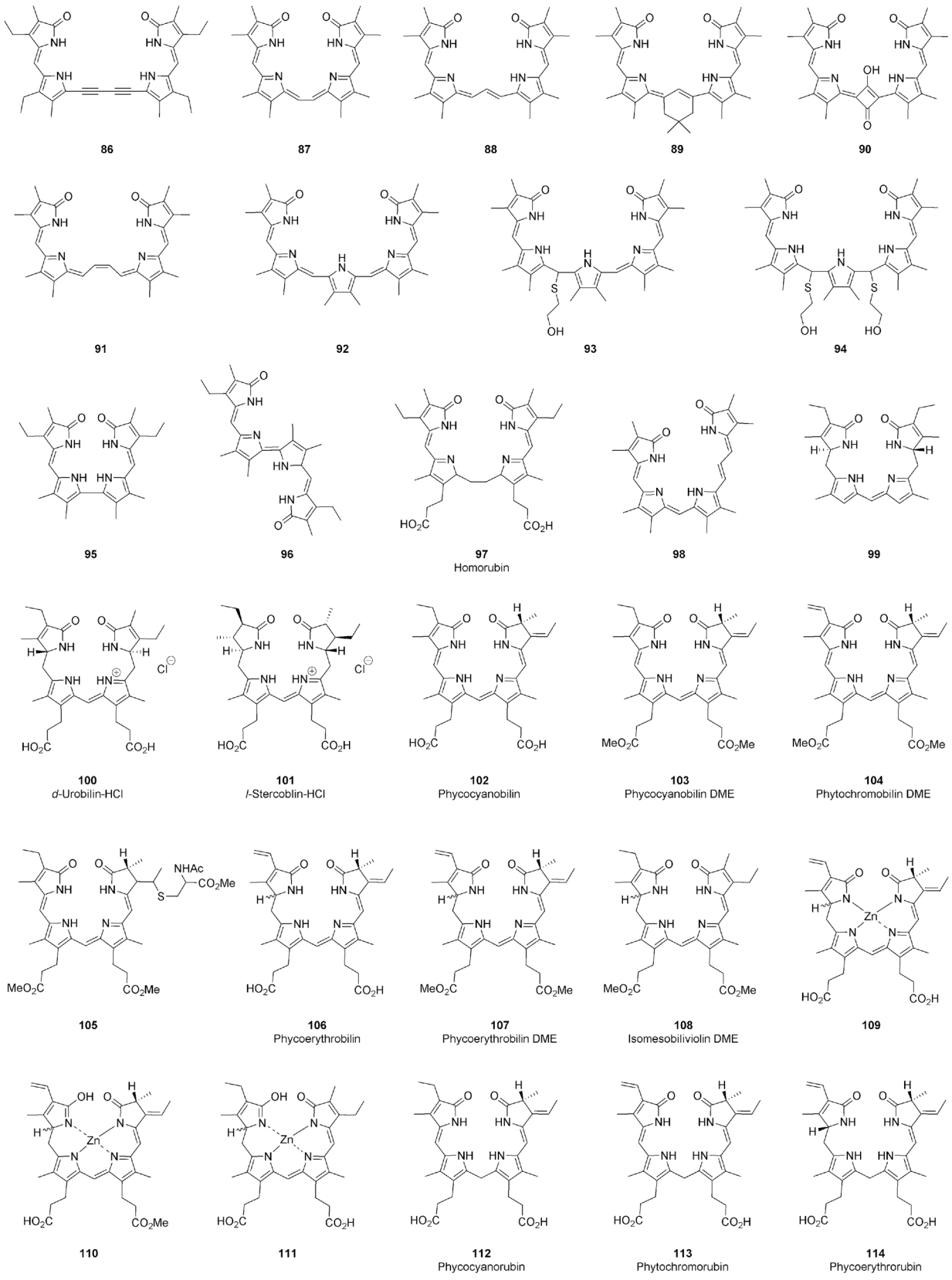

Chart 2. (*continued*).

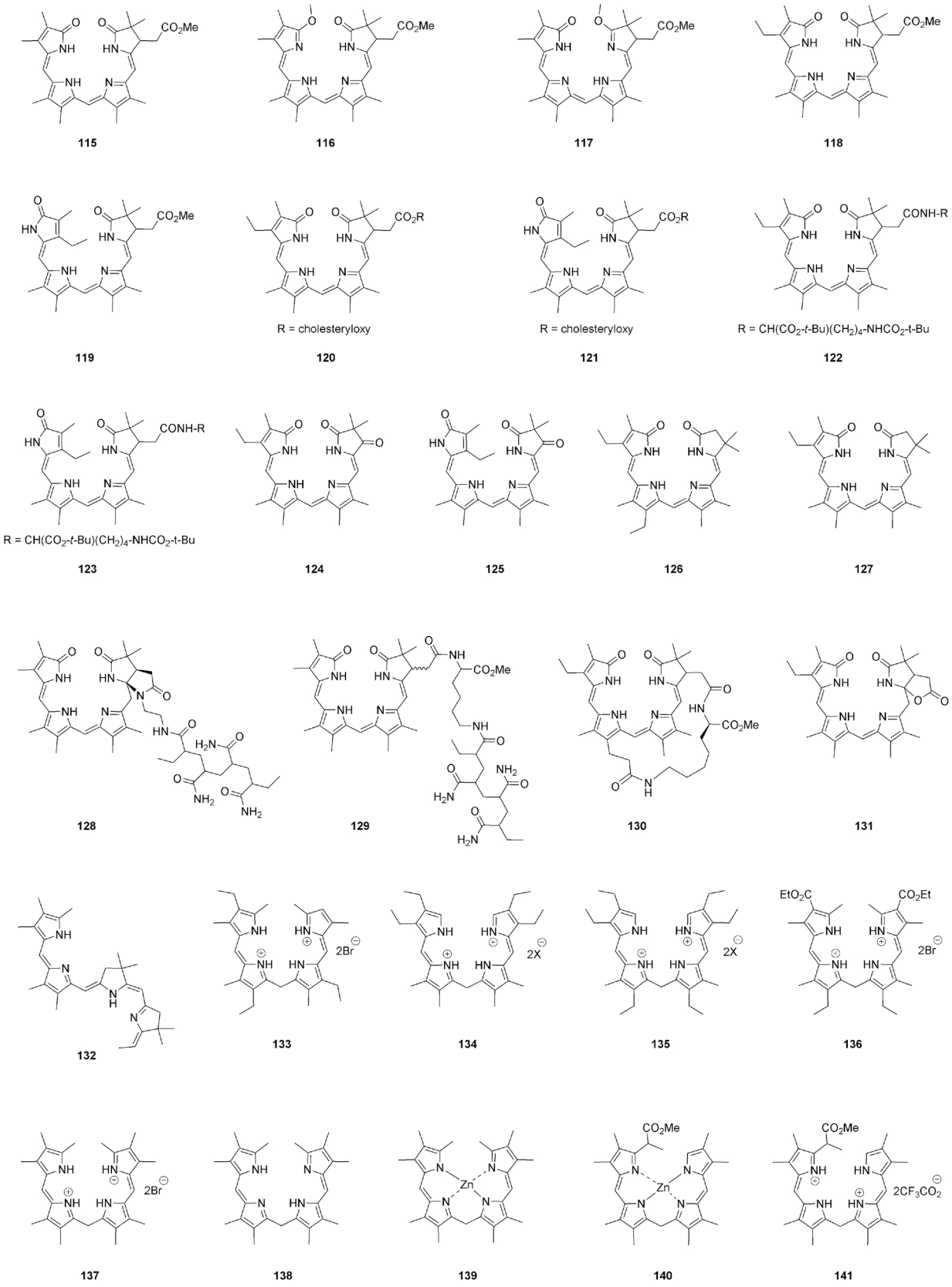

Chart 2. (*continued*).

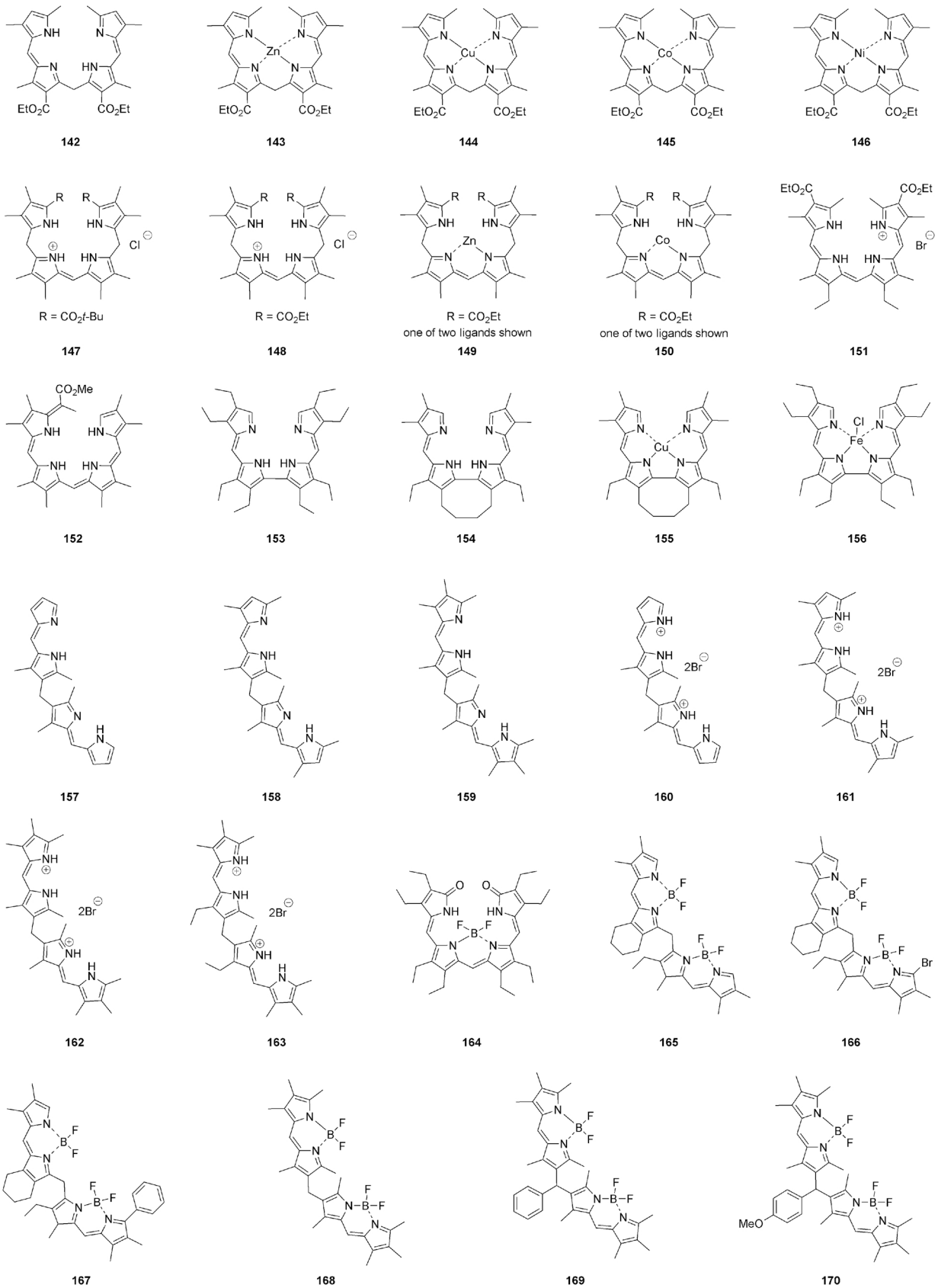

Chart 2. (*continued*).

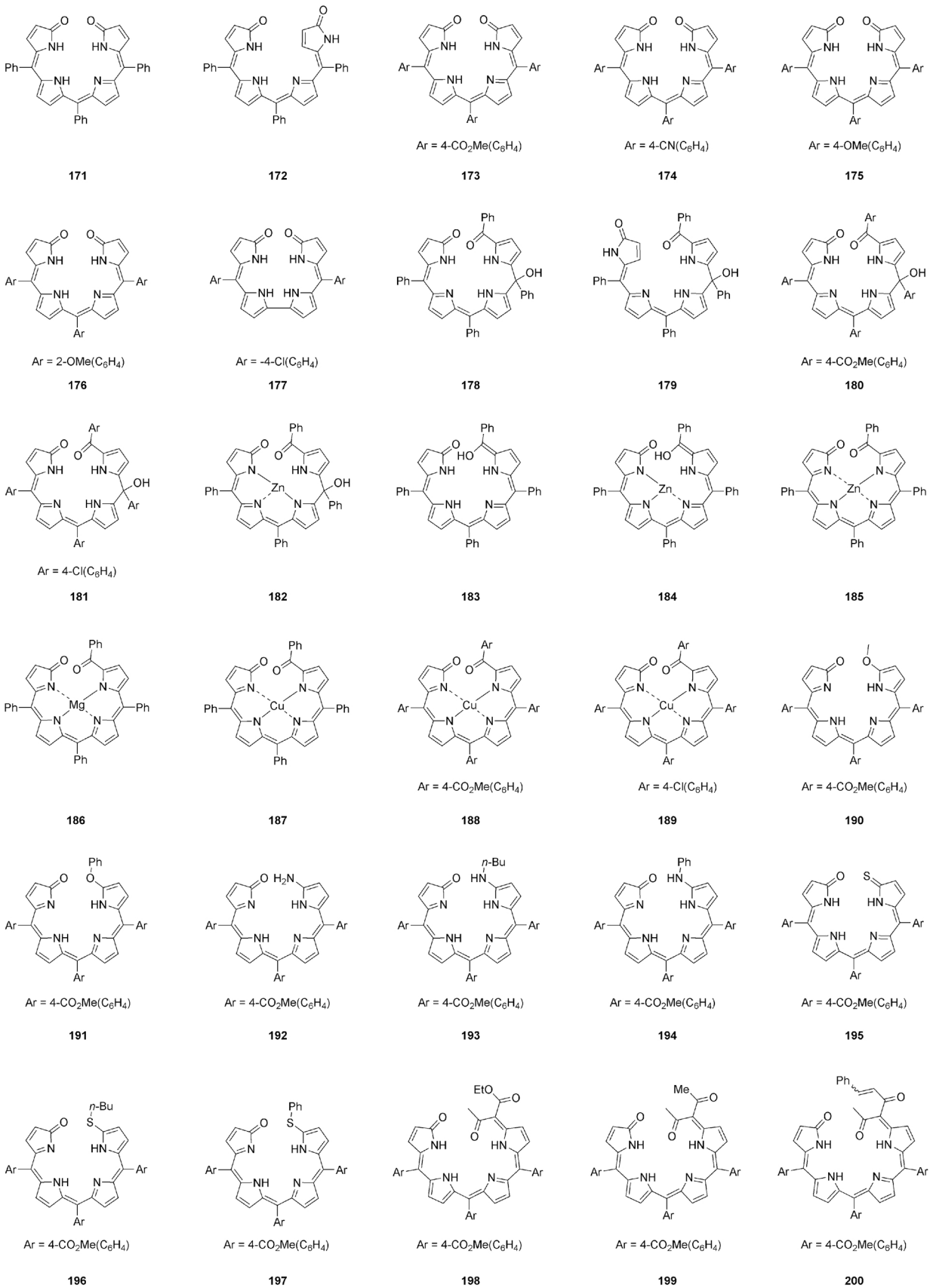

171 172 173 174 175 176 177 178 179 180 181 182 183 184 185 186 187 188 189 190 191 192 193 194 195 196 197 198 199 200

Chart 2. (*continued*).

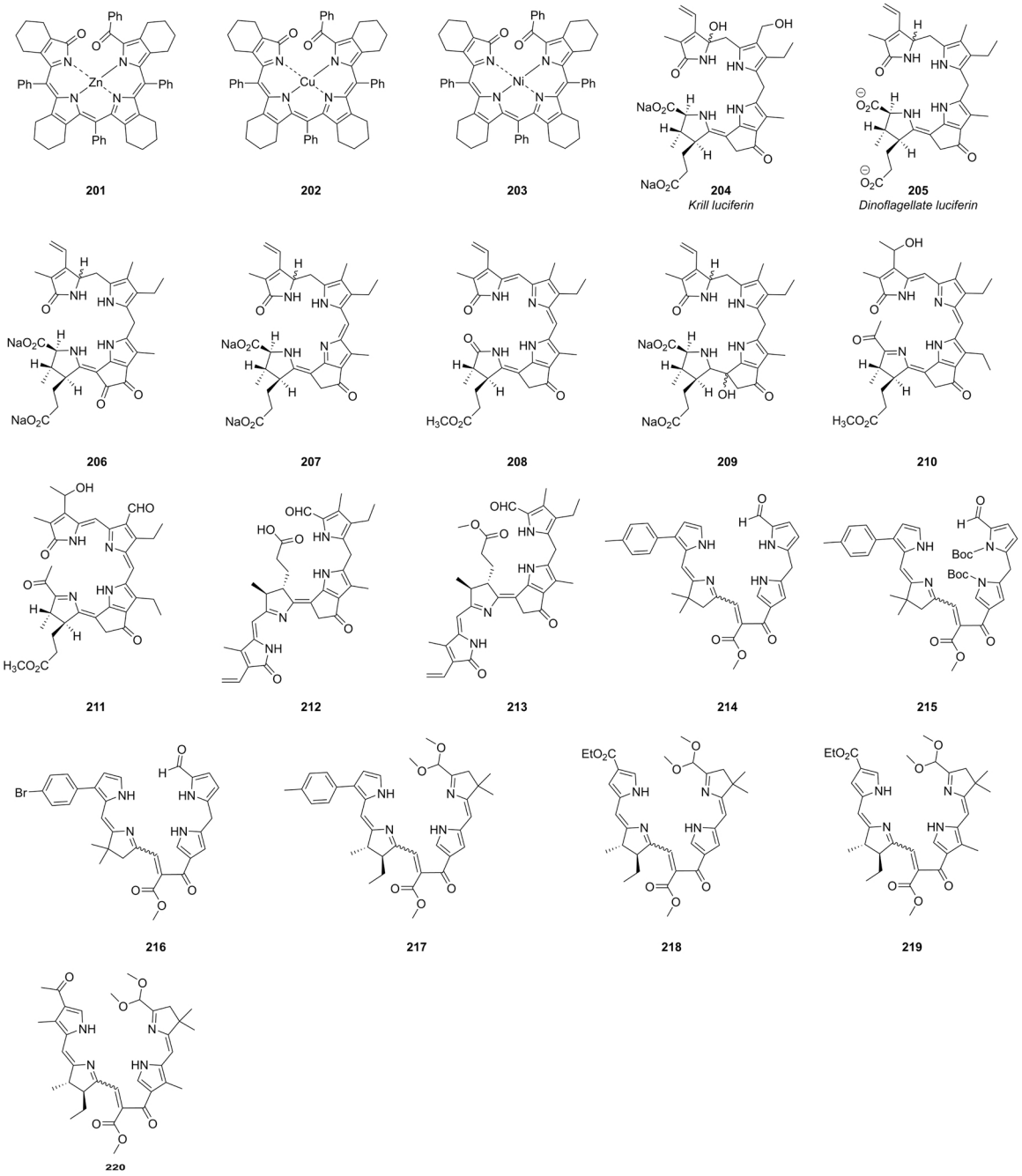

Chart 2. (*continued*).

open-chain tetrapyrroles are the substituents, metalation state, steric configuration (*E/Z*), and solvents. We now consider the ten groups in turn. In each case, every structure is called out with regards to spectral features.

4.1. Bilirubins and related compounds (1–19; panels A1–A6)

The classic bilirubin compound is bilirubin IXα (**1**), derived by oxidation of the heme ligand at the α-position (Scheme 1). The absorption maxima of bilirubin and derivatives (**1–11**) range from 378 nm (**8**) to 455 nm (**2**) in chloroform (except **5** in aqueous Tris buffer and **10** in methanol). The position of the peak maximum depends on the nature of the peripheral substituents (Fig. 1, panel A1). Each bilirubin contains two dipyrrinone units joined at the 10-methylene unit. Note that bilirubin derivatives exhibit significant spectral effects depending on the absence/presence of carboxylic acid substituents (typically propionic acid substituents). The bilirubin derivative in this set with the shortest wavelength maximum is mesobilirubin XIIIα dimethyl ester (**8**), which is nearly coincident with that of etiobilirubin (**11**). Both structures lack free carboxylic acid groups. The spectral distinction between **8** (378 nm) and **4** (431 nm) is significant, especially because both have identical chromophores and substituents except for the dimethyl ester and free carboxylic acids, respectively.

Bilirubin is known to fold upon itself in solution, with one of several folded conformations shown in Fig. 3. The self-folding is enabled by the pivot point provided by the 10-methylene unit and driven by a network of complementary intramolecular H-bonding pairs [203]. The intramolecular H-bonding arises from interactions of the carboxylic acid moiety of the first dipyrrinone with sites on the second dipyrrinone. The carboxylic acid is both a H-bond donor and a H-bond acceptor. The

Table 1
Absorption spectra data for open-chain tetrapyrroles in the database.

Cmpds	λ_{max} (relative intensities)	ε ($M^{-1}cm^{-1}$)	solvent	Ref
		(1) Bilirubins and related compounds		
1	451	55000 (451 nm)	chloroform	[61]
	450	62400 (450 nm)	chloroform	[199]
	454	37700 (454 nm)	chloroform	[131]
	455	43400 (455 nm)	methanol	[131]
	453	35500 (453 nm)	pyridine	[131]
	455	38700 (455 nm)	tetrahydrofuran	[131]
	443	65700 (443 nm)	Tris buffer[a]	[199]
2	455	57200 (455 nm)	chloroform	[199]
	443	37000 (443 nm)	Tris buffer[a]	[199]
3	451	40500 (451 nm)	chloroform	[199]
	442	42100 (442 nm)	Tris buffer[a]	[199]
4	431	58400 (431 nm)	chloroform	[199]
	431	57800 (431 nm)	chloroform	[117]
	426	57000 (426 nm)	dimethyl sulfoxide	[117]
	439	59000 (439 nm)	dimethyl sulfoxide	[103]
	418	36700 (418 nm)	Tris buffer[a]	[199]
5	392	32200 (392 nm)	Tris buffer[a]	[199]
6	400	75100 (400 nm)	carbon tetrachloride	[161]
	405	55800 (405 nm)	chloroform	[161]
	401	32500 (401 nm)	chloroform	[131]
	399	44700 (399 nm)	cyclohexane	[131]
	453	62200 (453 nm)	dimethyl sulfoxide	[161]
	451	33400 (451 nm)	methanol	[131]
	421	50400 (421 nm)	pyridine	[161]
	438	25700 (438 nm)	pyridine	[131]
	406	28300 (406 nm)	tetrahydrofuran	[131]
7	393		chloroform	[162]
8	378	58000 (378 nm)	chloroform	[119]
	427	65000 (427 nm)	dimethyl sulfoxide	[119]
9	432	53000 (432 nm)	chloroform	[119]
	426	60000 (426 nm)	dimethyl sulfoxide	[119]
10	444		methanol	[111]
11	382	64700 (382 nm)	chloroform	[131]
	430	49300 (430 nm)	methanol	[131]
	392	46300 (392 nm)	pyridine	[131]
	380	63300 (380 nm)	tetrahydrofuran	[131]
12	394	19900 (394 nm)	chloroform	[132]
	378	50700 (378 nm)	chloroform	[131]
	375	47000 (375 nm)	cyclohexane	[131]
	387	57000 (387 nm)	methanol	[131]
13	442	33500 (442 nm)	chloroform	[104]
	423	31900 (423 nm)	methanol	[104]
14	428	46500 (428 nm)	methanol	[193]
15	428	46500 (428 nm)	methanol	[151]
16	389	33400 (389 nm)	chloroform	[117]
	383	40500 (383 nm)	dimethyl sulfoxide	[117]
17	432		methanol	[167]
	437	33000 (437 nm)	methanol	[168]
18	416		chloroform	[162]
19	432		chloroform	[162]
		(2) Biliverdins/bilindiones and related compounds		
20	374 (1), 668 (0.25)		water	[188]
21	380 (1), 663 (0.27)	49900 (380 nm)	chloroform	[125]
	377 (1), 667 (0.28)	56200 (377 nm)	ethanol	[61]
22	372 (1), 638 (0.3)	35800 (372 nm)	dimethyl sulfoxide	[103]
	360 (1), 680 (0.55)		ethanol	[197]
23	369 (1), 639 (0.29)	55100 (369 nm)	chloroform	[105]
	372 (1), 635 (0.33)	55900 (372 nm)	dimethyl sulfoxide	[105]
24	370 (1), 650 (0.29)	49900 (370 nm)	chloroform	[106]
25	371 (1), 636 (0.29)	52000 (371 nm)	chloroform	[125]
26	369 (1), 598 (0.49)	41000 (369 nm)	chloroform	[125]
27	373 (1), 571 (0.35)	50700 (373 nm)	chloroform	[129]
28	367 (1), 635 (0.29)	52500 (367 nm)	chloroform	[178]
	373 (1), 640 (0.29)		methanol	[178]
29	368 (1), 640 (0.29)	23600 (368 nm)	chloroform	[129]
30	370 (1), 650 (0.28)	51300 (370 nm)	chloroform	[125]
31	370 (1), 605 (0.31)	44200 (370 nm)	chloroform	[125]
32	322 (1), 525 (0.46)	50500 (322 nm)	chloroform	[106]
33	387	44000 (387 nm)	chloroform	[143]
	440	31600 (440 nm)	dimethyl sulfoxide	[143]
34	402	24000 (402 nm)	chloroform	[143]
35	385 (1), 656 (0.27)		chloroform	[145]

(*continued on next page*)

Table 1 (*continued*)

Cmpds	λ_{max} (relative intensities)	ε ($M^{-1}cm^{-1}$)	solvent	Ref
36	368 (1), 608 (0.47)	41700 (368 nm)	chloroform	[177]
37	317 (1), 559 (0.78)	41700 (317 nm)	chloroform	[177]
38	365 (1), 595 (0.41)	23700 (365 nm)	methanol	[126]
39	365 (1), 595 (0.56)	20300 (365 nm)	methanol	[126]
40	360 (0.92), 575 (1)	7700 (575 nm)	methanol	[126]
41	360 (1), 585 (0.45)	12500 (360 nm)	chloroform	[130]
42	360 (1), 575 (0.74)	11100 (360 nm)	chloroform	[130]
43	360 (1), 570 (0.63)	10900 (360 nm)	chloroform	[130]
44	366 (1), 600 (0.44)	10900 (366 nm)	chloroform	[128]
45	363 (1), 573 (0.55)	10300 (363 nm)	chloroform	[128]
46	385 (0.48), 534 (1)	27700 (534 nm)	chloroform	[105]
	385 (0.61), 545 (1)	25800 (545 nm)	dimethyl sulfoxide	[105]
47	296 (1), 362 (0.58), 678 (0.13)	39100 (296 nm)	chloroform	[165]
48	296 (1), 374 (0.58), 724 (0.28)	49300 (296 nm)	chloroform	[165]
49	380 (1), 642 (0.28)	67000 (380 nm)	dichloromethane	[100]
50	350 (1), 906 (0.33)	35000 (350 nm)	pyridine	[100]
51	375 (1), 654 (0.22)	35000 (375 nm)	pyridine	[99]
52	381 (1), 749 (0.28)		water	[197]
53	355 (0.78), 615 (1)	28300 (615 nm)	methanol	[127]
54	370 (1), 670 (0.3)	40800 (370 nm)	methanol	[127]
55	369 (1), 687 (0.81)	44000 (369 nm)	methanol	[127]
56	390 (1), 706 (0.66)	30000 (390 nm)	chloroform	[149]
57	405 (1), 670 (0.8)	23800 (405 nm)	methanol	[149]
58	388 (1), 910 (0.41)	24000 (388 nm)	chloroform	[149]
59	402 (1), 790 (0.47)	33600 (402 nm)	dichloromethane	[163]
60	400 (1), 823 (0.34)		dichloromethane	[163]
61	358 (1), 726 (0.32)	39700 (358 nm)	dichloromethane	[170]
62	762	42400 (762 nm)	methanol	[124]
63	380 (1), 726 (0.32)	50000 (380 nm)	chloroform	[158]
64	388 (1), 790 (0.32)	50300 (388 nm)	chloroform	[158]
65	412 (1), 778 (0.31)		chloroform	[158]
66	430 (1), 868 (0.33)	16300 (430 nm)	chloroform	[158]
67	444 (1), 906 (0.3)	13700 (444 nm)	chloroform	[158]
68	422 (1), 896 (0.22)	65000 (422 nm)	chloroform	[158]
69	413 (1), 822 (0.4)	30800 (413 nm)	dichloromethane	[157]
70	425 (1), 846 (0.35)	22100 (425 nm)	dichloromethane	[157]
71	412 (1), 834 (0.45)	26100 (412 nm)	methanol	[148]
72	383 (1), 854 (0.2)	35600 (383 nm)	methanol	[148]
73	310 (1), 400 (0.7), 766 (0.2)	26000 (310 nm)	dichloromethane	[160]
74	308 (1), 424 (0.95), 802 (0.32)	29000 (308 nm)	dichloromethane	[160]
75	308 (0.98), 432 (1), 752 (0.29), 844 (0.29)	39000 (432 nm)	dichloromethane	[160]
76	277 (1), 345 (0.66), 431 (0.56)	33350 (277 nm)	ethanol	[147]
77	312 (1), 438 (0.55), 780 (0.55)	11000 (312 nm)	chloroform	[166]
78	361 (0.87), 551 (1)	20000 (551 nm)	chloroform	[178]
	355 (1), 550 (0.61)	38900 (355 nm)	methanol	[178]
79	361 (1), 551 (0.36)	56200 (361 nm)	chloroform	[178]
	360 (1), 546 (0.5)	43700 (360 nm)	methanol	[178]
80	325 (1), 556 (0.73)	48000 (325 nm)	chloroform	[106]
81	620	55000 (620 nm)	methanol	[124]
	(3) Extended bilindiones			
82	308 (0.37), 516 (1)		methanol	[169]
83	311 (0.34), 499 (1)		methanol	[169]
84	470		dimethyl sulfoxide	[169]
85	457		dimethyl sulfoxide	[169]
86	461	40600 (461 nm)	chloroform	[194]
	456	43900 (456 nm)	dimethyl sulfoxide	[194]
87	284 (1), 533 (0.76)	50000 (284 nm)	dichloromethane	[114]
88	381 (1), 820 (0.9)	37100 (381 nm)	dichloromethane	[115]
89	367 (1), 627 (0.33)	32500 (367 nm)	dichloromethane	[115]
90	372 (0.17), 760 (1)	65000 (760 nm)	dichloromethane	[115]
91	368 (1), 644 (0.41), 844 (0.13)	34000 (368 nm)	dichloromethane	[116]
	364 (0.58), 486 (1), 650 (0.19)	50500 (486 nm)	dimethyl sulfoxide	[116]
92	319 (1), 725 (0.14)	60000 (319 nm)	chloroform	[138]
93	318 (1), 394 (0.82), 554 (0.71)	32000 (394 nm)	chloroform	[139]
94	394 (1), 510 (0.12)	6400 (394 nm)	chloroform	[139]
95	354 (1), 445 (0.67)	20100 (354 nm)	dichloromethane	[142]
96	518	30000 (518 nm)	dichloromethane	[142]
97	424	57000 (424 nm)	dichloromethane	[183]
98	391 (1), 699 (0.27)	58300 (391 nm)	chloroform	[146]
	(4) Urobilins and related compounds			
99	445 (1), 503 (0.41)	15800 (445 nm)	methanol	[182]
100	496	94000 (496 nm)	dichloromethane-d_2	[150]
101	493	78400 (493 nm)	dichloromethane	[150]

(*continued on next page*)

Table 1 (*continued*)

Cmpds	λ_{max} (relative intensities)	ε ($M^{-1}cm^{-1}$)	solvent	Ref
		(5) Phycocyanobilin and related compounds		
102	361 (1), 605 (0.38)		water	[191]
	363 (1), 623 (0.4)		methanol	[197]
103	369 (1), 600 (0.35)	54200 (369 nm)	chloroform	[112]
	368 (1), 600 (0.39)	43000 (368 nm)	methanol	[108]
	362 (1), 600 (0.36)	41700 (362 nm)	methanol	[152]
104	372 (1), 610 (0.29)	57500 (372 nm)	methanol	[195]
105	345 (1), 590 (0.46)	38000 (345 nm)	methanol	[102]
106	295 (0.72), 505 (1)		chloroform	[113]
107	316 (0.65), 530 (1)	17700 (530 nm)	methanol	[118]
108	330 (1), 565 (0.64)	17500 (330 nm)	methanol	[118]
109	320 (0.7), 583 (1)		chloroform	[113]
110	336 (0.45), 604 (1)	33200 (604 nm)	methanol	[118]
111	338 (0.89), 629 (1)	24100 (629 nm)	methanol	[118]
112	366 (0.92), 416 (1)		dichloromethane	[192]
113	361 (0.67), 442 (1)		dichloromethane	[192]
114	358		dichloromethane	[192]
115	347 (1), 582 (0.43)	16100 (347 nm)	chloroform	[133]
116	353 (1), 616 (0.44)	38000 (353 nm)	chloroform	[133]
117	349 (1), 673 (0.53)	39700 (349 nm)	chloroform	[133]
118	349 (1), 600 (0.45)	34800 (349 nm)	dimethyl sulfoxide/water	[135]
119	350 (1), 560 (0.65)	25500 (350 nm)	dimethyl sulfoxide/water	[135]
120	344 (1), 580 (0.42)	34700 (344 nm)	chloroform	[122]
121	348 (1), 550 (0.7)	24800 (348 nm)	chloroform	[122]
122	348 (1), 582 (0.47)	32300 (348 nm)	chloroform	[123]
123	348 (1), 540 (0.75)	23600 (348 nm)	chloroform	[123]
124	339 (1), 645 (0.43)		chloroform	[136]
125	365 (1), 636 (0.59)		chloroform	[136]
126	345 (1), 580 (0.45)		chloroform	[140]
127	345 (2), 585 (0.44)		carbon tetrachloride	[137]
128	328 (1), 555 (0.78)	28600 (328 nm)	dimethyl sulfoxide	[144]
	323 (1), 536 (0.65)	29600 (323 nm)	water	[144]
129	346 (1), 595 (0.45)	33400 (346 nm)	dimethyl sulfoxide	[144]
	335 (1), 570 (0.45)	35200 (335 nm)	water	[144]
130	335 (1), 563 (0.43)	17200 (335 nm)	chloroform	[141]
131	320 (1), 545 (0.84)	19100 (320 nm)	dimethyl sulfoxide	[134]
		(6) Biladiene derivatives		
132	387 (0.35), 547 (1)	39800 (547 nm)	benzene	[164]
133	445 (0.6), 511 (1)		methanol	[190]
134	450 (1), 520 (0.84)		dichloromethane	[181]
135	451 (0.31), 519 (1)		chloroform/methanol	[180]
136	454 (0.11), 524 (1)	210000 (524 nm)	chloroform	[120]
137	485	97200 (485 nm)	dimethyl sulfoxide	[185]
138	441	36300 (441 nm)	dimethyl sulfoxide	[185]
139	502	98900 (502 nm)	dimethyl sulfoxide	[185]
140	473 (1), 540 (0.52)		dichloromethane	[175]
141	447 (1), 518 (0.41)	24600 (447 nm)	dichloromethane	[175]
142	425 (1), 490 (0.54)	27700 (425 nm)	chloroform	[173]
143	454 (0.92), 475 (1)	153000 (475 nm)	chloroform	[173]
144	461	97800 (461 nm)	chloroform	[173]
145	488	124000 (488 nm)	chloroform	[172]
146	476	73600 (476 nm)	chloroform	[172]
147	498		dichloromethane	[175]
148	509	58900 (509 nm)	chloroform	[174]
149	521	140000 (521 nm)	chloroform	[174]
150	524	125000 (524 nm)	chloroform	[174]
151	432 (1), 724 (0.45)	60000 (432 nm)	ethanol	[120]
152	424 (1), 774 (0.53)	81900 (424 nm)	dichloromethane	[175]
153	334 (0.21), 590 (1)	85000 (590 nm)	dichloromethane	[109]
154	330 (0.62), 565 (1)	36000 (565 nm)	dichloromethane	[109]
155	405 (0.78), 495 (1)	76000 (495 nm)	dichloromethane	[109]
156	398 (1), 812 (0.18)	39800 (398 nm)	dichloromethane	[110]
157	420		*n*-propanol	[121]
158	463		*n*-propanol	[121]
159	458	22300 (458 nm)	*N,N*-dimethylformamide	[154]
159	468		*n*-propanol	[121]
160	479		*n*-propanol	[121]
161	496		*n*-propanol	[121]
162	464 (0.39), 504 (1)	120000 (504 nm)	dichloromethane	[153]
	505		*n*-propanol	[121]
163	504		chloroform	[97]
		(7) Boron difluoride complexes		

(*continued on next page*)

Table 1 (*continued*)

Cmpds	λ_{max} (relative intensities)	ε ($M^{-1}cm^{-1}$)	solvent	Ref
164	364 (0.66), 629 (1)	57500 (629 nm)	chloroform	[107]
	634	62500 (634 nm)	xylene	[96]
165	556	157000 (556 nm)	tetrahydrofuran	[186]
166	566	108000 (566 nm)	tetrahydrofuran	[186]
167	577	139000 (577 nm)	tetrahydrofuran	[186]
168	550		benzene	[98]
169	550		benzene	[98]
170	547	170000 (547 nm)	benzene	[98]
	(8) Bilins derived from synthetic tetraarylporphyrins			
171	335 (0.58), 400 (1), 616 (0.45)		chloroform	[198]
172	333 (0.69), 400 (1), 609 (0.45)		chloroform	[198]
173	327 (0.62), 402 (1), 628 (0.49)	39200 (402 nm)	chloroform	[159]
174	400 (1), 631 (0.49)		chloroform	[176]
175	419 (1), 632 (0.51)		chloroform	[176]
176	394 (1), 613 (0.69)		chloroform	[176]
177	330 (0.57), 412 (0.6), 590 (1)	39000 (590 nm)	dichloromethane	[101]
178	352 (1), 561 (0.63)		chloroform	[198]
179	316 (0.97), 358 (0.85), 527 (1)		chloroform	[198]
180	337 (1), 554 (0.58)		dichloromethane	[171]
181	359 (1), 416 (0.98), 561 (0.38)		dichloromethane	[187]
182	345 (0.9), 583 (0.49), 627 (1)		benzene	[95]
183	346 (1), 560 (0.63)		dichloromethane	[189]
184	339 (0.86), 585 (0.63), 628 (1)		dichloromethane	[189]
185	360 (1), 489 (0.99), 820		benzene	[95]
186	790		dichloromethane	[189]
187	364 (1), 478 (0.99), 760 (0.28), 861 (0.23)	24700 (364 nm)	dichloromethane	[187]
188	361 (1), 486 (0.88), 757 (0.23), 857 (0.2)	25870 (361 nm)	dichloromethane	[187]
189	371 (0.73), 414 (1), 485 (0.49), 754 (0.12)	40000 (414 nm)	dichloromethane	[187]
190	325 (0.81), 402 (1), 644 (0.4)	44200 (402 nm)	chloroform	[159]
191	328 (0.77), 409 (1), 651 (0.29)	50500 (409 nm)	chloroform	[159]
192	331 (0.8), 408 (1), 673 (0.35)	45100 (408 nm)	chloroform	[159]
193	336 (0.89), 420 (1), 699 (0.39)	42100 (420 nm)	chloroform	[159]
194	366 (0.92), 433 (1), 706 (0.28)	44600 (433 nm)	chloroform	[159]
195	360 (0.7), 444 (1), 676 (0.36)	47500 (444 nm)	chloroform	[159]
196	346 (0.83), 427 (1), 668 (0.27)	41700 (427 nm)	chloroform	[159]
197	342 (0.68), 430 (1), 667 (0.24)	54700 (430 nm)	chloroform	[159]
198	371 (0.87), 463 (1), 706 (0.37)	48200 (463 nm)	chloroform	[159]
199	371 (0.87), 463 (1), 712 (0.37)	40900 (463 nm)	chloroform	[159]
200	372 (0.88), 480 (1), 723 (0.4)	51800 (480 nm)	chloroform	[159]
201	330 (1), 455 (0.87), 752 (0.27)		benzonitrile	[179]
202	344 (0.96), 484 (1), 814 (0.4)		benzonitrile	[179]
203	326 (1), 442 (0.95), 804 (0.42)		benzonitrile	[179]
	(9) Chlorophyll catabolites			
204	242 (1), 386 (0.37)		acetonitrile (40%)[a]	[20]
	246 (1), 388 (0.37)		ethanol (50%)[a]	[19]
205	247 (1), 392 (0.31)		ethanol/water	[196]
206	233 (0.98), 348 (1)		acetonitrile (30%)[a]	[18]
207	313 (0.12), 370 (0.2), 633 (1)		methanol (80%)[a]	[18]
208	336 (1), 605 (0.41), 690 (0.30)		dichloromethane	[155]
209	237		acetonitrile	[18]
210	366 (1), 569 (0.58), 587 (0.57)		no solvent specified	[184]
211	363 (1), 549 (0.69), 577 (0.69)		no solvent specified	[184]
212	314 (1), 486 (0.55), 528 (0.56)	28200 (314 nm)	dichloromethane	[156]
213	310 (1), 486 (0.68), 526 (0.68)	28200 (310 nm)	dichloromethane	[156]
	(10) Knoevenagel enones			
214	236 (0.9), 294 (1), 495 (0.27)		acetonitrile	[38]
215	239 (1), 295 (0.75), 501 (0.32)		acetonitrile	[38]
216	295 (1), 487 (0.41)	30500 (295 nm)	acetonitrile	[38]
217	319 (1), 505 (0.61)	26000 (319 nm)	chloroform	[37]
218	330 (1), 474 (0.57)		toluene	[39]
219	339 (1), 454 (0.51)		toluene	[40]
220	337 (1), 480 (0.56)		toluene	[40]

[a] In aqueous solution.

dipyrrinone contains two N–H units that serve as H-bond donors, and a carbonyl group that serves as a H-bond acceptor. The integral role of H-bonding in the self-folding implies that a bilirubin bearing a dipropionic acid dimethyl ester, which lacks H-bond donor capability, is unlikely to fold in the same manner. Conversion of the sp^3-hybridized 10-methylene of a bilirubin to the sp^2-hybridized 10-methine of a biliverdin also would abolish the folding process. Such structural features – folded or not folded – underlie some of the observed spectral features of the bilins described herein.

The absorption spectrum of bilirubin IXα (**1**) bearing free carboxylic acid substituents shows almost no change with solvent across the range of chloroform, tetrahydrofuran, ethanol, and pyridine (Fig. 1, panel A2).

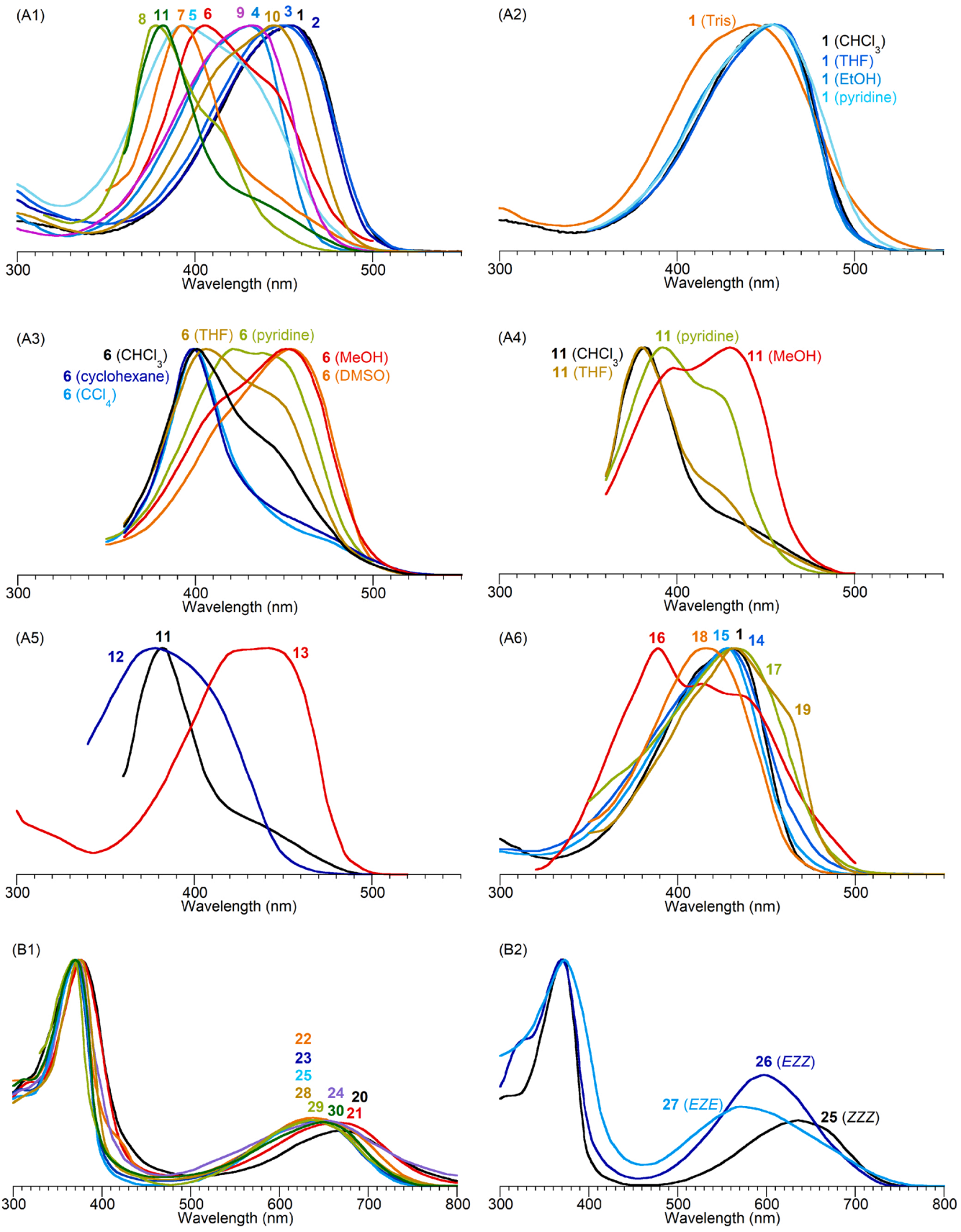

Fig. 1. Absorption spectra of open-chain tetrapyrroles in the database.

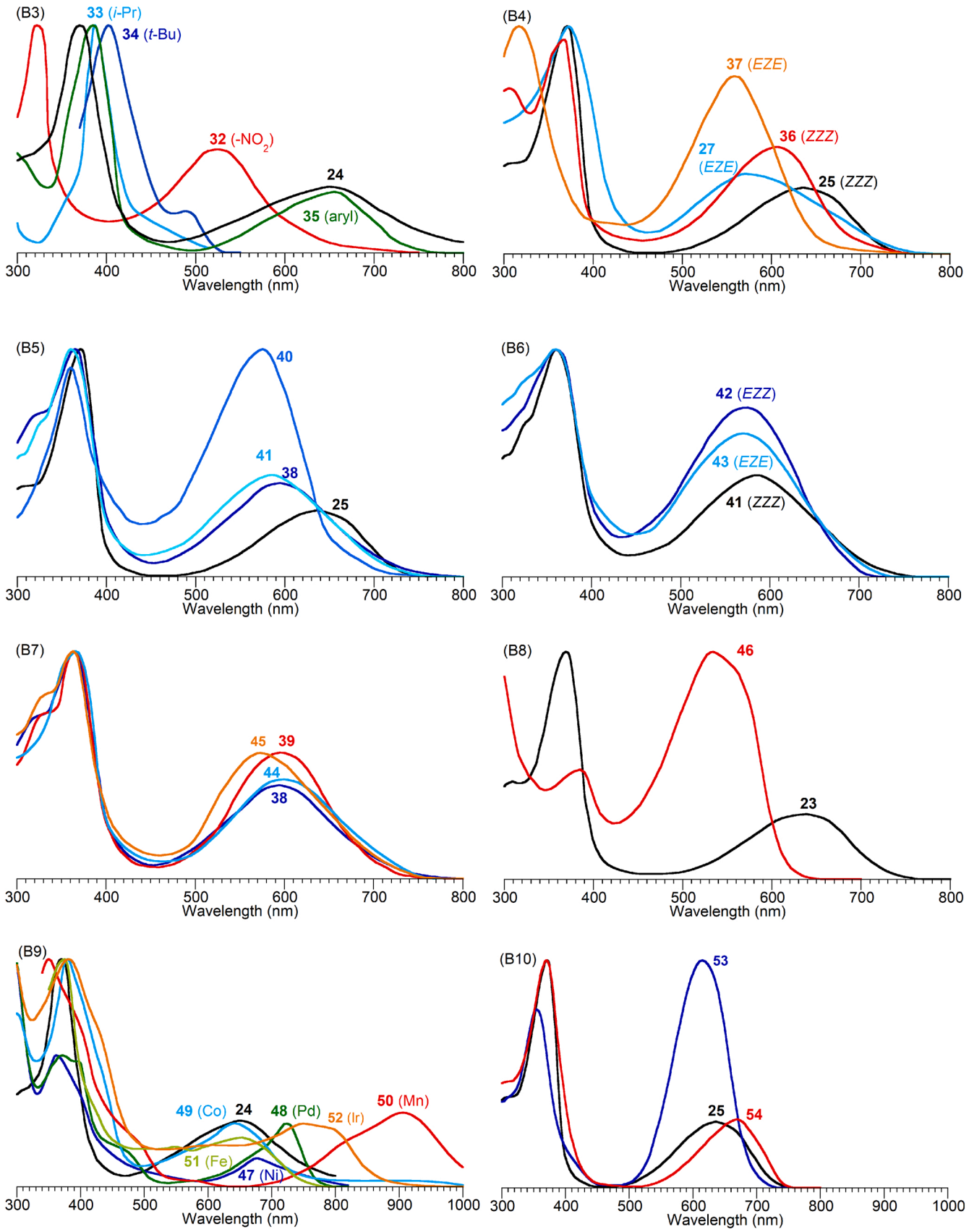

Fig. 1. (*continued*).

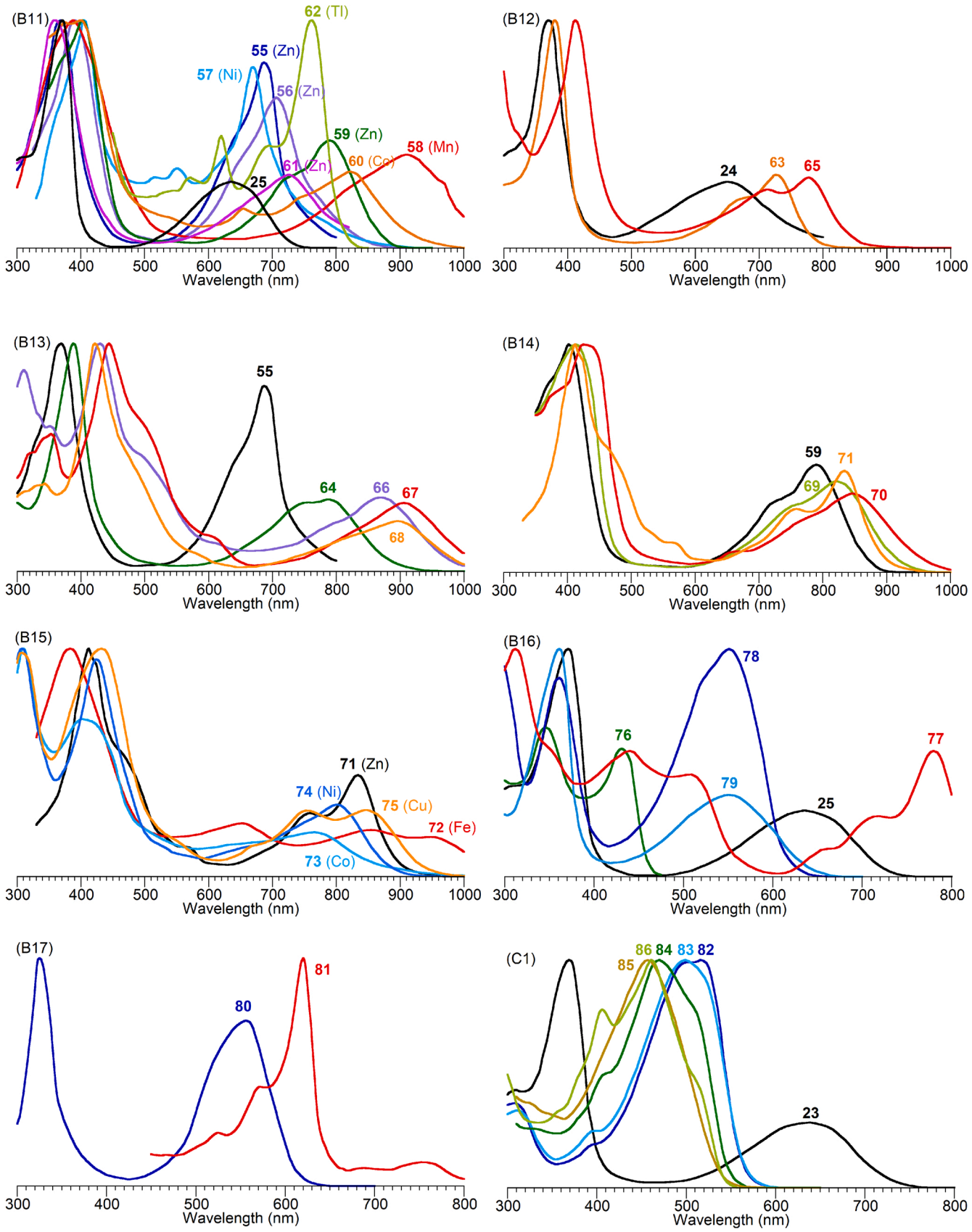

Fig. 1. (*continued*).

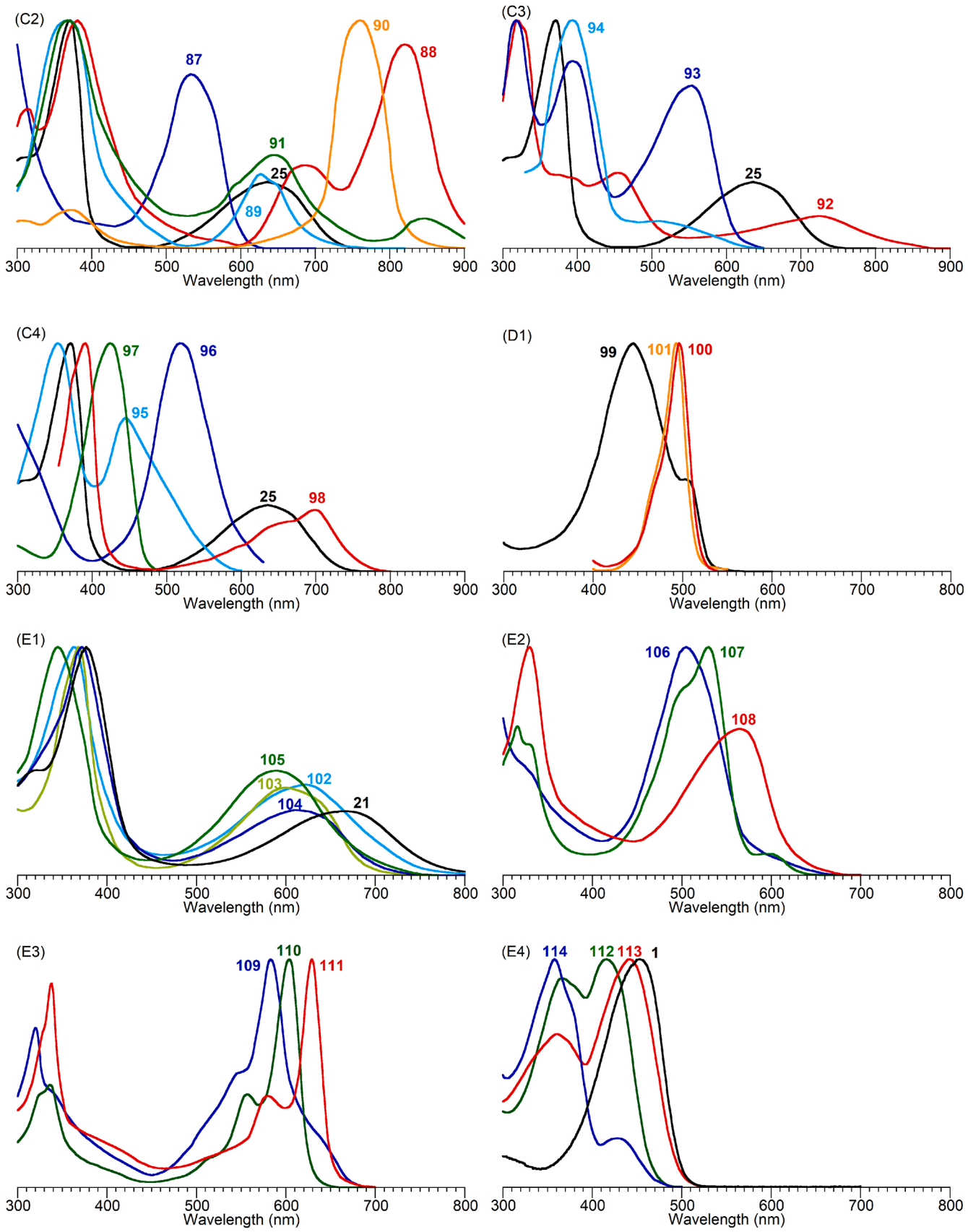

Fig. 1. (*continued*).

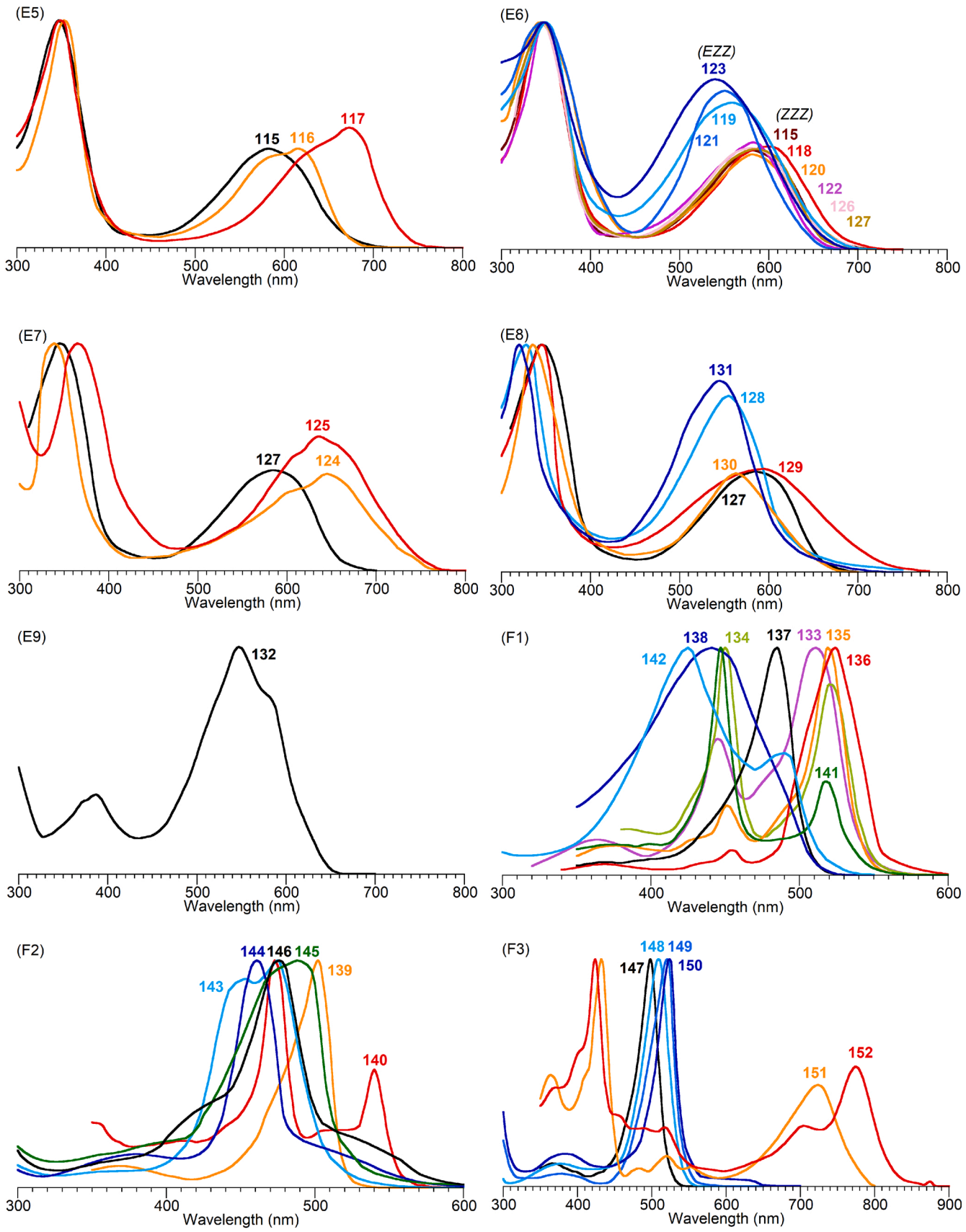

Fig. 1. (*continued*).

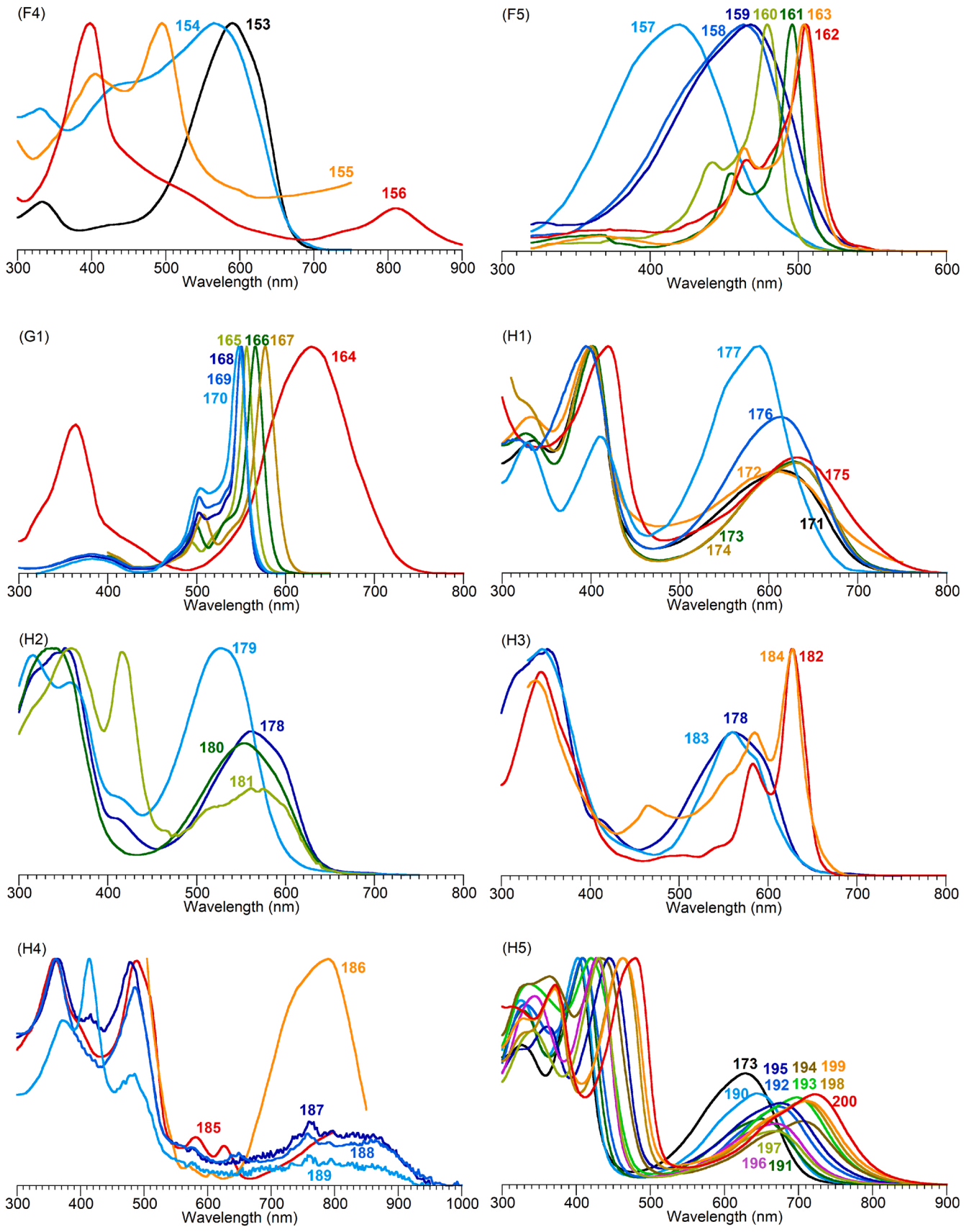

Fig. 1. (*continued*).

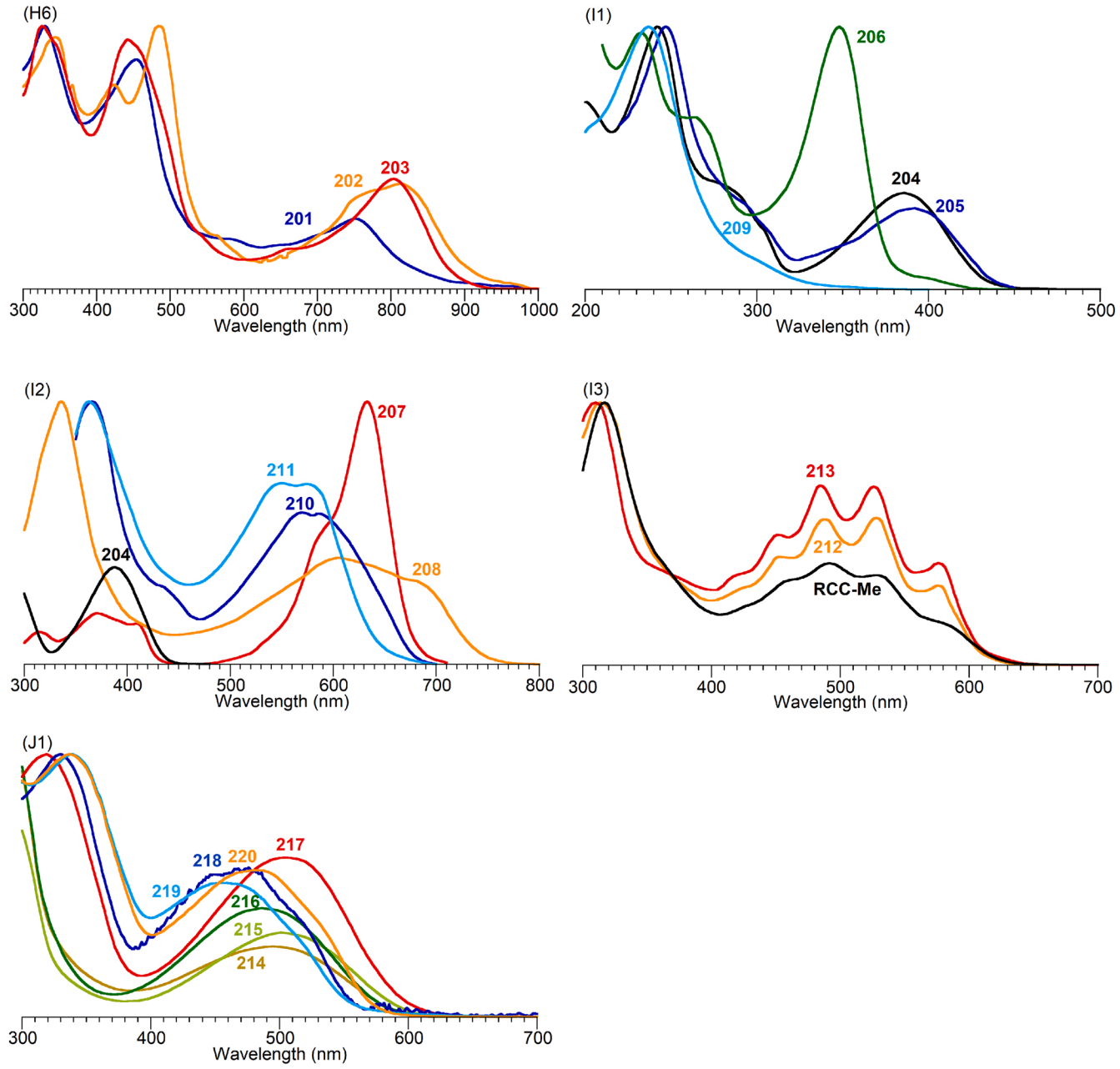

Fig. 1. (*continued*).

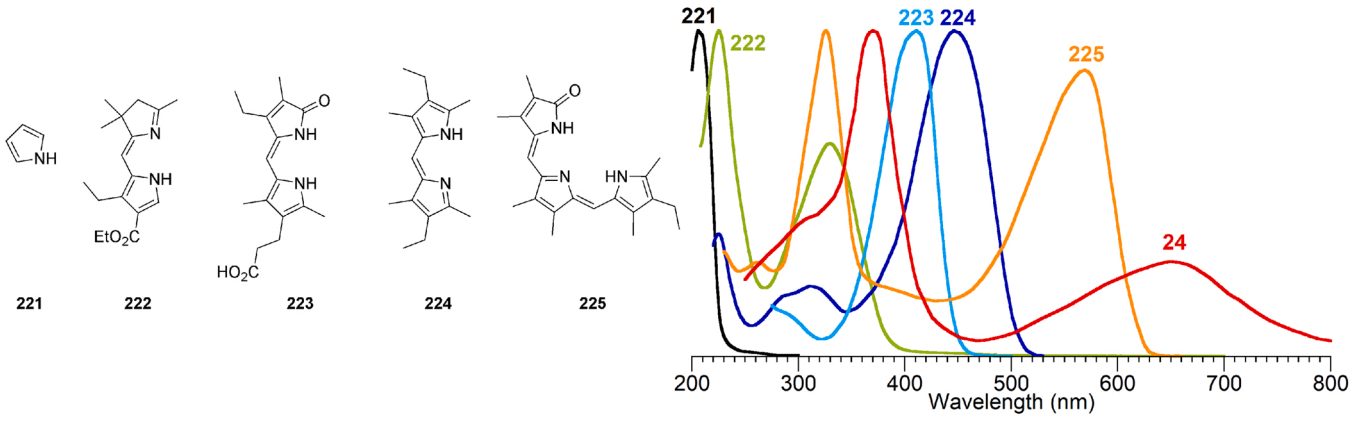

Fig. 2. Absorption spectra of pyrrolic compounds.

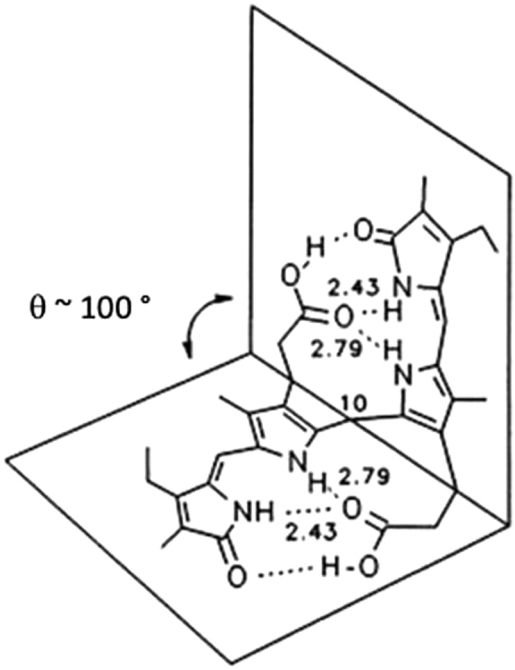

Fig. 3. Self-folding of bilirubin about the 10-methylene group to give a ridge-tile conformation. The non-bonded H···C distances are displayed in Å. Adapted from Nogales and Lightner [203].

On the other hand, the absorption spectrum of bilirubin IXα dimethyl ester (DME) (**6**) bearing carboxylic esters changes significantly with solvent, ranging from 400 nm in non-polar solvents (chloroform, cyclohexane, or carbon tetrachloride) to 453 nm in polar solvents (methanol, dimethylsulfoxide), with spectra intermediate between the two limits in solvents of intermediate polarity (tetrahydrofuran, pyridine) (Fig. 1, panel A3). Similar solvent effects are observed for etiobilirubin (**11**), which lacks carboxylic acids altogether (Fig. 1, panel A4).

The absorption spectra of bilirubins **12** and **13**, wherein the nitrogen atoms are bridged by covalent moieties, are compared to that of etiobilirubin (**11**) (Fig. 1, panel A5). Bilirubin **12** is bridged across nitrogen atoms N^{21}–N^{24}, whereas bilirubin **13** is bridged across N^{21}–N^{22} and N^{23}–N^{24}; in both cases the bridge comprises a methylene unit. Etiobilirubin exhibits a fairly narrow absorption band. Introduction of a methylene bridge between distal nitrogen atoms (N^{21}–N^{24}) in compound **12** causes substantial spectral broadening. Introduction of carbonyl bridges between each of two adjacent nitrogen atoms (N^{21}–N^{22} and N^{23}–N^{24}) in compound **13** causes both broadening and a significant bathochromic shift.

Bilirubins **14** and **15** are modified wherein a thia or selena atom replaces the 10-methylene to join the two dipyrrinone halves. The absorption spectra of **14** and **15** closely resemble that of the parent bilirubin IXα (**1**) itself (Fig. 1, panel A6). Oxidation of the 10-methylene to give a ketone (10-oxo-mesobilirubin, **16**) results in a hypsochromic shift and extensive spectral broadening. Isolumirubin IX (**17**) is an analogue of bilirubin IXα (**1**) that has undergone photocyclization, thereby creating annulation across positions 3 and 7. Phorcarubin DME **18**, a bilirubin derived by γ-oxidative scission (and methylation of the propionic acid groups), contains a 1,2-ethane bridge derived by addition of the N^{22} nitrogen at the β-position of the 12-vinyl group. Isophorcarubin DME **19** is a further derivative wherein cyclization also has occurred by addition of the N^{21} nitrogen to the α-position of the 7-vinyl group. Phorcarubin DME **18** is thus a bilirubin containing one seven-membered cycle, whereas isophorcarubin DME **19** is a bilirubin containing one seven-membered cycle and one six-membered cycle; both cycles impart structural rigidification. The absorption spectra of photocyclized bilirubin (isolumirubin IX, **17**) and nitrogen-β-pyrrole bridged bilirubins (phorcarubin DME, **18**; isophorcarubin DME, **19**) are rather similar to that of bilirubin IXα (**1**) (Fig. 1, panel A6).

4.2. Biliverdins/bilindiones and related compounds (20–81; panels B1–B17)

Biliverdins, often also referred to as bilindiones, contain three methine carbons (5,10,15-positions) in the tetrapyrrolic structure and pyrrolinone termini. In contrast, bilirubins contain only two methines (5,15-positions) and one methylene (10-position). As such, biliverdin/bilindiones have a longer path of conjugation, which is manifested in the absorption spectra. The classic biliverdin example is biliverdin IXα (**20**), derived, like bilirubin IXα, by oxidation of the heme ligand at the α-position (Scheme 1). The absorption spectra of nine biliverdins/bilindiones (**20–25** and **28–30**) are similar with each other. Each exhibits two bands, in the regions ~370 and ~650 nm, with an intensity ratio of ~3:1 (Fig. 1, panel B1). Etiobiliverdin has been characterized in three isomeric forms (**25–27**) depending on the configuration of two of the three carbon-carbon double bonds that encompass the 5-, 10-, and 15-methine carbons and bridge the pyrrolic and pyrrolinone units. The effect of steric configurations of the double bonds (*E/Z*) are compared for the three isomers (Fig. 1, panel B2). The absorption maxima shift hypsochromically in the series *ZZZ*-isomer **25** (λ_{max} = 635 nm) to the *EZZ*-isomer **26** (λ_{max} = 598 nm) to the *EZE*-isomer **27** (λ_{max} = 571 nm). The consequences of conformational distortion on absorption spectra are described in the landmark book by Falk [2]. In a similar manner, the absorption maxima shift hypsochromically in going from the *ZZZ*-isomer **30** (λ_{max} = 650 nm) to the *EZZ*-isomer **31** (λ_{max} = 605 nm) (not shown).

Several meso-substituted bilindiones have been prepared and characterized. The absorption spectra of meso-substituted bilindiones **32–35** are compared with that of the corresponding parent bilindione **24** (Fig. 1, panel B3). Introduction of the 10-isopropyl or 10-*tert*-butyl group (**33** or **34**) causes the bands at ~650 nm to be diminished due to the strong structural distortion [143]. The absorption maximum of the isopropyl-bilindione **33** shows a further hypsochromic shift due to tautomerization to the isopropyliden-biladiene-*ac*, where the double bond resides between the meso-carbon and the secondary carbon of the attached isopropyl moiety, affording four N–H protons rather than three for the tautomer shown [143]. Introduction of a 5-nitro substituent causes a profound hypsochromic shift (from **24**: λ_{max} = 650 nm to **32**: λ_{max} = 533 nm). The shift has been ascribed to the prevention of conjugation due to the bulkiness of meso-nitro substituent (alternatively, electronic perturbation due to resonance giving the dioxoimine moiety as a canonical form cannot be ruled out); regardless of origin, the absorption spectrum of **32** is somewhat similar to that of a tripyrrinone [106] as seen by the spectrum of **25** (Fig. 2). On the other hand, the absorption spectrum is relatively unchanged by the introduction of a 10-aryl substituent as observed for **35**.

Several so-called "stretched" bilindiones have been prepared wherein a large molecular entity spans the two propionic acid substituents, altering the conformation of the bilindione unit, or at least restricting the suite of possible conformations to a more limited set. The absorption spectra of *ZZZ*-isomer **36** and *EZE*-isomer **37** exhibit hypsochromic shifts compared to spectra of the unstretched parental compounds *ZZZ*-isomer **25** and *EZE*-isomer **27** (Fig. 1, panel B4) [177]. Strictly speaking, **36** and **37** are not "open-chain" tetrapyrroles; however, the spectra are listed herein because the tetrapyrrole chromophore remains an open-chain and the "stretching" unit is joined via non-conjugated, ester moities.

Methylation at one or more of the nitrogen atoms causes a hypsochromic shift in comparison with the parent compound. Thus, the peak maximum for the parent etiobiliverdin (**25**, λ_{max} = 636 nm) differs from that upon introduction of a single *N*-methyl group given by **38** (N^{24}-methyl, λ_{max} = 595 nm) and **40** (N^{23}-methyl, λ_{max} = 575 nm), as well as two *N*-methyl groups given by **41** (N^{21},N^{24}-dimethyl, λ_{max} = 585 nm) (Fig. 1, panel B5). The shifts are attributed to distortion of the

conjugation [130].

Once *N*-methyl groups are introduced and absorption spectra have been hypsochromically shifted, the effects of *Z*/*E* configuration are less pronounced. Thus, the absorption maxima of several isomers are relatively similar exemplified by the following: *ZZZ*-isomer **41** (λ_{max} = 585 nm), *EZZ*-isomer **42** (λ_{max} = 575 nm), and *EZE*-isomer **43** (λ_{max} = 570 nm) (Fig. 1, panel B6). In other words, the effects of different *Z*/*E* configurations and the presence of *N*-methyl groups are not additive.

The conversion of the carbonyl group of a pyrrolinone moiety in an *N*-methyl etiobiliverdin (from **38** and **39**) to a methoxypyrrole unit (**44** and **45**) causes a nominal effect on the resulting absorption spectra (Fig. 1, panel B7). Thus, **44** and **45** are 1-methoxybilin-19-ones (or *vice versa*, 19-methoxybilin-1-ones). One interpretation is that the pyrrolinone structure itself is better represented via resonance as an oxypyrrolenine unit, the latter isoelectronic with the chromophore irrevocably enforced by the introduction of the methoxy group.

The introduction of a carbonyl bridge between adjacent nitrogen atoms (N^{23} and N^{24}) in biliverdin **25** to form **46** causes a large hypsochromic shift (Fig. 1, panel B8) [105]. This result is in the opposite direction from the similar N^{21}–N^{22}, N^{23}–N^{24} carbonyl bridge modifications of bilirubin **13**, or even the methylene bridge across distal nitrogens N^{21}–N^{24} of bilirubin **12**, versus the parent etiobilirubin **11** as described in the previous section (Fig. 1, panel A5), which causes a bathochromic shift. The conjugation in a biliverdin is fundamentally different from that of a bilirubin, and distinct spectral effects are not surprising.

A more facile and more versatile approach to achieve bridging across nitrogen atoms in bilins is by metal coordination. The absorption spectra of metal complexes of bilindiones **47–52** are compared to the spectrum of the free base bilindione **24** (Fig. 1, panel B9). Metal chelation often imparts a substantial bathochromic shift. The magnitude of bathochromic shift of absorption maxima compared to free base bilindione **24** (λ_{max} = 650 nm) are nickel(II) **47** (λ_{max} = 678 nm) < palladium(II) **48** (λ_{max} = 724 nm) < manganese(III) **50** (λ_{max} = 749 nm) < iridium (III) **52** (λ_{max} = 906 nm). The absorption spectra of cobalt(III) complex **49** and iron(III) complex **51** are relatively unchanged compared to that of free base bilindione **24**. The free base bilindione contains three N–H units, which are replaced by M–N dative bonds upon metal (M) chelation. In the case of trivalent metals, no counterion is expected or observed. In the case of divalent metals, an accompanying anion is present; for the nickel(II) **47** and palladium(II) **48** chelates, the accompanying anion is triiodide. For the manganese(III) **50** and iron(III) **51**, apical coordination by one or two pyridine molecules, respectively, is observed.

There are occcasional structures described in the literature that are difficult to reconcile with the reported spectra. In one such instance, compound **53** is reported to be a mono-hydroxy mono-oxo bilin. In other words, a tautomer of bilindione **25**. The absorption spectrum assigned to structure **53** exhibits a hyperchromic and hypsochromic shift (to 615 nm) compared with that of **25** (λ_{max} = 635 nm). Further study is required to reconcile this apparent discrepancy. On the other hand, and more reasonably, the conversion of a pyrrolinone to a methoxypyrrole in **54**, where dipyrrinone – hydroxydipyrrin tautomerism (Chart 1) is not possible, causes a bathochromic shift of the absorption maximum, from 635 to 670 nm (Fig. 1, panel B10).

Complexation of a bilindione with a metal can induce bonding changes in the organic ligand. Thus, each metal complex **55–62** is displayed with the bilin moiety comprised of one oxo group and one hydroxy group along with the formal dianionic ligand and dicationic metal; the tautomerism to form one hydroxydipyrrin from the dipyrrinone is required for complementary coordination. The resulting ligand is best regarded as a bilatrienone. The metal-coordination complexes **55–62** exhibit absorption spectra that are sharp and bathochromically shifted versus that of the free base bilindione **25** (Fig. 1, panel B11). Very large bathochromic shits of absorption maxima are observed for chelates of manganese(II) (**58**, λ_{max} = 910 nm), cobalt(II) (**60**, λ_{max} = 823 nm), and thallium(III) (**62**, λ_{max} = 762 nm) compared to the free base bilindione **25** (λ_{max} = 635 nm). The position of the absorption maxima of zinc(II) complexes **55**, **56**, **59**, **61** varies depending on the nature of the peripheral substituents.

Cyano-substituted bilins **63–68** were prepared by treatment of verdohemes with cyanide, as reported by Balch and co-workers [158]. The installation of a single meso-cyano group generally causes a significant bathochromic shift. The absorption maxima of 10-cyanobilindione **63** (λ_{max} = 726 nm) and 1,5-dicyanobilatrienone **65** (λ_{max} = 778 nm) are considerably bathochromically shifted compared to that of the parent bilindione **24** (λ_{max} = 650 nm) (Fig. 1, panel B12). Similar results are observed for the absorption spectra of cyano-substituted zinc(II) bilatrienones **64–68**, wherein the absorption maxima are bathochromically shifted up to ~200 nm compared to that of the parent zinc(II) bilatrienone **55** (λ_{max} = 687 nm) (Fig. 1, panel B13). The zinc bilatrienones bear 10-cyano (**64**), 1,5-dicyano (**66**), 1,5,10-tricyano (**67**), and 1,10-dicyano (**68**) substituents.

Derivatives of bilindiones bearing various terminal substituents in lieu of one oxo moiety have been prepared and converted to the zinc(II) chelate. The replacement of the oxo group entails concomitant conversion of the pyrrolinone to the substituted pyrrolenine, affording the resulting bilatrienone. The substituents include methoxy (**59**, λ_{max} = 790 nm), *N,N*-dimethylamino (**69**, λ_{max} = 822 nm), methylthio (**70**, λ_{max} = 846 nm), and formyl (**71**, λ_{max} = 834 nm). Regardless of the disparate substituents, which range from potent electron-donating via resonance (*N,N*-dimethylamino) to strongly electron-withdrawing via induction (formyl), the spectra are quite similar with each other (Fig. 1, panel B14).

A free base formyl-substituted bilatrienone has been chelated with a variety of metals, including zinc(II), iron(II), cobalt(II), nickel(II), and copper(II), affording **71–75**, respectively. The resulting absorption spectra of the diverse metal complexes exhibit λ_{max} > 800 nm due to the dual effects of metalation and the presence of the 1-formyl substituent (Fig. 1, panel B15). For example, the absorption maximum of the zinc(II) chelate with the 1-formyl group **71** (834 nm) shows a bathochromic shift compared to that of the zinc(II) chelate with the 1-methoxy group **59** (790 nm).

Several core-modified bilindiones have been prepared and can be compared with the representative unmodified bilindione **25** (Fig. 1, panel B16). The installation of a pyridine ring in lieu of a pyrrole ring causes a large hypsochromic shift, from 636 nm (**25**) to 431 nm (**76**). The installation of a furan ring (**78**, λ_{max} = 551 nm) or thiophene ring (**79**, λ_{max} = 550 nm) also causes a hypsochromic shift. Balch and coworkers prepared a tripyrrinone bearing an appended pyridine-2,5-dione **77** as a palladium(II) complex [166], which exhibits NIR absorption (λ_{max} = 780 nm). The pyridine-2,5-dione was attached via a single carbon-carbon bond linkage, in effect replacing not only the terminal pyrrolinone unit but also the 5-methine carbon. Accordingly, the pyridyl nitrogen atom is in a 1,4-relationship with the N^{22} atom as opposed to the ordinary 1,5-relationship of N^{22} and N^{23} atoms in an unmodified bilindione (as in **25**).

Compound **80** derives from a bilindione to which two molecules of ethanol have been added, interrupting the conjugation across the length of the tetrapyrrole structure. Compound **80** can thus be regarded as a tripyrrinone with an appended, non-conjugated pyrrolinone unit. The absorption spectrum of **80** (λ_{max} = 556 nm) is similar to that of a free base tripyrrinone (Fig. 1, panel B17). Bilindione derivative **80** was isolated as an unexpected byproduct in the attempted halogenation of biliverdin **24** in chloroform, where the two added ethoxy groups originated from the use of ethanol as a stabilizer of the solvent chloroform [106]. Note that while the added ethanol for stabilization may only comprise 0.75% on a volume basis (7.5 mL of ethanol per liter), for example, such a fraction corresponds to 0.13 M [204], which is in considerable excess of the typical concentration of tetrapyrrole species in many cases. Compound **81** has a more explicit origin, arising from exposure of thallium(III) complex **62** to air and methanol [124].

Compound **81** can be regarded as a bilindione to which two molecules of methanol have been added, followed by stabilization of the hydroxypyrrolenine tautomer rather than the pyrrolinone tautomer in the thallium(III) chelate. The absorption spectrum of **81** (λ_{max} = 620 nm) is similar to that of a metal tripyrrinone. The structure and absorption spectrum of a free base tripyrrinone (**225**, λ_{max} = 326 and 569 nm, in ethanol) are shown in Fig. 2.

4.3. Extended bilindiones (82–98; panels C1–C4)

Most of the examples included in this category contain conjugated groups interjected between the two halves of the classic bilirubin (e.g., **1**) or biliverdin (e.g., **20**) molecules. The structures have been created for multiple basic science purposes, including to explore the interplay of structure variation, molecular conformation, and absorption properties.

Bilindione analogues wherein one or more alkynes replaces the central, 10-methylene (or 10-methine) have been prepared by Lightner and co-workers [169,194]. The absorption spectra of bis(dipyrrinone)s bridged with carbon-carbon triple bonds (1,2-ethyne or 1,4-butadiyne) **82–86** are compared to the spectrum of mesobiliverdin XIIIα DME (**23**) (Fig. 1, panel C1). Compounds **82–86** do not display an absorption band at ~650 nm, which is a characteristic spectral feature of bilindiones. Rather, their absorption spectra are ascribed to a dipyrrinone framework, e.g., xanthobilirubic acid (**223**) shown in Fig. 2, plus a bathochromic shift due to the presence of the ethyne unit. The absorption maxima of ethyne-bridged bis(dipyrrinone)s **82** and **83** appear at 516 and 499 nm, respectively. The bathochromic shift of the butadiyne-bridged bis(dipyrrinone)s is slightly weaker than that of the ethyne-bridged structures, with absorption maxima as follows: 470 nm (**84**), 457 nm (**85**), and 461 nm (**86**).

Chen and Falk synthesized a series of conjugation-elongated bilindiones, **87–91**, wherein an additional alkene is inserted in lieu of the central, 10-methine carbon [114–116]. The absorption spectra of **87–91** are overlayed with that of the parent bilindione **25** for comparison (Fig. 1, panel C2). The presence of the additional carbon-carbon double bond in **87** (λ_{max} = 533 nm) causes an unexpected hypsochromic shift of the absorption spectrum compared to that of **25** (λ_{max} = 636 nm). The hypsochromic shift is explained by twisting of the single bond bridging the two dipyrrinones, which causes dihedral deformation and thwarted conjugation [114]. The addition of one carbon atom in going from **87** (two-carbon bridge) to **88** (three-carbon bridge) resolves the configurational strain and enables a planar arrangement; accordingly, the absorption spectrum of **88** (λ_{max} = 820 nm) exhibits a profound bathochromic shift compared to that of **25**. The entirety of the bathochromic shift is attributed to the extended conjugation [115]. Partial rigidification of the π-system through use of a fused 6-membered ring in going from **88** to **89** imparts a hypsochromic shift (λ_{max} = 627 nm) compared to the absorption spectrum of **88** and affords a spectrum more similar to that of **25**. Incorporation of a squaric acid moiety in **90** should provide the same conjugation level as in **88**. The absorption maximum of **90** (λ_{max} = 760 nm) is not as bathochromically shifted compared with **88**, which is explained by charge interaction from the zwitterionic squaric acid [115]. Further addition of conjugation in **91**, which contains a four-carbon bridge, causes an extra bathochromic shift (λ_{max} = 844 nm) together with a hypochromic shift, and solvatochromism is observed. Molecular modeling of **90** suggested very few planar conformations [116]. These prominent examples illustrate that absorption spectral properties are not simply governed by the ostensible degree of conjugation, and steric factors need to be considered.

Compounds **92–94** each contain an additional pyrrolic unit and hence are pentapyrroles. Compound **92** can be regarded as a homologue of biliverdin, containing five pyrroles rather than the canonical four. Compounds **93** and **94** are derivatives of **92** derived by addition of one and two molecules of 2-mercaptoethanol, respectively, to the carbon(s) flanking the central pyrrole. Compound **93** effectively is comprised of a dipyrrinone and tripyrrinone, whereas **94** is comprised of two dipyrrinones and a lone pyrrole. The absorption spectra of pentapyrroles **92–94** are overlayed with the spectrum of the parent tetrapyrrole **25** for comparison (Fig. 1, panel C3). The absorption spectrum of **92** (λ_{max} = 725 nm) is bathochromically shifted and broadened compared to that of tetrapyrrole **25**. Due to the interruption of conjugation, the absorption spectrum of **93** (λ_{max} = 554 nm) resembles that of tripyrrinone **225**, and the absorption spectrum of **94** (λ_{max} = 394 nm) resembles that of dipyrrinone **223** (see Fig. 2).

Assorted bilindiones have been prepared that are sufficiently singular or exotic as to best be considered individually rather than within a systematic series. Such structures here are **95–98**, for which the absorption spectra are overlayed with that of the tetrapyrrole etiobiliverdin **25** for comparison (Fig. 1, panel C4). Compound **95** (λ_{max} = 445 nm) contains a direct carbon-carbon single-bond linkage between the two dipyrrinones – effectively an α,α-linked bis(dipyrrinone) – entailing loss of one double bond, which is reflected in a hypsochromic shift compared to that of **25**. Oxidation of diene **95**, which contains four N–H groups and two carbon-carbon double bonds, one in each dipyrrinone unit, resulted in formation of **96**, which contains three N–H groups and three carbon-carbon double bonds between pyrrolic units. The resulting absorption maximum (λ_{max} = 518 nm) is bathochromically shifted compared to that of **95**; however, the shift does not reach the long-wavelength position exhibited by the *ZZZ*-isomer **25** (λ_{max} = 635 nm) perhaps owing to the *ZEZ* configuration of **96** [142]. The absorption spectrum of homorubin **97**, which lacks conjugation between the two dipyrrinones because the linker is a saturated 1,2-ethane unit in lieu of the single 10-methylene, is almost identical to that of a lone dipyrrinone **223** (see Fig. 2). An extension of conjugation between the pyrrole and pyrrolinone rings in **98** (λ_{max} = 699 nm) causes a bathochromic shift of the absorption spectra compared to that of **25** [146].

4.4. Urobilins and related compounds (99–101; panel D1)

Compounds **99**–**101** are defined by two distinct structural features, a free base dipyrrin core to which are appended two pyrrolinone units without intervening conjugation. The absorption spectra of *d*-urobilin hydrochloride salt (**100**) and *l*-stercobilin hydrochloride salt (**101**) are almost identical, given that the chromophore is a dipyrrin structure (Fig. 1, panel D1). Protonated dipyrrins and metal-chelated dipyrrins generally afford sharp absorption bands, whereas free base dipyrrins tend to give a very broad absorption band [201,204,205]. The absorption spectrum of urobilin **99** exhibits a very broad band at short wavelength and a sharp band as a bathochromic shoulder [182]. The latter shoulder is coincident with the absorption band of **100** and **101**.

4.5. Phycocyanobilin and related compounds (102–131; panels E1–E9)

Phycocyanobilin (**102**) is a red, light-harvesting pigment found in cyanobacteria and some additional photosynthetic organisms. Phycocyanobilin (**102**) differs from biliverdin IXα (**20**) in the presence of an ethyl substituent rather than a vinyl substituent at position 18, and an exocyclic ethylidene moiety rather than a vinyl group at position 3. The exocyclic ethylidene group causes the terminal heterocycle to be a pyrrolidone. Phycocyanobilin and derivatives **102–104** each contains such a pyrrolidone unit, whereas in phycocyanobilin derivative **104** the exocyclic ethylidene group has been further derivatized by addition of an *N*-acetylcysteine methyl ester molecule. The absorption spectra of phycocyanobilin derivatives **102–105** (λ_{max} 590–610 nm) show a hypsochromic shift (~60 nm) of the main absorption band compared to that of biliverdin IXα DME (**21**, λ_{max} = 667 nm) due to the diminished conjugation, yet the absorption spectral pattern of biliverdins is generally retained (Fig. 1, panel E1).

Phycoerythrobilin (**106**) is a blue, light-harvesting pigment found in cyanobacteria and some additional photosynthetic organisms. Phycoerythrobilin (**106**) is an analogue of phycocyanobilin (**102**), differing in the presence of saturation at positions 15 and 16, and a vinyl group at

position 18 rather than an ethyl group. The diminished conjugation among tetrapyrrolic units causes the absorption spectra of phycoerythrobilin **106** (λ_{max} = 505 nm) and phycoerythrobilin dimethyl ester **107** (λ_{max} = 530 nm) to fall in between the absorption of dipyrrin **224** (λ_{max} = 446 nm) and that of tripyrrinone **225** (λ_{max} = 569 nm) (Fig. 1, panel E2 and Fig. 2). The core chromophore of the compound named isomesobiliviolin DME (**108**) is a tripyrrinone framework; thus, the absorption spectrum of **108** (λ_{max} = 565 nm) closely matches that of tripyrrinone **225**. Moss argues against usage of the term violin because of structural ambiguity, stating in a sly footnote deep within an otherwise dry tome on nomenclature [11] "*the violins are muted in these recommendations.*" The absorption spectra of the zinc(II) complexes **109** (λ_{max} = 583 nm), **110** (λ_{max} = 604 nm) and **111** (λ_{max} = 629 nm) are more narrow and bathochromically shifted compared to those of the free base counterparts **106–108** (Fig. 1, panel E3). It warrants mention that bilin pigments employed in biological light-harvesting are invariably housed in protein scaffolds, which can substantially alter the spectra and photophysics (vide infra).

Phycocyanorubin (**112**) and phytochromorubin (**113**) are analogues of bilirubins that each contains an exocyclic ethylidene bond [192]. Phycocyanorubin (**112**) is to phycocyanobilin (**102**) what bilirubin IXα (**1**) is to biliverdin IXα (**20**). Phytochromorubin (**113**) contains a 18-vinyl group whereas phycocyanorubin (**112**) contains a 18-ethyl group. The absorption spectra of **112** (λ_{max} = 416 nm) and **113** (λ_{max} = 442 nm) are hypsochromically shifted compared to that of bilirubin IXα **1** (λ_{max} = 451 nm) (Fig. 1, panel E4). Further reduction to saturate the 15,16-positions of phytochromorubin (**113**) gives phycoerythrorubin (**114**: λ_{max} = 358 nm), which causes an additional hypsochromic shift. In phytochromorubin (**113**), meso-position 10 is saturated. In phycoerythrorubin (**114**), meso-positions 10 and 15 are saturated.

Bilindione **115** contains a gem-dimethyl group at position 2. As such, the gem-dimethyl-substituted terminal heterocycle is a pyrrolidinone. A gem-dimethyl group locks in the saturation level in a manner that is resilient toward adventitious dehydrogenation as might occur upon routine handling [92]. A gem-dimethyl (or gem-dialkyl) group is found in a number of naturally occurring hydroporphyrins, including the well known cofactors cobalamin and F_{430}, and the lesser known tolyporphins and bonellin [206,207]. The conversion of the remaining pyrrolinone unit of **115** (λ_{max} = 582 nm) to a pyrrolenine, concomitant with the conversion of the carbonyl group to a methoxy group, gives **116** (λ_{max} = 616 nm). Conversion of the pyrrolidinone of **115** to a 1-pyrroline moiety gives **117** (λ_{max} = 673 nm). In both cases, the change in structure causes a bathochromic shift (Fig. 1, panel E5).

Falk and co-workers prepared an extensive series of synthetic phycocyanobilin analogues [121,132–136,139,140,144] Each compound **118–127** contains one gem-dimethyl group causing the terminal heterocycle to be a pyrrolidinone. In structures **118–125**, the gem-dimethyl group is at position 2 whereas in **126** and **127**, the gem-dimethyl group is at position 3. The location of the structural lock at position 3 or 2 appears inconsequential. On the other hand, the absorption spectra of the *EZZ*-isomers (**119**, **121**, and **123**) are hypsochromically shifted compared to those of the *ZZZ*-isomers (**115**, **118**, **120**, **122**, **126**, and **127**) (Fig. 1, panel E6).

The installation of an additional oxo group by oxidation of the 3-methylene group flanking the 2-gem-dimethyl group affords bilintriones **124** and **125**, where the oxo groups are located at positions 1, 3, and 19. The two bilintriones are isomers that differ with regard to the configuration about the double bond spanning positions 15 and 16. The absorption spectra of **124** (λ_{max} = 645 nm) and **125** (λ_{max} = 636 nm) exhibit a bathochromic shift compared to that of **127** (λ_{max} = 585 nm), which is a bilindione analogue (Fig. 1, panel E7).

The final group of structures in this set contain peripheral modifications. Compounds **128** and **131** are bilintriones with an annulation at positions 3 and 4 in the pyrrolidinone ring. Position 3 has proved versatile for elaboration. Compounds **115–121** each contain an acetic acid ester moiety attached to position 3; compounds **122** and **123** each contain an *N*-substituted acetamide moiety attached to position 3. Compounds **129** and **130** extend the latter examples: **129** is an analogue of **122** that bears a longer *N*-acetamide-substituted peptide chain; **130** contains an α,ε-linked lysine bridging the two propionic acid units via amide bonds, forming a macrolactam. The absorption spectra of **128–131** are overlayed with the spectrum of the benchmark compound **127** for comparison (Fig. 1, panel E8). The conjugation level of **129** and **130** is unchanged from that of **127** by the presence of the peripheral amide bonds; thus, the absorption spectra of **129** (λ_{max} = 595 nm) and **130** (λ_{max} = 563 nm) are similar to that of **127** (λ_{max} = 595 nm). Compound **127** contains the same chromophore of **129** and **130** but lacks the acetamide substituent entirely. On the other hand, the presence of a fused five-membered ring (2-pyrrolidone for **128** and γ-butyrolactone for **131**) spanning positions 3 and 4 causes diminished conjugation. As a result, the absorption spectra of **128** (λ_{max} = 536 nm) and **131** (λ_{max} = 545 nm) are hypsochromically shifted compared to that of **127**.

Compound **132** was separated as a side product upon β-methylation of a hexahydroporphyrin (a pyrrocorphinate) by Eschenmoser and coworkers [164]. Compound **132** contains two gem-dimethyl groups (positions 2 and 7) and an exocyclic ethylidene group at position 1; the ethylidene π-system can be regarded as effectively isoelectronic with an oxo group. The absorption spectra of **132** (λ_{max} = 547 nm) is similar to that of tripyrrinone **225** (Fig. 1, panel E9 and Fig. 2).

4.6. Biladiene derivatives (132–163; panels F1–F5)

The compounds in this group contain a bilene, biladiene, or bilatriene chromophore and furthermore lack 1,19-diones. Compounds **133–138**, **141** and **142** are *a,c*-biladienes. The absorption spectra are shown in Fig. 1, panel F1. The absorption spectra of free base biladienes **138** (λ_{max} = 441 nm) and **142** (λ_{max} = 425 nm) are similar to that of a single dipyrrin **224** (λ_{max} = 446 nm). The absorption maxima of biladiene salts **133–137**, **140**, and **141** (485–524 nm) are sharper and bathochromically shifted compared to those of corresponding free base species **138** and **142**. The absorption spectra of metal complexes of the biladienes (**139**, **140**, **143–146**) are similar to those of biladiene salts described above (Fig. 1, panel F2). Protonation and metal complexation have similar effects on the spectra of dipyrrins [204,205].

Compounds **147–150** are *b*-bilenes whereas **151** is an *a,b,c*-bilatriene. Compound **152** is an *a,b,c*-bilatriene with a lone alkylidene extension of the π-system. Bilenes **147–150** are either salts or metal complexes; thus, each resulting absorption spectrum exhibits a sharp band (λ_{max} = 498–524 nm) (Fig. 1, panel F3). The sharp band is typical of that observed for bis(dipyrrinato)metal complexes [201,204,205]. The bilatriene framework of salt **151** (λ_{max} = 724 nm) and free base **152** (λ_{max} = 774 nm) gives rise to the absorption band in the NIR region. Not surprisingly, the extended conjugation in **152** results in the most bathochromic absorption in this subset.

Compounds **153–156** are α,α-bidipyrrins synthesized by Bröring and co-workers [109]. The compounds contain two dipyrrins directly linked by a carbon-carbon single bond across the respective dipyrrin α-positions (i.e., the dipyrrin 9- and 11-positions were the 10-carbon present). The absorption spectra of bridged bidipyrrin **154** (λ_{max} = 565 nm) is significantly broader than that of corresponding **153** (λ_{max} = 590 nm) (Fig. 1, panel F4), which has been explained by the inaccessibility of a single minimum conformation due to restricted rotation. The absorption spectra of copper(II) complex **155** (only a partial spectral trace is available) and **156** exhibit a broad band in the NIR region.

Dundia and co-workers prepared a series of *a,c*-biladiene analogues **157–163** wherein the central, 10-methylene unit bridges each dipyrrin chromophore at a β-position (i.e, corresponding to the 8- and 12-positions in an ordinary *a,c*-biladiene) [121,153]. The absorption spectra of **157–163** (Fig. 1, panel F5) are similar to those of the ordinary, α,α-linked (i.e., 9,11-linked) analogues **133** and **138** (Fig. 1, panel F1), where each free base species **157–159** (λ_{max} = 420–463 nm) exhibits a

broad band, while each salt **160–163** (λ_{max} 479–504 nm**)** presents a sharp band.

4.7. Boron-difluoride complexes (164–170; panel G1)

The formation of difluoroboronato complexes of a dipyrrin originated with the pioneering work of Treibs and Kreuzer [208]. While the modern era of BODIPY chemistry chiefly focuses on dipyrrins given the desirable fluorescent properties of the dipyrrinato-borondifluoride complexes, analogous complexes have also been formed of bilins and derivatives. Compound **164** is a bilindione to which is complexed one difluoroboron unit, on the central dipyrrin moiety (i.e., spanning the "*b*" unit, linking the N^{22}–N^{23} atoms). Compounds **165–170** are bilins to which are complexed two difluoroboron units, one on each of the dipyrrin moieties (i.e., spanning the "*a*" and "*c*" units, linking the N^{21}–N^{22} and N^{23}–N^{24} atoms). Each bis(difluoroboron–dipyrrin) complex joined via pyrrolic α-positions **165–167** [186] or pyrrolic β-positions **168–170** [98] exhibits a typical sharp, BODIPY-type absorption band (Fig. 1, panel G1) [201]. The presence of an aryl group attached to the saturated 10-methylene site in **169** or **170** does not impart a noticeable change in absorption, as expected given the lack of conjugation at this position. On the other hand, the absorption spectrum of **164** (λ_{max} = 634 nm), the bilindione to which is complexed one difluoroboron unit across the "*b*" unit, shows a broad band (fwhm ~100 nm) with shape resembling that of BODIPY derivatives with extended conjugation [209].

4.8. Bilins derived from synthetic tetraarylporphyrins (171–203; panels H1–H6)

This section focuses on bilins derived from oxidative cleavage of meso-tetraarylporphyrins. The meso-tetraarylporphyrins were first reported by Rothemund in the 1930s, are readily synthesized [94], and have become workhorse molecules across chemistry, materials science, and the photosciences. Since the initial report of bilindiones derived from meso-tetraarylporphyrins in 1980 by Smith and co-workers [189], Mizutani and co-workers have made extensive contributions [95,159, 171,176,187,198]. The absorption spectra of bilindiones bearing diverse aryl substituents at the 5,10,15-positions **171–176** are rather similar with each other (Fig. 1, panel H1). The absorption spectra of meso-triaryl bilindiones **171–176**, which exhibit absorption maxima in the range 609–632 nm, are comparable to those of β-alkyl-substituted bilindiones **24**, **25**, **28–30** (636–650 nm) (Fig. 1, panel B1). The similarity implies that the presence of a full complement of meso-aryl or β-alkyl substituents have little effect on the general spectral features of bilindiones. The term "full complement" indicates each meso-position or each β-alkyl position is so substituted; in this case there is a 5,10,15-triarylbilindione or a 2,3,7,8,12,13,17,18-octaalkylbilindione. Compound **177** is an α,α-linked bis(dipyrrinone) that contains 5,15-diaryl substitution and no β-alkyl groups. The absorption spectrum of **177** is hypsochromically shifted with respect to that of **176**, although there are differences in the nature of the meso-aryl groups: *p*-chlorophenyl in **177** and *o*-methoxyphenyl in **176**. Analysis of additional compounds would be required to draw definitive conclusions about the role of structure and substituents in altering spectra for these distinct compounds.

Bilindiones **171–176** each contain three carbon-carbon double bonds linking the pyrrolic moieties. Compounds **178–181** differ in several significant ways from **171–176**. First, the terminal heterocycle is a pyrrole rather than a pyrrolinone; second, position 1 bears an aroyl group; and third, one molecule of water has been added to the pyrrolenine unit encompassing methine carbon 5. Alteration of the conjugation level from a triene (**171–176**: λ_{max} = 609–632 nm, Fig. 1, panel H1) to a diene (**178**, **180** and **181**; λ_{max} = 554–561 nm) causes an expected hypsochromic shift of the absorption maximum (Fig. 1, panel H2). Compounds **178–181** display a tripyrrinone chromophore that bears two meso-aryl substituents. The diene **178** (λ_{max} = 561 nm) is a *ZZZ*-isomer. The absorption spectrum of the *EZZ*-isomer diene **179** (λ_{max} = 527 nm) is further hypsochromically shifted (Fig. 1, panel H2).

Compound **182** is the zinc(II) chelate of **178**. The absorption maximum of the zinc(II) chelate **182** (λ_{max} = 627 nm) is bathochromically shifted compared to that of the free base **178** (λ_{max} = 561 nm) (Fig. 1, panel H3). Compound **183** is a reduction product of **178**. The relationship is most easily seen by visualizing a tautomer of **183** that contains a 1-benzoyl group and a saturated 5-methylene site. The tautomer of **183** (H and Ph at the 5-position) effectively contains the same chromophore as **178** (HO and Ph at the 5-position). The absorption spectra of **178** and **183** are almost identical with each other regardless of their distinct compositions and ostensibly distinct structures, suggesting the aforementioned tautomer is a likely contributor to the solution structure of **183**. Similarly, the absorption spectra of the respective zinc (II) complexes (**182** and **184**) are almost identical with each other. One possible coordination sphere for **184** is displayed in Chart 1; the actual coordination geometry is unclear given the requirement for a formal dianionic ligand to complement zinc(II) and the presence of three N–H units in the parent, free base ligand.

The formal oxidative scission of meso-tetraphenylporphyrin by addition of a molecule of oxygen across the bond between a meso-carbon and the α-pyrrolic position affords a free base open-chain tetrapyrrole that at the respective termini contains a pyrrolinone unit (19-oxo group) and a benzoylpyrrole (1-benzoyl group). The open-chain tetrapyrrole also contains a phenyl group at each of the 5-, 10-, and 15-positions. An appropriate term for the ligand is a bilatrienone. Compounds **185–188** are so derived and are chelated with zinc(II), magnesium(II), and copper(II), respectively. Each of the bilatrienone metal complexes exhibits a very broad band at ~800 nm (Fig. 1, panel H4).

Bilatrienones bearing three meso-aryl groups have been prepared that contain a wide variety of substituents at the 1-position (**190–200**). The 1-substituents range from methoxy, phenoxy, amino, alkyl or aryl amino, alkyl or aryl thio, alkylidenyl, and thionyl. The absorption spectra of **190–200** are overlayed with the absorption spectrum of bilindione **173** for comparison (Fig. 1, panel H5). The groups that impart a substantial extension of conjugation cause a bathochromic shift (**198**, λ_{max} = 706 nm; **199**, λ_{max} = 712 nm; **200**, λ_{max} = 723 nm) compared to that of bilindione **173** (λ_{max} = 628 nm). Comparison also can be made with bilatrienones **55–61** and companion spectra (Fig. 1, panel B11).

meso-Tetraarylporphyrins have been prepared from pyrroles that bear β,β'-annulated alkyl moieties. Such porphyrins tend to be structurally deformed due to the steric interactions of the flanking meso-aryl and β-alkyl groups [210]. Bilatrienones derived from such porphyrins (**201–203**) were prepared by Smith and co-workers [179]. Like compounds **185–189**, the bilatrienones bear 5,10,15-triphenyl groups and a 1-benzoyl group, but unlike **185–189**, also contain a full complement of β-alkyl substituents, namely a tetramethylene unit spanning each of the three β,β'-pyrrolic sites. The absorption spectra of the metal chelates show that the absorption band appears in the NIR region. The peak maxima include 752 nm for the zinc(II) chelate (**201**), 840 nm for the copper(II) chelate (**202**), and 804 nm for the nickel(II) chelate (**203**) (Fig. 1, panel H6).

4.9. Chlorophyll catabolites (204–213; panels I1–I3)

Chlorophylls are produced globally in gargantuan quantities yet until recently relatively little was known about the processes by which chlorophylls are degraded. The products in plants derived from chlorophyll *a*, termed phyllobilins, are derived by oxidative scission at the chlorophyll α-position. Some 73 native or native-derived phyllobilins have been identified over the past three decades, and the absorption spectra have been compiled in a database [17]. In this section, the absorption spectra of open-chain tetrapyrroles produced by scission of chlorophyll *a* at the δ-position are compared (Scheme 1).

The chlorophyll catabolites of interest here are referred to as

Table 2
Fluorescence spectra data for open-chain tetrapyrroles in the database.[a]

Cmpds	λ_{flu}	Φ_f	solvent	Ref
13	510	0.09	chloroform	[104]
101	534		dichloromethane	[150]
134	555	0.014	dichloromethane	[181]
163	510		chloroform	[97]
164	672	0.37[b]	xylene	[96]
165	571	0.99	tetrahydrofuran	[186]
166	581	0.77	tetrahydrofuran	[186]
167	598	0.96	tetrahydrofuran	[186]
168	559		benzene	[98]
169	556		benzene	[98]
170	556	0.85	benzene	[98]
212	612		dichloromethane	[156]
213	611		dichloromethane	[156]

[a] All spectral data were determined in solution at room temperature. [b]The Φ_f value was determined in ethanol.

luciferins. Compounds **204**–**211** each are pyrochlorophylls indicating loss of the carbomethoxy group at the 13^2-position of chlorophyll. The absorption spectra of *Krill luciferin* (**204**, λ_{max} = 386 nm) and *Dinoflagellate luciferin* (**205**, λ_{max} = 392 nm) match each other closely (Fig. 1, panel I1). Each contains a limited path of conjugation given the saturation at two of the three meso-carbons, as reflected in the absorption maxima in the near-UV region. Embedding a second carbonyl group in the five-membered, exocyclic ring (so called ring E) creates a 1,2-dione motif and causes a hypsochromic shift (**206**, λ_{max} = 348 nm) compared to that of *Dinoflagellate luciferin* (**205**, λ_{max} = 392 nm). The absorption spectrum of **209** (λ_{max} = 237 nm), where the addition of a hydroxy group further interrupts any conjugation, is similar to that of pyrrole (λ_{max} = 209 nm) [61].

The absorption spectra of **207** (λ_{max} = 633 nm) shows an immense bathochromic shift compared to that of *Krill luciferin* (**204**, λ_{max} = 386 nm) due to the presence of additional conjugation that encompasses two pyrrolic units (Fig. 1, panel I2). Further added conjugation (**208**, shoulder ~690 nm) to encompass three pyrrolic units causes a commensurably increased bathochromic shift and broadening of the absorption spectrum. The absorption spectra of **210** (λ_{max} = 567 and 587) and **211** (λ_{max} = 549 and 577) show bathochromic shifts compared to the spectrum of *Krill luciferin* (**204**); however, the shift is less extensive compared to the spectrum of **208**. The distinctions are attributed to the fact that compounds **210** and **211** each contain a hydrated vinyl group, which removes a significant auxochrome from the bilin chromophore.

Compounds **212** and **213** are derivatives of the red chlorophyll catabolite (RCC), which is a universal precursor to phyllobilins, and are mentioned here only for comparison purposes. The structures differ from RCC itself (see Scheme 1) in that both are pyro derivatives and both are *ZEZ*-isomers rather than the *ZZZ*-isomer presented by RCC. Furthermore, **212** contains a free propionic acid whereas **213** is a methyl ester thereof (**RCC-Me**) [156]. The absorption spectra of **212** and **213** are almost identical to that of RCC methyl ester (Fig. 1, panel I3). This observation is at odds with the features exhibited by bilindiones (Fig. 1, panel B2) and phycocyanobilins (Fig. 1, panel E1), wherein a substantial hypsochromic shift is observed due to the change in stereoconfiguration.

4.10. Knoevenagel enones (214–220; panel J1)

The total synthesis of native photosynthetic pigments has largely been neglected [206]. A program aimed at the total synthesis of native photosynthetic tetrapyrroles, including chlorophyll *a* and

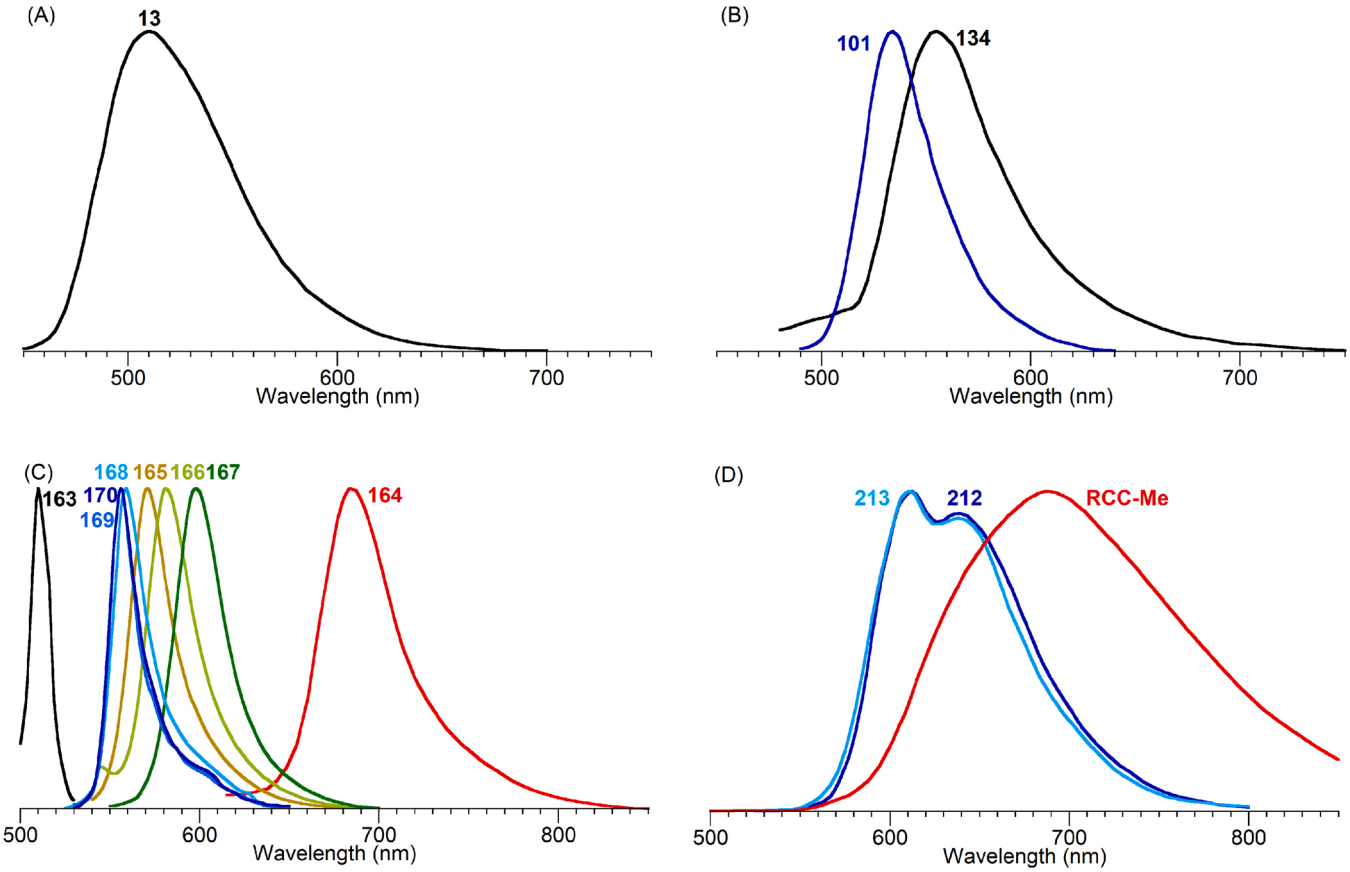

Fig. 4. Fluorescence spectra of open-chain tetrapyrroles in the database. The reader is referred to the text or original citations for solvent and other information. (A) Nitrogen-bridged bilirubin **13**. (B) *l*-Stercobilin hydrochloride (**101**) [150] and *a,c*-biladiene salt **134**. (C) Bis(difluoroboron–dipyrrin) complexes **165–170**. (D) RCC derivatives **212** and **213** as well as the methyl ester of the red chlorophyll catabolite (**RCC-Me**).

bacteriochlorophyll *a*, has yielded analogues of bilins as reaction intermediates. The intermediates are derived from Knoevenagel condensation of a dihydrodipyrrin-carboxaldehyde and a β-ketoester to which is attached a dihydrodipyrrin (for bacteriochlorophylls) or dipyrromethane (for chlorophylls). The products of the Knoevenagel condensation thus contain a propenone unit that links the two halves (**214–220**). Compounds **214–216** are synthetic precursors of chlorophyll analogues and contain a dihydrodipyrrin in conjugation with a propenone–dipyrromethane [38], whereas compounds **217–220** are precursors of bacteriochlorophyll analogues and contain two dihydrodipyrrins in conjugation with a propenone [37,39,40]. The absorption spectra of **214–220** show a visible band from 454 to 501 nm, and absorption in the UV region that is slightly different for the set **214–216** (band <300 nm) versus the set **217–220** (band ~319–339 nm) (Fig. 1, panel J1). Each member of the former set contains a formylpyrrole that is not conjugated with the dihydrodipyrrin-propenone pyrrole, whereas each member of the latter set contains a dimethoxymethyl (acetal) group attached to the terminus of one of the dihydrodipyrrin halves. While **214–220** are not bilins, the structures are similar, and the relatively facile synthesis of such compounds may open doors for comparative studies of reduced, open-chain tetrapyrroles.

5. Fluorescence spectra

The literature provides numerous examples of absorption spectra of compounds in the bilin family, as delineated in the prior sections. By contrast, the literature on fluorescence spectra of the same compounds is very sparse. At first glance, the contrast is astonishing. On further inspection, the reason for the dearth of fluorescence spectra has to do with the often, but not always, very low fluorescence yield of bilin compounds in solution. Here, we provide a necessarily short section on the fluorescence spectra and properties of members of the bilin family.

In general, "normal' open-chain tetrapyrroles are weakly fluorescent at room temperature. The metric for fluorescence intensity is the fluorescence quantum yield (Φ_f), which takes on values from 0 to 1. A Φ_f value of 1 indicates that for each photon absorbed, one photon is emitted as fluorescence. The Φ_f value of bilirubin **1** is $< 10^{-5}$ in Tris buffer at room temperature [211]. The Φ_f of bilirubin IXα DME (**6**) increases from 7.6×10^{-4} in ethanol at room temperature to 0.31 at 77 K in ethanol [162]. Metal chelation with "innocent" metal ions [2] generally increases the Φ_f value for bilins, as evidenced for biliverdin DME (**21**, $\Phi_f = 1.1 \times 10^{-4}$) [212] converted to zinc(II) biliverdin DME ($\Phi_f = 0.036$) [213]. The synthetic phycocyanobilin analogue **118** ($\Phi_f = 8 \times 10^{-4}$) is also weakly fluorescent [214].

Concerning the fluorescence of bilins, we harken back to the notion proffered over 80 years ago by Lewis and Calvin [215], who stated *"All of these groups that cause a rapid dissipation of the energy of electronic excitation, whether this is manifested by diminution of fluorescence or by diminution of structure, may be likened to loose bolts in some moving part of a machine. They provide a process by which the energy of the system is lost or degraded."* Conversely, one can understand the profound increase in fluorescence of bilins upon application of conditions – temperature, medium, or structural – that limit conformational motion. Said differently, the diminution of the rate constant for internal conversion (k_{ic}) upon restricted conformational motion causes a concomitant increase in excited-state lifetime (τ_s) and hence a commensurate increase in fluorescence quantum yield (Φ_f). The competition among photophysical processes is given by Eq. 1, which includes the rate constant for fluorescence (k_f) and intersystem crossing (k_{isc}) as well as that for internal conversion (k_{ic}). This simple heuristic – that constraining motion about a chromophore can increase the Φ_f – is as important today as it was in 1939 [215], and certainly helps to explain many cases of substances that exhibit aggregation-induced emission, which often stems from the same phenomenon of restricted motion.

$$\Phi_f = k_f / (k_{ic} + k_{isc} + k_f) = k_f \cdot \tau_s \quad (1)$$

The notion of restricted conformational motion of bilins leading to an increased Φ_f value has been described by Falk [2]. A further point germane to the fluorescence of bilins warrants mention: a compound with dim fluorescence (i.e., low value of Φ_f) can still be a potent photosensitizer, as long as the rate constant for the excited-state sensitization process is of significant magnitude relative to the sum of the other rate constants for depopulating the excited state [216]. The processes are competitive. In this regard, while the Φ_f value is often taken as a proxy for the excited-state lifetime, a low Φ_f value does not imply an impotent photosensitizer. For perspective, the benchmark molecules meso-tetraphenylporphyrin and zinc(II) meso-tetraphenylporphyrin exhibit a Φ_f value of 0.090 and 0.030, respectively [217]; such values are ostensibly low (or at least often regarded as low), but both compounds are valuable photoactive entities used across the photosciences.

The fluorescence spectral data for 13 open-chain tetrapyrroles are listed in Table 2. The table includes the wavelength of fluorescence maxima (λ_{flu}), Φ_f value if available, solvent for data collection, and literature citation. The compounds selected here have published fluorescence spectra (compounds **1**, **6**, **21**, and **118** mentioned above have reported Φ_f values but were not accompanied by published fluorescence spectra). The fluorescence spectral traces of the 15 open-chain tetrapyrroles are displayed in Fig. 4. The fluorescence spectra in Fig. 4 are

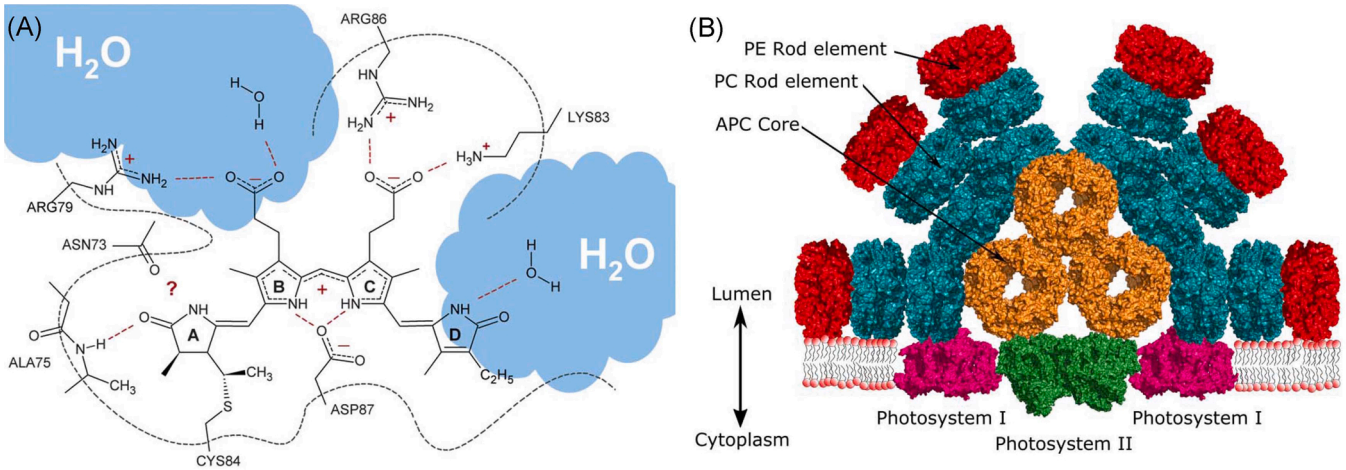

Fig. 5. (A) Structural rigidification of phycocyanobilin in the protein binding pocket of C-phycocyanin, one of the major biliproteins of phycobilisomes [223]. (B) Phycobilisome showing the pigment–proteins phycoerythrin (PE), phycocyanin (PC) and allophycocyanin (APC) [221].
(a) Adapted from Elgabarty. (b) Adapted from Saer and Blankenship.

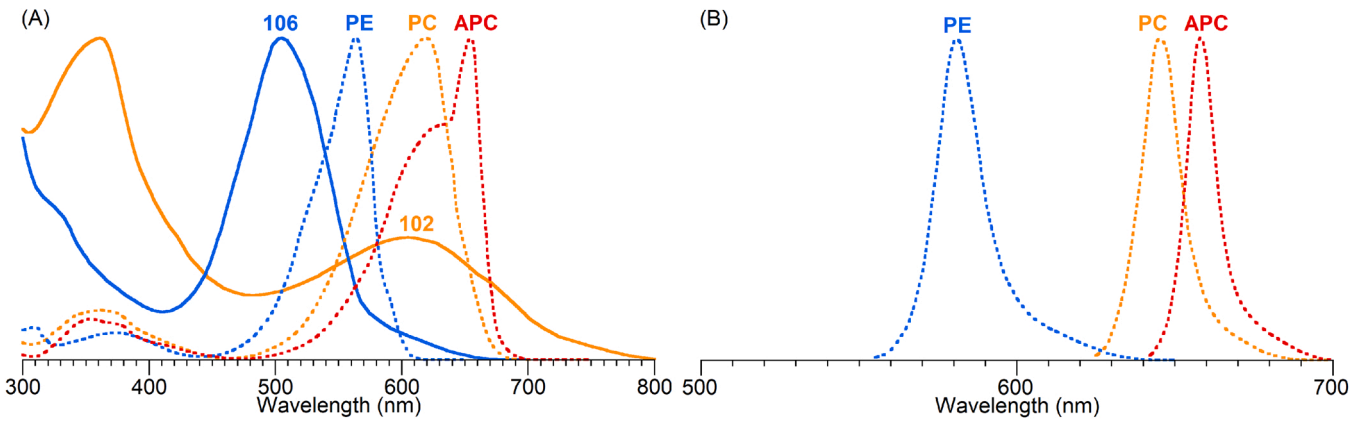

Fig. 6. (A) Absorption spectra of open-chain tetrapyrroles [phycoerythrobilin (**106**) and phycocyanobilin (**102**)] alone in solution and of biliproteins phycoerythrin (**PE**), phycocyanin (**PC**), and allophycocyanin (**APC**). (B) Fluorescence spectra of the biliproteins **PE**, **PC**, and **APC**.

normalized to unity. The reader should realize that the magnitude of fluorescence might vary.

We now briefly summarize key structural features for the compounds described in Table 2 and Fig. 4, as well as selected counterparts of the compounds.

- Compound **13**, a bilirubin derivative that bears carbonyl bridges between N^{21}–N^{22} and N^{23}–N^{24}, exhibits $\Phi_f = 0.09$ at room temperature [104] (Fig. 4, panel A). Similar intensification of fluorescence is observed for the nitrogen-β-pyrrole bridged bilirubins phorcarubin DME (**18**) and isophorcarubin DME (**19**), where the Φ_f value is 0.0015 and 0.04, respectively, in ethanol at room temperature [162].
- Compounds **101** (*l*-stercobilin hydrochloride) [150] and **134** (a diprotonated *a,c*-biladiene salt) [181] contain one or two protonated dipyrrin moieties, respectively (Fig. 4, panel B). Compound **134** exhibits $\Phi_f = 0.014$.
- The bilindione difluoroboron complex **164** ($\Phi_f = 0.37$) exhibits a broad fluorescence band and spectral shape similar to BODIPYs with extended conjugation [209] (Fig. 4, panel C).
- Each compound **165–170** is a bis(difluoroboron) complex of a biladiene and exhibits a sharp fluorescence band characteristic of typical BODIPYs and a value of Φ_f up to 0.99.
- A difluoroboron complex of an analogue of urobilin **100**, which is a bilene-*b* (i.e., contains a single dipyrrin chromophore), exhibits $\Phi_f = 0.57$, although the spectral trace is apparently not available [218].
- Now we turn to derivatives of the red chlorophyll catabolite (RCC), namely the methyl ester **RCC-Me** and **212** and **213**, all of which are phyllobilins. The fluorescence spectra of **212** and **213** in dichloromethane (with 1% methanol) are overlayed with that of **RCC-Me** in ethanol [156,219] for comparison (Fig. 4, panel D). While **212**, **213**, and **RCC-Me** exhibit nearly identical absorption spectra (Fig. 1, panel I3), the fluorescence spectra of **212** ($\lambda_{em} = 612$ nm) and **213** ($\lambda_{em} = 611$ nm) differ significantly from that of **RCC-Me** ($\lambda_{em} = 687$ nm, $\Phi_f = 0.036$). A reasonable number of fluorescence spectra of phyllobilins have been reported, albeit generally without information concerning Φ_f values [17]. Where data are available, phyllobilins exhibit moderate Φ_f values (e.g., phyllolumibilin exhibits $\Phi_f = 0.21$ in ethanol at room temperature [220]) compared to the puny emission of most bilirubins and biliverdins.

The larger values of Φ_f given by the above examples versus that typical of bilirubin alone can be attributed to rigidification of the molecular architecture (i.e., suppression of rotation that leads to an increase in internal conversion), in accord with the heuristic enunciated by Lewis and Calvin [215] and in accord with data assembled by Falk [2]. On the basis of the limited data available, it appears that rigidification of an open-chain tetrapyrrole by the mere presence of an exocyclic, five-membered ring (ring E of chlorophylls) contributes to an increased Φ_f value. Additional study is required to ensure that such a perspective is reflective of a large number of compounds and is not biased by a small number of positive reports on selected compounds.

To close, we return now to bilins, which lack the exocyclic, five-membered ring. Selected bilins are embedded as pigments in pigment-protein assemblies, known as phycobilisomes, that function as light-harvesting elements in phototropic bacteria [221,222]. The bilins include phycoerythrin (PE), phycocyanin (PC), and allophycocyanin (APC). Incorporation of the bilins in proteins imparts structural rigidification. One example, drawn chiefly from X-ray studies, is illustrated for phycocyanobilin in such a protein in Fig. 5 panel A [223]. Several features are noteworthy: (1) the open-chain tetrapyrrole is covalently bound by cysteine thiol addition to the vinyl group of ring A; (2) the dipyrrin unit (rings B and C) is protonated by an aspartate; (3) multiple hydrogen-bonds are extant with protein residues including lysine and arginine, as well as the alanine backbone. The structural rigidification results in a sharp absorption band relative to that in solution, where many conformations are available, and also a profound increase in Φ_f value in the biliprotein when measured apart from the rest of the phycobilisome architecture. Typical Φ_f values include the following: PE, 0.41–0.98 [224–226]; PC, 0.51–0.81 [224–226]; and APC, 0.68 [225].

A representative structure of a phycobilisome is shown in Fig. 5 panel B. The pigment-protein assemblies include phycoerythrin (PE) at the outer section of the rod, distal from the thylakoid membrane. Beneath the PE elements are phycocyanin (PC) elements. Beneath the PC elements are allophycocyanin (APC) elements at the core of the assembly. The flow of excitation energy following absorption of light is exceptionally rapid and essentially quantitative, in a downhill cascade, from PE to PC to APC constituents and on to the chlorophylls of photosystem II. The phycobilisomes are dynamic structures and can undergo alteration to accommodate different illumination conditions. The phycobilisomes serve to augment the light-harvesting capacity attained from chlorophylls alone [221,222].

The absorption spectra of selected open-chain tetrapyrroles and biliproteins [227,228] are compared in Fig. 6. Phycoerythrobilin (**106**) is the chromophore of the biliprotein PE, and phycocyanobilin (**102**) is the chromophore of the biliproteins PC and APC. The sharp absorption spectra upon incorporation in the protein assembly is profound and resembles that observed upon protonation or metal chelation of a dipyrrin or bilin containing a more extended π-system. The fluorescence bands of the biliproteins also are sharp. Such features are readily attributable to the rigidification, and perhaps protonation or hydrogen-bonding, of the bilin chromophore in the protein matrix. These examples illustrate the profound change of spectral and photophysical features that can be exercised upon incorporation of appropriate bilin chromophores in a suitable environment.

6. Outlook

The bile pigments may have had a lowly origin, identified as mere waste products, but members of the ever-increasing family of bilins have been found to occupy diverse roles in the life sciences. Constituents of bilins such as dipyrrins are now of central importance in fields that range from coordination chemistry to clinical diagnostics. The spectral database of open-chain tetrapyrroles described herein should support fundamental research concerning individual compounds as well as comparative studies among compounds. Of considerable interest is to gain a deeper understanding of the relationship between molecular structure and spectral properties, including the type of Aufbau-like progression outlined herein to visualize how increasing conjugation underpins a spectral progression. An understanding of the structure–spectra relationship of bilins provides a valuable juxtaposition for analogous phyllobilins, which differ in particular due to the presence of the fifth, exocyclic ring characteristic of photosynthetic tetrapyrroles. The present database of spectra for bilins in conjunction with the database for phyllobilins [17] should enable systematic comparisons and deepen understanding of these often-disregarded yet valuable members of the tetrapyrrole family.

Declaration of Competing Interest

The authors declare that they have no known competing financial interests or personal relationships that could have appeared to influence the work reported in this paper.

Data availability

All data are available at www.photochemcad.com for downloading at no cost.

Acknowledgements

This work was supported by the NSF (CHE-2054497).

References

[1] A.F. McDonagh, Bile pigments: Bilatrienes and 5,15-biladienes, in: D. Dolphin (Ed.), The Porphyrins, Vol. 6, Academic Press, New York, 1979, pp. 293–491, https://doi.org/10.1016/B978-0-12-220106-6.50013-9.
[2] H. Falk, The Chemistry of Linear Oligopyrroles and Bile Pigments, Springer-Verlag Wien, New York, 1989, https://doi.org/10.1007/978-3-7091-6938-4.
[3] S.E. Boiadjiev, D.A. Lightner, Optical activity and stereochemistry of linear oligopyrroles and bile pigments, Tetrahedron Asymm. 10 (1999) 607–655, https://doi.org/10.1016/S0957-4166(99)00037-3.
[4] N. Frankenberg, J.C. Lagarias, Biosynthesis and biological functions of bilins, in: K.M. Kadish, K.M. Smith, R. Guilard (Eds.), The Porphyrin Handbook, Vol. 13, Academic Press, San Diego, 2003, pp. 211–235, https://doi.org/10.1016/B978-0-08-092387-1.50013-8.
[5] A. Bennett, H.W. Siegelman, Bile pigments of plants, in: D. Dolphin (Ed.), The Porphyrins, Vol. 6, Academic Press, New York, 1979, pp. 493–520, https://doi.org/10.1016/B978-0-12-220106-6.50014-0.
[6] A.N. Glazer, Light guides: directional energy transfer in a photosynthetic antenna, J. Biol. Chem. 264 (1989) 1–4, https://doi.org/10.1016/S0021-9258(17)31212-7.
[7] G.J. Wedemayer, D.G. Kidd, A.N. Glazer, Cryptomonad biliproteins: bilin types and locations, Photosynth. Res. 48 (1996) 163–170, https://doi.org/10.1007/BF00041006.
[8] F. Pagels, A.C. Guedes, H.M. Amaro, A. Kijjoa, V. Vasconcelos, Phycobiliproteins from cyanobacteria: chemistry and biotechnological applications, Biotechnol. Adv. 37 (2019) 422–443, https://doi.org/10.1016/j.biotechadv.2019.02.010.
[9] R. Schmid, A.F. McDonagh, Formation and metabolism of bile pigments in vivo, in: D. Dolphin (Ed.), The Porphyrins, Vol. 6, Academic Press, New York, 1979, pp. 257–292, https://doi.org/10.1016/B978-0-12-220106-6.50012-7.
[10] P.R.O. De Montellano, K. Auclair, Heme oxygenase structure and mechanism, in: K.M. Kadish, K.M. Smith, R. Guilard (Eds.), The Porphyrin Handbook, Vol. 12, Academic Press, San Diego, 2003, pp. 183–210, https://doi.org/10.1016/B978-0-08-092386-4.50013-7.
[11] G.P. Moss, Nomenclature of tetrapyrroles (Recommendations 1986), Pure Appl. Chem. 59 (1987) 779–832, https://doi.org/10.1351/pac198759060779.
[12] H. Chakdar, S. Pabbi, Cyanobacterial phycobilins: production, purification, and regulation, in: P. Shukla (Ed.), Frontier Discoveries and Innovations in Interdisciplinary Microbiology, Springer India, New Delhi, India, 2015, pp. 45–69, https://doi.org/10.1007/978-81-322-2610-9_4.
[13] B. Ledermann, M. Aras, N. Frankenberg-Dinkel, Biosynthesis of cyanobacterial light-harvesting pigments and their assembly into phycobiliproteins, in: P. C. Hallenbeck (Ed.), Modern Topics in the Phototrophic Prokaryotes: Metabolism, Bioenergetics, and Omics, Springer International Publishing, Cham, Switzerland, 2017, pp. 305–340, https://doi.org/10.1007/978-3-319-51365-2_9.
[14] B. Kräutler, Chlorophyll breakdown and chlorophyll catabolites, in: K.M. Kadish, K.M. Smith, R. Guilard (Eds.), The Porphyrin Handbook, Vol. 13, Academic Press, San Diego, 2003, pp. 183–209, https://doi.org/10.1016/B978-0-08-092387-1.50012-6.
[15] A. Pérez-Gálvez, M. Roca, Phyllobilins: a new group of bioactive compounds, in: F.R.S. Atta-ur-Rahman (Ed.), Studies in Natural Products Chemistry, Vol. 52, Elsevier, Amsterdam, Netherlands, 2017, pp. 159–191, https://doi.org/10.1016/B978-0-444-63931-8.00004-7.
[16] P. Wang, C.A. Karg, N. Frey, J. Frädrich, A.M. Vollmar, S. Moser, Phyllobilins as a challenging diverse natural product class: exploration of pharmacological activities, Arch. Pharm. 354 (2021) 2100061, https://doi.org/10.1002/ardp.202100061.
[17] C.A. Karg, M. Taniguchi, J.S. Lindsey, S. Moser, Phyllobilins – Bioactive natural products derived from chlorophyll – Plant origins, structures, absorption spectra, and biomedical properties (in press), Planta Med. 88 (2022), https://doi.org/10.1055/a-1955-4624.
[18] H. Nakamura, Y. Kishi, O. Shimomura, D. Morse, J.W. Hastings, Structure of dinoflagellate luciferin and its enzymic and nonenzymic air-oxidation products, J. Am. Chem. Soc. 111 (1989) 7607–7611, https://doi.org/10.1021/ja00201a050.
[19] O. Shimomura, The roles of the two highly unstable components F and P involved in the bioluminescence of euphausiid shrimps, J. Biolumin. Chemilumin. 10 (1995) 91–101, https://doi.org/10.1002/bio.1170100205.
[20] H. Nakamura, B. Musicki, Y. Kishi, O. Shimomura, Structure of the light emitter in krill (*Euphausia pacifica*) bioluminescence, J. Am. Chem. Soc. 110 (1988) 2683–2685, https://doi.org/10.1021/ja00216a070.
[21] H. Nakamura, Y. Oba, A. Murai, Synthesis and absolute configuration of the ozonolysis product of krill fluorescent compound F, Tetrahedron Lett. 34 (1993) 2779–2782, https://doi.org/10.1016/S0040-4039(00)73560-X.
[22] A. Yamaguchi, T. Horiguchi, Culture of the heterotrophic dinoflagellate *Protoperidinium Crassipes* (dinophyceae) with noncellular food items, J. Phycol. 44 (2008) 1090–1092, https://doi.org/10.1111/j.1529-8817.2008.00547.x.
[23] J. Janouškovec, G.S. Gavelis, F. Burki, D. Dinh, T.R. Bachvaroff, S.G. Gornik, K. J. Bright, B. Imanian, S.L. Strom, C.F. Delwiche, R.F. Waller, R.A. Fensome, B. S. Leander, F.L. Rohwer, J.F. Saldarriaga, Major transitions in dinoflagellate evolution unveiled by phylotranscriptomics, Proc. Natl. Acad. Sci. U. S. A. 114 (2017) E171–E180, https://doi.org/10.1073/pnas.1614842114.
[24] E. Nagababu, J.M. Rifkind, Heme degradation by reactive oxygen species, Antioxid. Redox Signal 6 (2004) 967–978, https://doi.org/10.1089/ars.2004.6.967.
[25] G.A.F. Hendry, J.D. Houghton, S.B. Brown, The degradation of chlorophyll – A biological enigma, N. Phytol. 107 (1987) 255–302, https://doi.org/10.1111/j.1469-8137.1987.tb00181.x.
[26] K. Inomata, Studies on the structure and function of phytochromes as photoreceptors based on synthetic organic chemistry, Bull. Chem. Soc. Jpn. 81 (2008) 25–59, https://doi.org/10.1246/bcsj.81.25.
[27] D.A. Lightner, Derivatives of bile pigments, in: D. Dolphin (Ed.), The Porphyrins, Vol. 6, Academic Press, New York, 1979, pp. 521–584, https://doi.org/10.1016/B978-0-12-220106-6.50015-2.
[28] A. Gossauer, H. Plieninger, Synthesis, purification, and characterization of bile pigments and related compounds, in: D. Dolphin (Ed.), The Porphyrins, Vol. 6, Academic Press, New York, 1979, pp. 586–650, https://doi.org/10.1016/B978-0-12-220106-6.50016-4.
[29] A. Gossauer, Synthesis of bilins, in: K.M. Kadish, K.M. Smith, R. Guilard (Eds.), The Porphyrin Handbook, Vol. 13, Academic Press, San Diego, 2003, pp. 237–274, https://doi.org/10.1016/B978-0-08-092387-1.50014-X.
[30] A.L. Balch, F.L. Bowles, Coordination chemistry of verdohemes and open-chain oligopyrrole systems involved in heme oxidation and porphyrin destruction, in: K. M. Kadish, K.M. Smith, R. Guilard (Eds.), Handbook of Porphyrin Science, Vol. 8, World Scientific, Singapore, 2010, pp. 293–342, https://doi.org/10.1142/9789814307246_0012.
[31] M. Bröring, Beyond dipyrrins: Coordination interactions and templated macrocyclizations of open-chain oligopyrroles, in: K.M. Kadish, K.M. Smith, R. Guilard (Eds.), Handbook of Porphyrin Science, Vol. 8, World Scientific, Singapore, 2010, pp. 343–501, https://doi.org/10.1142/9789814307246_0013.
[32] A.W. Johnson, Synthesis of porphyrins from 1,19-dideoxybiladienes-*ac* and 1,19-dideoxybilenes-*b*, in: D. Dolphin (Ed.), The Porphyrins, Vol. 1, Academic Press, New York, 1978, pp. 235–264, https://doi.org/10.1016/B978-0-12-220101-1.50012-3.
[33] P.S. Clezy, A.H. Jackson, Synthesis of porphyrins from oxobilane intermediates, in: D. Dolphin (Ed.), The Porphyrins, Vol. 1, Academic Press, New York, 1978, pp. 265–288, https://doi.org/10.1016/B978-0-12-220101-1.50013-5.
[34] K.M. Smith, Strategies for the synthesis of octaalkylporphyrins, in: K.M. Kadish, K.M. Smith, R. Guilard (Eds.), The Porphyrin Handbook, 1, Academic Press, San Diego, 2000, pp. 1–43.
[35] D.K. Dogutan, S.H.H. Zaidi, P. Thamyongkit, J.S. Lindsey, New route to ABCD-porphyrins via bilanes, J. Org. Chem. 72 (2007) 7701–7714, https://doi.org/10.1021/jo701294d.

[36] D.K. Dogutan, J.S. Lindsey, Investigation of the scope of a new route to ABCD-bilanes and ABCD-porphyrins, J. Org. Chem. 73 (2008) 6728–6742, https://doi.org/10.1021/jo8010396.
[37] S. Zhang, J.S. Lindsey, Construction of the bacteriochlorin macrocycle with concomitant Nazarov cyclization to form the annulated isocyclic ring: Analogues of bacteriochlorophyll *a*, J. Org. Chem. 82 (2017) 2489–2504, https://doi.org/10.1021/acs.joc.6b02878.
[38] P. Wang, F. Lu, J.S. Lindsey, Use of the nascent isocyclic ring to anchor assembly of the full skeleton of model chlorophylls, J. Org. Chem. 85 (2020) 702–715, https://doi.org/10.1021/acs.joc.9b02770.
[39] K.C. Nguyen, P. Wang, R.D. Sommer, J.S. Lindsey, Asymmetric synthesis of a bacteriochlorophyll model compound containing *trans*-dialkyl substituents in ring D, J. Org. Chem. 85 (2020) 6605–6619, https://doi.org/10.1021/acs.joc.0c00608.
[40] D.T.M. Chung, P.V. Tran, K. Chau Nguyen, P. Wang, J.S. Lindsey, Synthesis of model bacteriochlorophylls containing substituents of native rings A, C and E, New J. Chem. 45 (2021) 13302–13316, https://doi.org/10.1039/D1NJ02469H.
[41] N.C. Rockwell, J.C. Lagarias, A brief history of phytochromes, ChemPhysChem 11 (2010) 1172–1180, https://doi.org/10.1002/cphc.200900894.
[42] R.M. Kilner, The evolution of egg colour and patterning in birds, Biol. Rev. 81 (2006) 383–406, https://doi.org/10.1017/S1464793106007044.
[43] R. Hamchand, D. Hanley, R.O. Prum, C. Brückner, Expanding the eggshell colour gamut: Uroerythrin and bilirubin from Tinamou (*Tinamidae*) eggshells, Sci. Rep. 10 (2020) 11264, https://doi.org/10.1038/s41598-020-68070-7.
[44] S.T. Williams, Molluscan shell colour, Biol. Rev. 92 (2017) 1039–1058, https://doi.org/10.1111/brv.12268.
[45] M.M. Gagnon, Serum biliverdin as source of colouration upon sexual maturation in male blue-throated wrasse *Notolabrus tetricus*, J. Fish. Biol. 68 (2006) 1879–1882, https://doi.org/10.1111/j.0022-1112.2006.01033.x.
[46] A. Yamanaka, T. Ito, D. Koga, T. Sato, M. Ochiai, K. Endo, Purification and characterization of biliverdin-binding protein from larval hemolymph of the swallowtail butterfly, *Papilio xuthus* L, Biosci. Biotechnol. Biochem. 64 (2000) 1978–1981, https://doi.org/10.1271/bbb.64.1978.
[47] L. Jespersen, L.D. Strømdahl, K. Olsen, L.H. Skibsted, Heat and light stability of three natural blue colorants for use in confectionery and beverages, Eur. Food Res. Technol. 220 (2005) 261–266, https://doi.org/10.1007/s00217-004-1062-7.
[48] S.Y. Byeon, M.K. Cho, K.H. Shim, H.J. Kim, H.G. Song, H.S. Shin, Development of a *Spirulina* extract/alginate-imbedded PCL nanofibrous cosmetic patch, J. Microbiol. Biotechnol. 27 (2017) 1657–1663, https://doi.org/10.4014/jmb.1701.01025.
[49] S.A. Adli, F. Ali, A.S. Azmi, H. Anuar, N.A.M. Nasir, R. Hasham, M.K.H. Idris, Development of biodegradable cosmetic patch using a polylactic acid/phycocyanin–alginate composite, Polymers 12 (2020) 1669, https://doi.org/10.3390/polym12081669.
[50] Y. Zhang, H. Liu, X. Dai, H. Li, X. Zhou, S. Chen, J. Zhang, X.-J. Liang, Z. Li, Cyanobacteria-based near-infrared light-excited self-supplying oxygen system for enhanced photodynamic therapy of hypoxic tumors, Nano Res. 14 (2021) 667–673, https://doi.org/10.1007/s12274-020-3094-0.
[51] H. Keum, D. Yoo, S. Jon, Photomedicine based on heme-derived compounds, Adv. Drug Deliv. Rev. 182 (2022), 114134, https://doi.org/10.1016/j.addr.2022.114134.
[52] S. Sekar, M. Chandramohan, Phycobiliproteins as a commodity: trends in applied research, patents and commercialization, J. Appl. Phycol. 20 (2008) 113–136, https://doi.org/10.1007/s10811-007-9188-1.
[53] W. Li, Y. Pu, B. Ge, Y. Wang, D. Yu, S. Qin, Dye-sensitized solar cells based on natural and artificial phycobiliproteins to capture low light underwater, Int. J. Hydrog. Energy 44 (2019) 1182–1191, https://doi.org/10.1016/j.ijhydene.2018.10.176.
[54] F.-L. Xing, Z.-H. Zhang, C.-L. Yang, M.-S. Wang, X.-G. Ma, Phycoerythrobilin/phycourobilin as efficient sensitizers of dye-sensitized solar cell, Sol. Energy 243 (2022) 494–499, https://doi.org/10.1016/j.solener.2022.08.028.
[55] E.A. Rodriguez, G.N. Tran, L.A. Gross, J.L. Crisp, X. Shu, J.Y. Lin, R.Y. Tsien, A far-red fluorescent protein evolved from a cyanobacterial phycobiliprotein, Nat. Methods 13 (2016) 763–769, https://doi.org/10.1038/nmeth.3935.
[56] K. Fushimi, T. Miyazaki, Y. Kuwasaki, T. Nakajima, T. Yamamoto, K. Suzuki, Y. Ueda, K. Miyake, Y. Takeda, J.-H. Choi, H. Kawagishi, E.Y. Park, M. Ikeuchi, M. Sato, R. Narikawa, Rational conversion of chromophore selectivity of cyanobacteriochromes to accept mammalian intrinsic biliverdin, Proc. Natl. Acad. Sci. U. S. A. 116 (2019) 8301–8309, https://doi.org/10.1073/pnas.1818836116.
[57] Y. Uda, H. Miura, Y. Goto, K. Yamamoto, Y. Mii, Y. Kondo, S. Takada, K. Aoki, Improvement of phycocyanobilin synthesis for genetically encoded phytochrome-based opto-genetics, ACS Chem. Biol. 15 (2020) 2896–2906, https://doi.org/10.1021/acschembio.0c00477.
[58] K. Fushimi, R. Narikawa, Phytochromes and cyanobacteriochromes: Photoreceptor molecules incorporating a linear tetrapyrrole chromophore, in: H. Yawo, H. Kandori, A. Koizumi, R. Kageyama (Eds.), Opto-genetics: Light-Sensing Proteins and Their Applications in Neuroscience and Beyond, Springer Nature, Singapore, 2021, pp. 167–187, https://doi.org/10.1007/978-981-15-8763-4_10.
[59] S.E. Braslavsky, A.R. Holzwarth, K. Schaffner, Solution conformations, photophysics, and photochemistry of bile pigments; bilirubin and biliverdin, dimethyl esters and related linear tetrapyrroles, in: Angew. Chem. Int. Ed. Engl, 22, 1983, pp. 656–674, https://doi.org/10.1002/anie.198306561.
[60] M. Taniguchi, H. Du, J.S. Lindsey, PhotochemCAD 3: diverse modules for photophysical calculations with multiple spectral databases, Photochem. Photobiol. 94 (2018) 277–289, https://doi.org/10.1111/php.12862.
[61] M. Taniguchi, J.S. Lindsey, Database of absorption and fluorescence spectra of >300 common compounds for use in PhotochemCAD, Photochem. Photobiol. 94 (2018) 290–327, https://doi.org/10.1111/php.12860.
[62] M. Taniguchi, J.S. Lindsey, Absorption and fluorescence spectral database of chlorophylls and analogues, Photochem. Photobiol. 97 (2021) 136–165, https://doi.org/10.1111/php.13319.
[63] M. Taniguchi, D.F. Bocian, D. Holten, J.S. Lindsey, Beyond green with synthetic chlorophylls – Connecting structural features with spectral properties, J. Photochem. Photobiol. C: Photochem. Rev. 52 (2022), 100513, https://doi.org/10.1016/j.jphotochemrev.2022.100513.
[64] T.J. O'Donnell, J.R. Gurr, J. Dai, M. Taniguchi, P.G. Williams, J.S. Lindsey, Tolyporphins A–R, unusual tetrapyrrole macrocycles in a cyanobacterium from Micronesia, assessed quantitatively from the culture HT-58-2, New J. Chem. 45 (2021) 11481–11494, https://doi.org/10.1039/D1NJ02108G.
[65] M. Taniguchi, C.A. LaRocca, J.D. Bernat, J.S. Lindsey, Digital database of absorption spectra of diverse flavonoids enables structural comparisons and quantitative evaluations, J. Nat. Prod 86 (2023) 1087–1119, https://doi.org/10.1021/acs.jnatprod.2c00720.
[66] Y. Guo, Z. Xu, A.E. Norcross, M. Taniguchi, J.S. Lindsey, Developing a user community in the photosciences: a website for spectral data and PhotochemCAD, Proc. S. P. I. E. BiOS 10893 (2019) 108930O, https://doi.org/10.1117/12.2508077.
[67] Z. Wu, A. Kittinger, A.E. Norcross, M. Taniguchi, J.S. Lindsey, PhotochemCAD spectra viewer for web-based visualization of absorption and fluorescence spectra, Proc. S. P. I. E. BiOS 11660 (2021) 116600I, https://doi.org/10.1117/12.2577840.
[68] M. Taniguchi, J.S. Lindsey, Absorption and fluorescence spectra of organic compounds from 40 sources – archives, repositories, databases, and literature search engines, Proc. S. P. I. E. BiOS 11256 (2020) 112560J, https://doi.org/10.1117/12.2542859.
[69] M. Taniguchi, G. Hu, R. Liu, H. Du, J.S. Lindsey, Red and near-infrared fluorophores inspired by chlorophylls: Consideration of practical brightness in multicolor flow cytometry and biomedical sciences, Proc. S. P. I. E. BiOS 10508 (2018) 1050806, https://doi.org/10.1117/12.2302709.
[70] Q. Qi, M. Taniguchi, J.S. Lindsey, Heuristics from modeling of spectral overlap in Förster resonance energy transfer (FRET), J. Chem. Inf. Model. 59 (2019) 652–667, https://doi.org/10.1021/acs.jcim.8b00753.
[71] F. Wang, S. Sen, C. Chen, S. Bähring, C. Lei, Z. Duan, Z. Zhang, J.L. Sessler, A. Jana, Self-assembled cagelike receptor that binds biologically relevant dicarboxylic acids via proton-coupled anion recognition, J. Am. Chem. Soc. 142 (2020) 1987–1994, https://doi.org/10.1021/jacs.9b11566.
[72] F. Wang, K. Liang, M.C. Larsen, S. Bähring, M. Ishida, H. Furuta, A. Jana, Solvent-controlled self-assembled oligopyrrolic receptor, Molecules 26 (2021) 1771, https://doi.org/10.3390/molecules26061771.
[73] E. Tomat, C.J. Curtis, Biopyrrin pigments: from heme metabolites to redox-active ligands and luminescent radicals, Acc. Chem. Res. 54 (2021) 4584–4594, https://doi.org/10.1021/acs.accounts.1c00613.
[74] T.E. Wood, N.D. Dalgleish, E.D. Power, A. Thompson, X. Chen, Y. Okamoto, Stereochemically stable double-helicate dinuclear complexes of bis(dipyrromethene)s: A chiroptical study, J. Am. Chem. Soc. 127 (2005) 5740–5741, https://doi.org/10.1021/ja0500613.
[75] S. Saito, K. Furukawa, A. Osuka, Fully π-conjugated helices from oxidative cleavage of *meso*-aryl-substituted expanded porphyrins, J. Am. Chem. Soc. 132 (2010) 2128–2129, https://doi.org/10.1021/ja909929s.
[76] Z. Zhang, D. Dolphin, Synthesis of triple-stranded complexes using bis(dipyrromethene) ligands, Inorg. Chem. 49 (2010) 11550–11555, https://doi.org/10.1021/ic101694z.
[77] K. Yamanishi, M. Miyazawa, T. Yairi, S. Sakai, N. Nishina, Y. Kobori, M. Kondo, F. Uchida, Conversion of cobalt(II) porphyrin into a helical cobalt(III) complex of acyclic pentapyrrole, Angew. Chem. Int. Ed. 50 (2011) 6583–6586, https://doi.org/10.1002/anie.201102144.
[78] H. Maeda, T. Nishimura, R. Akuta, K. Takaishi, M. Uchiyama, A. Muranaka, Two double helical modes of bidipyrrin–Zn^{II} complexes, Chem. Sci. 4 (2013) 1204–1211, https://doi.org/10.1039/c2sc21913a.
[79] E.V. Antina, R.T. Kuznetsova, L.A. Antina, G.B. Guseva, N.A. Dudina, A. I. V'yugin, A.V. Solomonov, New luminophors based on the binuclear helicates of *d*-METALS with BIS(DIPYRRIN)S, Dyes Pigm. 113 (2015) 664–674, https://doi.org/10.1016/j.dyepig.2014.10.002.
[80] J. Kong, Q. Li, M. Li, X. Li, X. Liang, W. Zhu, H. Ågren, Y. Xie, Modulation of the structures and properties of bidipyrrin zinc complexes by introducing terminal α-methoxy groups, Dyes Pigm. 137 (2017) 430–436, https://doi.org/10.1016/j.dyepig.2016.10.038.
[81] A.A. Ksenofontov, E.V. Antina, G.B. Guseva, M.B. Berezin, L.A. Antina, A. I. Vyugin, Prospects of applications of fluorescent sensors based on zinc(II) and boron(III) bis(dipyrromethenate)s, J. Mol. Liq. 274 (2019) 681–689, https://doi.org/10.1016/j.molliq.2018.11.025.
[82] C. Eerdun, T.H.T. Nguyen, T. Okayama, S. Hisanaga, J. Setsune, Conformational changes and redox properties of bimetallic single helicates of hexapyrrole-α,ω-dicarbaldehydes, Chem. Eur. J. 25 (2019) 5777–5786, https://doi.org/10.1002/chem.201900353.
[83] K. Kupietz, M.J. Białek, K. Hassa, A. Białońska, L. Latos-Grażyński, Oxygenation of phenanthriporphyrin and copper(III) phenanthriporphyrin: an efficient route

to phenanthribilinones, Inorg. Chem. 58 (2019) 12446–12456, https://doi.org/10.1021/acs.inorgchem.9b02183.
[84] F. Zhang, A. Fluck, S.A. Baudron, M.W. Hosseini, Strapping a benzaldehyde-appended 2,2′-bis-dipyrrin Zn(II) double-stranded helicate using imine bond formation, Dalton Trans. 48 (2019) 4105–4108, https://doi.org/10.1039/C9DT00377K.
[85] E.V. Antina, N.A. Bumagina, M.B. Berezin, Bis(dipyrromethene)s as a new class of highly efficient chromo-fluorogenic ligands, Dyes Pigm. 195 (2021), 109656, https://doi.org/10.1016/j.dyepig.2021.109656.
[86] Ç. Baş, F. Doettinger, N. Klein, S. Tschierlei, M. Bröring, Pyrrolyl-appended zinc porphodimethenes: branched oligopyrrole products from the templated one-pot isoporphyrin synthesis, Eur. J. Inorg. Chem. 2021 (2021) 3239–3246, https://doi.org/10.1002/ejic.202100472.
[87] S. Panchavarnam, P. Pushpanandan, M. Ravikanth, Synthesis, structure, and properties of helical bis-Cu(II) complex of linear hexapyrrolic ligand, Inorg. Chem. 61 (2022) 1562–1570, https://doi.org/10.1021/acs.inorgchem.1c03329.
[88] N. Sakamoto, C. Ikeda, M. Yamamura, T. Nabeshima, α-Bridged BODIPY oligomers with switchable near-IR photoproperties by external-stimuli-induced foldamer formation and disruption, Chem. Commun. 48 (2012) 4818–4820, https://doi.org/10.1039/c2cc17513d.
[89] D. Taguchi, T. Nakamura, H. Horiuchi, M. Saikawa, T. Nabeshima, Synthesis and unique optical properties of selenophenyl BODIPYs and their linear oligomers, J. Org. Chem. 83 (2018) 5331–5337, https://doi.org/10.1021/acs.joc.8b00782.
[90] A. Rohatgi, WebPlotDigitizer version 4.6. (2019) ⟨https://automeris.io/WebPlotDigitizer⟩ (retrieved December 7, 2022).
[91] R.B. Fox, W.H. Powell. Nomenclature of Organic Compounds – Principles and Practice, 2nd ed.,, Oxford University Press, Oxford, 2001, pp. 16–17.
[92] J.S. Lindsey, De novo synthesis of gem-dialkyl chlorophyll analogues for probing and emulating our green world, Chem. Rev. 115 (2015) 6534–6620, https://doi.org/10.1021/acs.chemrev.5b00065.
[93] M. Taniguchi, J.S. Lindsey, Synthetic chlorins, possible surrogates for chlorophylls, prepared by derivatization of porphyrins, Chem. Rev. 117 (2017) 344–535, https://doi.org/10.1021/acs.chemrev.5b00696.
[94] J.S. Lindsey, Synthesis of meso-substituted porphyrins, in: K.M. Kadish, K. M. Smith, R. Guilard (Eds.), The Porphyrin Handbook, Vol. 1, Academic Press, San Diego, 2000, pp. 45–118.
[95] H. Akasaka, H. Yukutake, Y. Nagata, T. Funabiki, T. Mizutani, H. Takagi, Y. Fukushima, L.R. Juneja, H. Nanbu, K. Kitahata, Selective adsorption of biladien-*ab*-one and zinc biladien-*ab*-one to mesoporous silica, Micro Mesopor. Mat. 120 (2009) 331–338, https://doi.org/10.1016/j.micromeso.2008.11.025.
[96] T.H. Allik, R.E. Hermes, G. Sathyamoorthi, J.H. Boyer, Spectroscopy and laser performance of new BF_2-complex dyes in solution, Proc. SPIE 2115 (1994) 240–248, https://doi.org/10.1117/12.172742.
[97] E.V. Antina, G.B. Guseva, N.A. Dudina, A.I. V'yugin, A.S. Semeikin, Synthesis and spectral analysis of alkyl-substituted 3,3′-bis(dipyrrolylmethenes), Russ. J. Gen. Chem. 79 (2009) 2425–2434, https://doi.org/10.1134/S1070363209110243.
[98] L.A. Antina, A.A. Kalyagin, A.A. Ksenofontov, R.S. Pavelyev, O.A. Lodochnikova, D.R. Islamov, M.B. Berezin, E.V. Antina, Effects of *ms*-aryl substitution on the structure and spectral properties of new CH(Ar)-bis(BODIPY) luminophores, Spectrochim. Acta A Mol. Biomol. 265 (2022), 120393, https://doi.org/10.1016/j.saa.2021.120393.
[99] A.L. Balch, L. Latos-Grazynski, B.C. Noll, M.M. Olmstead, N. Safari, Isolation and characterization of an iron biliverdin-type complex that is formed along with verdohemochrome during the coupled oxidation of iron(II) octaethylporphyrin, J. Am. Chem. Soc. 115 (1993) 9056–9061, https://doi.org/10.1021/ja00073a022.
[100] A.L. Balch, M. Mazzanti, B.C. Noll, M.M. Olmstead, Coordination patterns for biliverdin-type ligands. Helical and linked helical units in four-coordinate cobalt and five-coordinate manganese(III) complexes of octaethylbilindione, J. Am. Chem. Soc. 116 (1994) 9114–9122, https://doi.org/10.1021/ja00099a029.
[101] S.A. Baudron, H. Ruffin, M.W. Hosseini, On Zn(II) 2,2′-bisdipyrrin circular helicates, Chem. Commun. 51 (2015) 5906–5909, https://doi.org/10.1039/C5CC00724K.
[102] J.E. Bishop, J.O. Nagy, J.F. O'Connell, H. Rapoport, Diastereoselective synthesis of phycocyanobilin-cysteine adducts, J. Am. Chem. Soc. 113 (1991) 8024–8035, https://doi.org/10.1021/ja00021a032.
[103] S.E. Boiadjiev, D.A. Lightner, A water-soluble synthetic bilirubin with carboxyl groups replaced by sulfonyl moieties, Mon. Chem. 132 (2001) 1201–1212, https://doi.org/10.1007/s007060170035.
[104] S.E. Boiadjiev, D.A. Lightner, Conformational control by remote stereogenic centers: Linear tetrapyrroles, Tetrahedron Asymm. 15 (2004) 3301–3305, https://doi.org/10.1016/j.tetasy.2004.08.029.
[105] S.E. Boiadjiev, D.A. Lightner, N_{21},N_{22}-Carbonyl-bridged biliverdin. Red-blue color change effected by conformation, J. Heterocycl. Chem. 42 (2005) 161–164, https://doi.org/10.1002/jhet.5570420126.
[106] J.V. Bonfiglio, R. Bonnett, D.G. Buckley, D. Hamzetash, M.B. Hursthouse, K.M. A. Malik, S.C. Naithani, J. Trotter, The *meso*-reactivity of porphyrins and related compounds. Part VIII. Substitution and addition reactions of octaethyl-21*H*,24*H*-bilin-1,19-dione, a model verdin system. X-Ray analyses of octaethyl-5-nitro-21*H*,24*H*-bilin-1,19-dione and of 4,5-diethoxy-octaethyl-4,5-dihydro-21*H*,24*H*-bilin-1,19-dione, J. Chem. Soc., Perkin Trans. 1 (1982) 1291–1302, https://doi.org/10.1039/p19820001291.
[107] J.V. Bonfiglio, R. Bonnett, D.G. Buckley, D. Hamzetash, M.B. Hursthouse, K.M. A. Malik, A.F. McDonagh, J. Trotter, Linear tetrapyrroles as ligands: Syntheses and X-ray analyses of boron and nickel complexes of octaethyl-21*H*,24*H*-bilin-1,19-dione, Tetrahedron 39 (1983) 1865–1874, https://doi.org/10.1016/S0040-4020(01)88700-7.
[108] S.E. Braslavsky, D. Schneider, K. Heihoff, S. Nonell, P.F. Aramendia, K. Schaffner, Phytochrome models. 11. Photophysics and photochemistry of phycocyanobilin dimethyl ester, J. Am. Chem. Soc. 113 (1991) 7322–7334, https://doi.org/10.1021/ja00019a033.
[109] M. Bröring, S. Link, C.D. Brandt, E.C. Tejero, Helical transition-metal complexes of constrained 2,2′-bidipyrrins, Eur. J. Inorg. Chem. 2007 (2007) 1661–1670, https://doi.org/10.1002/ejic.200600986.
[110] M. Bröring, S. Köhler, S. Link, O. Burghaus, C. Pietzonka, H. Kelm, H.-J. Krüger, Iron chelates of 2,2′-bidipyrrin: stable analogues of the labile iron bilins, Chem. Eur. J. 14 (2008) 4006–4016, https://doi.org/10.1002/chem.200701919.
[111] J.O. Brower, D.A. Lightner, A.F. McDonagh, Aromatic congeners of bilirubin: synthesis, stereochemistry, glucuronidation and hepatic transport, Tetrahedron 57 (2001) 7813–7827, https://doi.org/10.1016/S0040-4020(01)00773-6.
[112] S.B. Brown, J.A. Holroyd, R.F. Troxler, G.D. Offner, Bile pigment synthesis in plants. Incorporation of haem into phycocyanobilin and phycobiliproteins in *Cyanidium caldarium*, Biochem. J. 194 (1981) 137–147, https://doi.org/10.1042/bj1940137.
[113] P.Ó. Carra, C.Ó. hEocha, D.M. Carroll, Spectral properties of the phycobilins. II, Phycoerythrobilin, Biochem. 3 (1964) 1343–1350, https://doi.org/10.1021/bi00897a026.
[114] Q.-Q. Chen, H. Falk, On the chemistry of pyrrole pigments, XCIII: 1,2-*bis*-(dipyrrinon-9-ylidene)-ethane – a novel *b*-homoverdin chromophore, Mon. Chem. 126 (1995) 1097–1107, https://doi.org/10.1007/BF00811380.
[115] Q.Q. Chen, H. Falk, On the chemistry of pyrrole pigments, XCIV: 1-(Dipyrrinon-9-yl)-3-(dipyrrinon-9-ylidene)-1-propene – a novel *b*-vinylogous verdin chromophore, Mon. Chem. 126 (1995) 1233–1244, https://doi.org/10.1007/BF00824302.
[116] Q.-Q. Chen, H. Falk, On the chemistry of pyrrole pigments, XCV: 1,4-*bis*-(dipyrrinone-9-ylidene)-butene-2 – A novel *b*-*homo*-verdin chromophore, Mon. Chem. 126 (1995) 1323–1329, https://doi.org/10.1007/BF00807061.
[117] Q. Chen, M.T. Huggins, D.A. Lightner, W. Norona, A.F. McDonagh, Synthesis of a 10-oxo-bilirubin: effects of the oxo group on conformation, transhepatic transport, and glucuronidation, J. Am. Chem. Soc. 121 (1999) 9253–9264, https://doi.org/10.1021/ja991814m.
[118] L.-J. Cheng, J.-S. Ma, L.-C.C. (Li-J. Jiang), The complexes formed by biladiene a, b compounds with zinc ions and their application in determination of the chromophore composition of α- and β- subunits of R-phycoerythrin, Photochem. Photobiol. 52 (1990) 1071–1076, https://doi.org/10.1111/j.1751-1097.1990.tb08447.x.
[119] J. Crusats, A. Delgado, J.-A. Farrera, R. Rubires, J.M. Ribó, Solution structure of mesobilirubin XIIIα bridged between the propionic acid substituents, Mon. Chem. 129 (1998) 741–753, https://doi.org/10.1007/PL00013483.
[120] D. Dolphin, A.W. Johnson, J. Leng, P. van den Broek, The base-catalysed cyclisations of 1,19-dideoxybiladienes-ac, J. Chem. Soc., C (1966) 880–884, https://doi.org/10.1039/j39660000880.
[121] N.A. Dudina, E.V. Antina, D.I. Sozonov, A.I. V'yugin, Effect of alkyl substitution in 3,3′-bis(dipyrrin) on chemosensor activity of fluorescent detection of Zn^{2+} cations, Russ. J. Org. Chem. 51 (2015) 1155–1161, https://doi.org/10.1134/S107042801508014X.
[122] J. Edinger, H. Falk, N. Müller, Zur chemie der pyrrolpigmente, 54. mitt.: phytochrommodellstudien: Ein 2,3-dihydrobilatrien-abc-3-cholesterylderivat, Mon. Chem. 115 (1984) 837–852, https://doi.org/10.1007/BF01120979.
[123] J. Edinger, H. Falk, W. Jungwirth, N. Müller, U. Zrunek, Zur chemie der pyrrolpigmente, 56. mitt.: Phytochrommodellstudien: Die induzierten und natürlichen chiroptischen eigenschaften von bilatrienen-abc und 2,3-dihydrobilatrienen-abc, Mon. Chem. 115 (1984) 1081–1099, https://doi.org/10.1007/BF00798775.
[124] F. Eivazi, M.F. Hudson, K.M. Smith, Bile pigment studies III. Controlled oxidative degradation of 1,19(21,24)-bilindiones (bilitrienes), Tetrahedron 33 (1977) 2959–2964, https://doi.org/10.1016/0040-4020(77)88030-7.
[125] H. Falk, K. Grubmayr, E. Haslinger, T. Schlederer, K. Thirring, Beiträge zur chemie der pyrrolpigmente, 25. mitt.: Die diastereomeren (geometrisch isomeren) biliverdindimethylester – Struktur, konfiguration und konformation, Mon. Chem. 109 (1978) 1451–1473, https://doi.org/10.1007/BF00906057.
[126] H. Falk, K. Thirring, Beiträge zur Chemie der pyrrolpigmente, XXXIII. Darstellung, struktur und eigenschaften von isomeren N-methyl-bilatrienen-abc (N-methyl-etiobiliverdine-IV-γ), Z. Naturforsch. B 34 (1979) 1448–1453, https://doi.org/10.1515/znb-1979-1020.
[127] H. Falk, T. Schlederer, Beiträge zur Chemie der Pyrrolpigmente, XXX. Struktur und eigenschaften der laktimform eines bilatriens-abc (ätiobiliverdin-IV-γ), Liebigs Ann. Chem. 1979 (1979) 1560–1570, https://doi.org/10.1002/jlac.197919791015.
[128] H. Falk, K. Thirring, Beiträge zur chemie der pyrrolpigmente, XXXIV. Über die konfiguration und konformation von diastereomeren N-methyl-O-methyl-bilatrienen-abc, Z. Naturforsch. B 34 (1979) 1600–1605, https://doi.org/10.1515/znb-1979-1123.
[129] H. Falk, N. Müller, T. Schlederer, Beiträge zur chemie der pyrrolpigmente, 35. mitt.: Eine regioselektive, reversible addition an bilatriene-abc, Mon. Chem. 111 (1980) 159–175, https://doi.org/10.1007/BF00938725.
[130] H. Falk, K. Thirring, Beiträge zur chemie der pyrrolpigmente, XXXVI. Zur anaeroben photochemie von 21.24-dimethy-aetiobiliverdin-IV-γ, Z. Naturforsch. B 35 (1980) 376–380, https://doi.org/10.1515/znb-1980-0322.

[131] H. Falk, T. Schlederer, P. Wolschann, Beiträge zur chemie der pyrrolpigmente, 38. mitt.: Zur assoziation von gallenpigmenten, Mon. Chem. 112 (1981) 199–207, https://doi.org/10.1007/BF00911086.
[132] H. Falk, K. Thirring, Beiträge zur chemie der pyrrolpigmente-XXXVII: Überbrückte gallenpiqmente: N_{21}-N_{24}-methylen-aetiobiliverdin- IV-$_\gamma$ und N_{21}-N_{24}-methylen-aetiobilirubin-IV-$_\gamma$, Tetrahedron 37 (1981) 761–766, https://doi.org/10.1016/S0040-4020(01)97694-X.
[133] H. Falk, U. Zrunek, Beiträge zur chemie der pyrrolpigmente, 50. mitt.: phytochrommodellstudien: Das laktam – Laktimgleichgewicht des pyrrolidinonfragmentes von 2,3-dihydrobilatrienen-abc – Protonierungsgleichgewichte, Mon. Chem. 114 (1983) 983–998, https://doi.org/10.1007/BF00799958.
[134] H. Falk, U. Zrunek, Beiträge zur chemie der pyrrolpigmente, 52. mitt.: Phytochrommodellstudien: Eine reversible addition an Δ-4 von 2,3-dihydrobilatrienen-abc, Mon. Chem. 115 (1984) 101–111, https://doi.org/10.1007/BF00798426.
[135] H. Falk, P. Wolschann, U. Zrunek, Beiträge zur chemie der pyrrolpigmente, 53. mitt.: phytochrommodellstudien: Das säure-basen-gleichgewicht diastereomerer 2,3-dihydrobilatriene-abc, Mon. Chem. 115 (1984) 243–249, https://doi.org/10.1007/BF00798415.
[136] H. Falk, H. Gsaller, E. Hubauer, N. Müller, Beiträge zur chemie der pyrrolpigmente, 61. mitt.: phytochrommodellstudien – Absorptionsspektren und strukturelle aspekte von 2,3-dihydrobilatrienen-abc aus der sicht eines semiempirischen quantenchemischen verfahrens (*PPP*-SCF-LCAO-MO-CI), Mon. Chem. 116 (1985) 939–959, https://doi.org/10.1007/BF00809188.
[137] H. Falk, N. Müller, S. Wansch, Zur chemie der pyrrolpigmente, 63. mitt.: phytochrommodellstudien: Das system 2,3-dihydrobilatrien – Hexamethylphosphorsäuretriamid als modell für gestreckte chromophore, Mon. Chem. 116 (1985) 1087–1097, https://doi.org/10.1007/BF00809199.
[138] H. Falk, H. Flödl, Beiträge zur chemie der pyrrolpigmente, 64. mitt.: 2,3,7,8,12,13,17,18,22,23-Decamethyl-1,24,25,29-tetrahydro-27*H*-pentapyrrin-1,24-dion, der erste vertreter linearer pentapyrrole: Darstellung und struktur im gelösten zustand, Mon. Chem. 116 (1985) 1177–1187, https://doi.org/10.1007/BF00811251.
[139] H. Falk, H. Flödl, Beiträge zur chemie der pyrrolpigmente, 65. mitt.: 2,3,7,8,12,13,17,18,22,23-Decamethyl-1,24,25,29-tetrahydro-27*H*-pentapyrrin-1,24-dion, der erste vertreter linearer pentapyrrole: Eigenschaften und reaktionsweisen, Mon. Chem. 117 (1986) 57–67. ⟨https://doi.org/10.1007/BF00809173⟩.
[140] H. Falk, A. Hinterberger, Beiträge zur chemie der pyrrolpigmente, 67. mitt.: Bilatriene-abc und 2,3-dihydrobilatriene-abc in micellaren systemen, Mon. Chem. 117 (1986) 1081–1090, https://doi.org/10.1007/BF00811278.
[141] H. Falk, W. Medinger, N. Müller, Beiträge zur chemie der pyrrolpigmente, 75. mitt. Phytochrom-modell-studien: Stereochemische untersuchungen an einem zwischen den pyrrolischen ringen A und C peptidartig überbrückten 2,3-dihydrobilatrien-abc, Mon. Chem. 119 (1988) 113–126, https://doi.org/10.1007/BF00810093.
[142] H. Falk, H. Flödl, U.G. Wagner, Beiträge zur chemie der pyrrolpigmente, 77. mitt. Synthese und struktur von *b-Nor*-bilatrienen-*abc* und *b-Nor*-biladienen-*ac* bzw. Bi-9,9′-dipyrrinonylidenen und bi-9,9′-dipyrrinonylenen, Mon. Chem. 119 (1988) 739–749, https://doi.org/10.1007/BF00809688.
[143] H. Falk, N. Müller, H. Wöss, Beiträge zur chemie der pyrrolpigmente, 79. mitt.: Zum strukturellen einfluß stark raumerfüllender reste bei 10-substituierten 1,19-bilindionen, Mon. Chem. 120 (1989) 35–43, https://doi.org/10.1007/BF00809647.
[144] H. Falk, K. Grubmayr, M. Marko, Beiträge zur chemie der pyrrolpigmente, 82. mitt.: Wasserlösliche polymere mit kovalent gebundenen violinoiden und 2,3-dihydro-verdinoiden gallenfarbstoffen, Mon. Chem. 120 (1989) 771–779, https://doi.org/10.1007/BF00809971.
[145] H. Falk, H. Wöss, Beiträge zur chemie der pyrrolpigmente, 83. mitt.: Zum einfluß geladener zentren auf die absorptionsspektren von 1,19-bilindionen, Mon. Chem. 121 (1990) 59–66, https://doi.org/10.1007/BF00810295.
[146] H. Falk, M. Frühwirth, On the chemistry of pyrrole pigments, LXXXIX: vinylogous linear di- and tetrapyrroles, Mon. Chem. 123 (1992) 1213–1221, https://doi.org/10.1007/BF00808284.
[147] H. Falk, A. Šuste, On the chemistry of pyrrole pigments, XC: pyridinologous linear tri- and tetrapyrroles, Mon. Chem. 124 (1993) 881–891, https://doi.org/10.1007/BF00816411.
[148] J.-H. Fuhrhop, Peter K.W. Wasser, J. Subramanian, U. Schrader, Formylbiliverdine und ihre Metallkomplexe, Liebigs Ann. Chem. 1974 (1974) 1450–1466, https://doi.org/10.1002/jlac.197419740909.
[149] J.-H. Fuhrhop, A. Salek, J. Subramanian, C. Mengersen, S. Besecke, Metallkomplexe von biliverdinderivaten, Liebigs Ann. Chem. 1975 (1975) 1131–1147, https://doi.org/10.1002/jlac.197519750612.
[150] S. Ghidinelli, S. Abbate, S.E. Boiadjiev, D.A. Lightner, G. Longhi, *l* -Stercobilin-HCl and *d*-urobilin-HCl. analysis of their chiroptical and conformational properties by VCD, ECD, and CPL experiments and MD and DFT calculations, J. Phys. Chem. B 122 (2018) 12351–12362, https://doi.org/10.1021/acs.jpcb.8b07954.
[151] B. Ghosh, D.A. Lightner, A.F. McDonagh, Synthesis, conformation, and metabolism of a selenium bilirubin, Mon. Chem. 135 (2004) 1189–1199, https://doi.org/10.1007/s00706-004-0191-9.
[152] A. Gossauer, W. Hirsch, Synthesen von Gallenfarbstoffen, IV. Totalsynthese des racemischen phycocyanobilins (phycobiliverdins) sowie eines homophycobiliverdins, Liebigs Ann. Chem. 1974 (1974) 1496–1513, https://doi.org/10.1002/jlac.197419740913.
[153] G.B. Guseva, N.A. Dudina, E.V. Antina, A.I. V'yugin, A.S. Semeikin, 3,3′-bis (dipyrrolylmethenes) as new chelating ligands: synthesis and spectral properties, Russ. J. Gen. Chem. 78 (2008) 1215–1224, https://doi.org/10.1134/S1070363208060200.
[154] GalinaB. Guseva, E.V. Antina, A.A. Ksenofontov, The complex formation of indium(III) acetate with alkyl-substituted 3,3′-*bis*(dipyrromethene) ligands, Inorg. Chim. Acta 498 (2019), 119146, https://doi.org/10.1016/j.ica.2019.119146.
[155] M.S. Huster, K.M. Smith, Ring cleavage of chlorophyll derivatives: isolation of oxochlorin intermediates and ring opening via a two oxygen molecule mechanism, Tetrahedron Lett. 29 (1988) 5707–5710, https://doi.org/10.1016/S0040-4039(00)82168-1.
[156] J. Ituttaspe, N. Engel, P. Matzinger, V. Mooser, A. Gossauer, Chlorophyll catabolism. Part 3. Structure elucidation and partial synthesis of a new red bilin derivative from *Chlorella protothecoides*, Photochem. Photobiol. 58 (1993) 116–119, https://doi.org/10.1111/j.1751-1097.1993.tb04911.x.
[157] J.A. Johnson, M.M. Olmstead, A.L. Balch, Reactivity of the verdoheme analogues. Opening of the planar macrocycle by amide and thiolate nucleophiles to form helical complexes, Inorg. Chem. 38 (1999) 5379–5383, https://doi.org/10.1021/ic9904283.
[158] J.A. Johnson, M.M. Olmstead, A.M. Stolzenberg, A.L. Balch, Ring-opening and meso substitution from the reaction of cyanide ion with zinc verdohemes, Inorg. Chem. 40 (2001) 5585–5595, https://doi.org/10.1021/ic0103300.
[159] K. Kakeya, M. Aozasa, T. Mizutani, Y. Hitomi, M. Kodera, Nucleophilic ring opening of *meso*-substituted 5-oxaporphyrin by oxygen, nitrogen, sulfur, and carbon nucleophiles, J. Org. Chem. 79 (2014) 2591–2600, https://doi.org/10.1021/jo5000412.
[160] R. Koerner, M.M. Olmstead, A. Ozarowski, S.L. Phillips, P.M. Van Calcar, K. Winkler, A.L. Balch, Possible intermediates in biological metalloporphyrin oxidative degradation. Nickel, copper, and cobalt complexes of octaethylformybiliverdin and their conversion to a verdoheme, J. Am. Chem. Soc. 120 (1998) 1274–1284, https://doi.org/10.1021/ja973088y.
[161] C.C. Kuenzle, Bilirubin conjugates of human bile. Nuclear-magnetic-resonance, infrared and optical spectra of model compounds, Biochem. J. 119 (1970) 395–409, https://doi.org/10.1042/bj1190395.
[162] W. Kufer, H. Scheer, A.R. Holzwarth, Isophorcarubin – A conformationally restricted and highly fluorescent bilirubin, Isr. J. Chem. 23 (1983) 233–240, https://doi.org/10.1002/ijch.198300033.
[163] L. Latos-Grażyński, J. Johnson, S. Attar, M.M. Olmstead, A.L. Balch, Reactivity of the verdoheme analogues, 5-oxaporphyrin complexes of cobalt(II) and zinc(II), with nucleophiles: opening of the planar macrocycle by alkoxide addition to form helical complexes, Inorg. Chem. 37 (1998) 4493–4499, https://doi.org/10.1021/ic971584h.
[164] C. Leumann, A. Eschenmoser, Chemistry of pyrrocorphins: methylative opening of the macrocycle between rings A and D, a side reaction in the peripheral *C*-methylation of a 20-methyl-pyrrocorphinate, J. Chem. Soc., Chem. Commun. (1984) 583–585, https://doi.org/10.1039/c39840000583.
[165] P.A. Lord, M.M. Olmstead, A.L. Balch, Redox characteristics of nickel and palladium complexes of the open-chain tetrapyrrole octaethylbilindione: a biliverdin model, Inorg. Chem. 39 (2000) 1128–1134, https://doi.org/10.1021/ic9910209.
[166] P.A. Lord, B.C. Noll, M.M. Olmstead, A.L. Balch, A remarkable skeletal rearrangement of a coordinated tetrapyrrole: chemical consequences of palladium π-coordination to a bilindione, J. Am. Chem. Soc. 123 (2001) 10554–10559, https://doi.org/10.1021/ja010647z.
[167] A.F. McDonagh, L.A. Palma, D.A. Lightner, Phototherapy for neonatal jaundice. Stereospecific and regioselective photoisomerization of bilirubin bound to human serum albumin and NMR characterization of intramolecularly cyclized photoproducts, J. Am. Chem. Soc. 104 (1982) 6867–6869, https://doi.org/10.1021/ja00388a104.
[168] A.F. McDonagh, D.A. Lightner, M. Reisinger, L.A. Palma, Human serum albumin as a chiral template. Stereoselective photocyclization of bilirubin, J. Chem. Soc., Chem. Commun. (1986) 249–250, https://doi.org/10.1039/c39860000249.
[169] A.F. McDonagh, D.A. Lightner, Influence of conformation and intramolecular hydrogen bonding on the acyl glucuronidation and biliary excretion of acetylenic bis-dipyrrinones related to bilirubin, J. Med. Chem. 50 (2007) 480–488, https://doi.org/10.1021/jm0609521.
[170] T. Mizutani, S. Yagi, A. Honmaru, S. Murakami, M. Furusyo, T. Takagishi, H. Ogoshi, Helical chirality induction in zinc bilindiones by amino acid esters and amines, J. Org. Chem. 63 (1998) 8769–8784, https://doi.org/10.1021/jo980819j.
[171] T. Mizutani, Coupled oxidation of iron tetraarylporphyrins as a synthetic tool for linear tetrapyrroles, J. Porphyr. Phthalocyanines 20 (2016) 108–116, https://doi.org/10.1142/S1088424616300044.
[172] Y. Murakami, Y. Kohno, Y. Matsuda, Transition-metal complexes of pyrrole pigments, II. Cobalt(II) and nickel(II) complexes of 1,19-dideoxy- 8,12-dicarbethoxy-1,3,7,13,17,17-hexamethylbiladiene-ac, Inorg. Chim. Acta 3 (1969) 671–675, https://doi.org/10.1016/S0020-1693(00)92575-1.
[173] Y. Murakami, Y. Matsuda, Y. Kanaoka, Transition-metal complexes of pyrrole pigments. III. Copper(II) and zinc(II) complexes of 1,19-dideoxy-8,12-dicarbethoxy-1,3,7,13,17,19-hexamethylbiladiene-ac, Bull. Chem. Soc. Jpn. 44 (1971) 409–415, https://doi.org/10.1246/bcsj.44.409.
[174] Y. Murakami, Y. Matsuda, S.-I. Kobayashi, Transition-metal complexes of pyrrole pigments. Part VII. Cobalt(II) and zinc(II) chelates of some tripyrrene-*b* and bilene-*b*, Ligands, J. Chem. Soc., Dalton Trans. (1973) 1734–1737, https://doi.org/10.1039/dt9730001734.

[175] C. Mwakwari, F.R. Fronczek, K.M. Smith, *b*-Bilene to *a,c*-biladiene transformation during syntheses of isoporphyrins and porphyrins, Chem. Commun. (2007) 2258–2260, https://doi.org/10.1039/b705182d.
[176] R. Nakamura, K. Kakeya, N. Furuta, E. Muta, H. Nishisaka, T. Mizutani, Synthesis of *para*- or *ortho*-substituted triarylbilindiones and tetraarylbiladienones by coupled oxidation of tetraarylporphyrins, J. Org. Chem. 76 (2011) 6108–6115, https://doi.org/10.1021/jo2007994.
[177] P. Nesvadba, A. Gossauer, Synthesis of bile pigments. 14. Synthesis of a bilindionostilbenoparacyclophane as a model for "stretched" bile pigment chromophores of biliproteins, J. Am. Chem. Soc. 109 (1987) 6545–6546, https://doi.org/10.1021/ja00255a069.
[178] P. Nesvadba, D. Ngoc-Phan, F. Nydegger, A.E. Ferao, A. Gossauer, Syntheses of bile pigments. Part 18. Synthesis and conformational studies of oxa- and thia-deaza-biliverdin analogues, Helv. Chim. Acta 77 (1994) 1837–1850, https://doi.org/10.1002/hlca.19940770715.
[179] O. Ongayi, M.G.H. Vicente, Z. Ou, K.M. Kadish, M.R. Kumar, F.R. Fronczek, K. M. Smith, Synthesis and electrochemistry of undeca-substituted metallo-benzoylbiliverdins, Inorg. Chem. 45 (2006) 1463–1470, https://doi.org/10.1021/ic050841c.
[180] R. Paolesse, A. Froiio, S. Nardis, M. Mastroianni, M. Russo, D.J. Nurco, K. M. Smith, Novel aspects of the chemistry of 1,19-diunsubstituted a,c-biladienes, J. Porphyr. Phthalocyanines 07 (2003) 585–592, https://doi.org/10.1142/S1088424603000744.
[181] R. Paolesse, A. Alimelli, A. D'Amico, M. Venanzi, G. Battistini, M. Montalti, D. Filippini, I. Lundström, C. Di Natale, Insights on the chemistry of *a,c*-biladienes from a CSPT investigation, New J. Chem. 32 (2008) 1162–1166, https://doi.org/10.1039/b800512e.
[182] C. Pasquier, A. Gossauer, W. Keller, C. Kratky, Syntheses of bile pigments. Part 15. First unequivocal assignment of the absolute configuration of an urobilinoid bile pigment by X-ray diffraction analysis of its synthetic precursor, Helv. Chim. Acta 70 (1987) 2098–2109, https://doi.org/10.1002/hlca.19870700815.
[183] W.P. Pfeiffer, D.A. Lightner, Homorubin. A centrally homologated bilirubin, Tetrahedron Lett. 35 (1994) 9673–9676, https://doi.org/10.1016/0040-4039(94)88356-4.
[184] N. Risch, A. Schormann, H. Brockmann, Photobilin e. Photooxidation von bacteriochlorophyll-e-derivaten, Tetrahedron Lett. 25 (1984) 5993–5996, https://doi.org/10.1016/S0040-4039(01)81741-X.
[185] E.V. Rumyantsev, S.P. Makarova, E.V. Antina, Protonation and solvation effects in the reaction of zinc 1,2,3,7,8,12,13,17,18,19-decamethylbiladien-*a,c* complex formation, Russ. J. Gen. Chem. 79 (2009) 2420–2424, https://doi.org/10.1134/S1070363209110231.
[186] A. Savoldelli, R. Paolesse, F.R. Fronczek, K.M. Smith, M.G.H. Vicente, BODIPY dyads from a,c-biladiene salts, Org. Biomol. Chem. 15 (2017) 7255–7257, https://doi.org/10.1039/C7OB01797A.
[187] K. Shimada, T. Mizutani, Synthesis and reactivity of 10,15,20-triaryl-5-oxaporphyrin copper complexes, Tetrahedron Lett. 103 (2022), 153977, https://doi.org/10.1016/j.tetlet.2022.153977.
[188] J.W. Singleton, L. Laster, Biliverdin reductase of guinea pig liver, J. Biol. Chem. 240 (1965) 4780–4789, https://doi.org/10.1016/S0021-9258(18)97023-7.
[189] K.M. Smith, S.B. Brown, R.F. Troxler, J.-J. Lai, Mechanism of photo-oxygenation of meso-tetraphenylporphyrin metal complexes, Tetrahedron Lett. 21 (1980) 2763–2766, https://doi.org/10.1016/S0040-4039(00)78600-X.
[190] K.M. Smith, O.M. Minnetian, Cyclizations of 1′,8′-dimethyl-*a,c*-biladiene salts to give porphyrins: a study with various oxidizing agents, J. Chem. Soc., Perkin Trans. 1 (1986) 277–280, https://doi.org/10.1039/P19860000277.
[191] M. Suresh, S.K. Mishra, S. Mishra, A. Das, The detection of Hg^{2+} by cyanobacteria in aqueous media, Chem. Commun. (2009) 2496–2498, https://doi.org/10.1039/b821687h.
[192] M.J. Terry, M.D. Maines, J.C. Lagarias, Inactivation of phytochrome- and phycobiliprotein-chromophore precursors by rat liver biliverdin reductase, J. Biol. Chem. 268 (1993) 26099–26106, https://doi.org/10.1016/S0021-9258(19)74286-0.
[193] A.K. Tipton, D.A. Lightner, A.F. McDonagh, Synthesis and metabolism of the first thia-bilirubin, J. Org. Chem. 66 (2001) 1832–1838, https://doi.org/10.1021/jo001598w.
[194] B.B. Tu, D.A. Lightner, A novel diacetylenic bilirubin, J. Heterocycl. Chem. 40 (2003) 707–712, https://doi.org/10.1002/jhet.5570400424.
[195] J. Weller, A. Gossauer, Synthesen von Gallenfarbstoffen, X. Synthese und Photoisomerisierung des *racem*. Phytochromobilin-dimethylesters, Chem. Ber. 113 (1980) 1603–1611, https://doi.org/10.1002/cber.19801130439.
[196] C. Wu, H. Akimoto, Y. Ohmiya, Tracer studies on dinoflagellate luciferin with [^{15}N]-glycine and [^{15}N]-L-glutamic acid in the dinoflagellate *Pyrocystis lunula*, Tetrahedron Lett. 44 (2003) 1263–1266, https://doi.org/10.1016/S0040-4039(02)02815-0.
[197] K. Yamada, T. Yatabe, K.-S. Yoon, S. Ogo, Cp*Ir complex with mesobiliverdin ligand isolated from *Thermoleptolyngbya* sp. O-77, J. Organomet. Chem. 964 (2022), 122302, https://doi.org/10.1016/j.jorganchem.2022.122302.
[198] T. Yamauchi, T. Mizutani, K. Wada, S. Horii, H. Furukawa, S. Masaoka, H.-C. Chang, S. Kitagawa, A facile and versatile preparation of bilindiones and biladienones from tetraarylporphyrins, Chem. Commun. (2005) 1311, https://doi.org/10.1039/b414299c.
[199] B. Yang, M.D. Morris, M. Xie, D.A. Lightner, Resonance Raman spectroscopy of bilirubins: band assignments and application to bilirubin/lipid complexation, Biochemistry 30 (1991) 688–694, https://doi.org/10.1021/bi00217a015.
[200] K.R. Reddy, E. Lubian, M.P. Pavan, H.-J. Kim, E. Yang, D. Holten, J.S. Lindsey, Synthetic bacteriochlorins with integral spiro-piperidine motifs, New J. Chem. 37 (2013) 1157–1173, https://doi.org/10.1039/C3NJ41161C.
[201] H. Falk, O. Hofer, H. Lehner, Beiträge zur chemie der pyrrolpigmente, 1. mitt.: Der induzierte circulardichroismus einiger pyrromethenderivate in cholesterischer mesophase, Mon. Chem. 105 (1974) 169–178, https://doi.org/10.1007/BF00911302.
[202] H. Falk, S. Gergely, K. Grubmayr, O. Hofer, Beiträge zur chemie der pyrrolpigmente, XVII: Struktur- und konformationsanalytische untersuchungen am chromophoren system der bilivioline [biladiene-(a.b)], Z. Naturforsch. B 32 (1977) 299–303, https://doi.org/10.1515/znb-1977-0313.
[203] D. Nogales, D.A. Lightner, The structure of bilirubin in solution, J. Biol. Chem. 270 (1995) 73–77, https://doi.org/10.1074/jbc.270.1.73.
[204] J.S. Lindsey, R.W. Wagner, Investigation of the synthesis of ortho-substituted tetraphenylporphyrins, J. Org. Chem. 54 (1989) 828–836, https://doi.org/10.1021/jo00265a021.
[205] L. Yu, K. Muthukumaran, I.V. Sazanovich, C. Kirmaier, E. Hindin, J.R. Diers, P. D. Boyle, D.F. Bocian, D. Holten, J.S. Lindsey, Excited-state energy-transfer dynamics in self-assembled triads composed of two porphyrins and an intervening bis(dipyrrinato)metal complex, Inorg. Chem. 42 (2003) 6629–6647, https://doi.org/10.1021/ic034559m.
[206] Y. Liu, S. Zhang, S, J.S. Lindsey, Total synthesis campaigns toward chlorophylls and related natural hydroporphyrins – diverse macrocycles, unrealized opportunities, Nat. Prod. Rep. 35 (2018) 879–901, https://doi.org/10.1039/C8NP00020D.
[207] J.S. Lindsey, Considerations of the biosynthesis and molecular diversity of tolyporphins, New J. Chem. 45 (2021) 12097–12107, https://doi.org/10.1039/d1nj01761f.
[208] A. Treibs, F.-H. Kreuzer, Difluorboryl-komplexe von di- und tripyrrylmethenen, Liebigs Ann. Chem. 718 (1968) 208–223, https://doi.org/10.1002/jlac.19687180119.
[209] Z. Dost, S. Atilgan, E.U. Akkaya, Distyryl-boradiazaindacenes: Facile synthesis of novel near IR emitting fluorophores, Tetrahedron 62 (2006) 8484–8488, https://doi.org/10.1016/j.tet.2006.06.082.
[210] M.O. Senge, Highly substituted porphyrins, in: K.M. Kadish, K.M. Smith, R. Guilard (Eds.), The Porphyrin Handbook, Vol. 1, Academic Press, San Diego, 2000, pp. 239–347.
[211] A.A. Lamola, J. Eisinger, W.E. Blumberg, S.C. Patel, J. Flores, Fluorometric study of the partition of bilirubin among blood components: Basis for rapid microassays of bilirubin and bilirubin binding capacity in whole blood, Anal. Biochem. 100 (1979) 25–42, https://doi.org/10.1016/0003-2697(79)90105-2.
[212] A.R. Holzwarth, H. Lehner, S.E. Braslavsky, K. Schaffner, Phytochrome models, II. The fluorescence of biliverdin dimethyl ester, Liebigs Ann. Chem. 1978 (1978) 2002–2017, https://doi.org/10.1002/jlac.197819781215.
[213] I.M. Tegmo-Larsson, S.E. Braslavsky, S. Culshaw, R.M. Ellul, C. Nicolau, K. Schaffner, Phytochrome models. 6. Conformation control by membrane of biliverdin dimethyl ester incorporated into lipid vesicles, J. Am. Chem. Soc. 103 (1981) 7152–7158, https://doi.org/10.1021/ja00414a019.
[214] H. Falk, U. Zrunek, Beiträge zur chemie der pyrrolpigmente, 51. mitt.: Phytochrommodellstudien: Zur deprotonierung von 3,4-dihydropyrromethenonen und 2,3-dihydrobilatrienen-abc, Mon. Chem. 114 (1983) 1107–1123, https://doi.org/10.1007/BF00799035.
[215] G.N. Lewis, M. Calvin, The color of organic substances, Chem. Rev. 25 (1939) 273–328, https://doi.org/10.1021/cr60081a004.
[216] J.S. Lindsey, M. Taniguchi, D.F. Bocian, D. Holten, The fluorescence quantum yield parameter in Förster resonance energy transfer (FRET) – Meaning, misperception, and molecular design, Chem. Phys. Rev. 2 (2021), 011302, https://doi.org/10.1063/5.0041132.
[217] M. Taniguchi, J.S. Lindsey, D.F. Bocian, D. Holten, Comprehensive review of photophysical parameters (ε, Φ_f, τ_s) of tetraphenylporphyrin (H_2TPP) and zinc tetraphenylporphyrin (ZnTPP) – Critical benchmark molecules in photochemistry and photosynthesis, J. Photochem. Photobiol. C: Photochem. Rev. 46 (2021), 100401, https://doi.org/10.1016/j.jphotochemrev.2020.100401.
[218] A. Gossauer, F. Fehr, F. Nydegger, H. Stöckli-Evans, Synthesis and conformational studies of urobilin difluoroboron complexes. Unprecedented solvent-dependent chiroptical properties of the BF_2 chelate of an urobilinoid analogue, J. Am. Chem. Soc. 119 (1997) 1599–1608, https://doi.org/10.1021/ja961883q.
[219] S. Jockusch, B. Kräutler, The red chlorophyll catabolite (RCC) is an inefficient sensitizer of singlet oxygen – photochemical studies of the methyl ester of RCC, Photochem. Photobiol. Sci. 19 (2020) 668–673, https://doi.org/10.1039/d0pp00071j.
[220] S. Jockusch, N.J. Turro, S. Banala, B. Kräutler, Photochemical studies of a fluorescent chlorophyll catabolite–source of bright blue fluorescence in plant tissue and efficient sensitizer of singlet oxygen, Photochem. Photobiol. Sci. 13

(2014) 407–411, https://doi.org/10.1039/c3pp50392e.
[221] R.G. Saer, R.E. Blankenship, Light harvesting in phototrophic bacteria: Structure and function, Biochem. J. 474 (2017) 2107–2131, https://doi.org/10.1042/BCJ20160753.
[222] B.R. Green, What happened to the phycobilisome? Biomolecules 9 (2019) 748, https://doi.org/10.3390/biom9110748.
[223] H. Elgabarty, P. Schmieder, D. Sebastiani, Unraveling the existence of dynamic water channels in light-harvesting proteins: alpha-C-Phycocyanobilin in vitro, Chem. Sci. 4 (2013) 755–763, https://doi.org/10.1039/C2SC21145A.
[224] R.E. Dale, F.W.J. Teale, Number and distribution of chromophore types in native phycobiliproteins, Photochem. Photobiol. 12 (1970) 99–117, https://doi.org/10.1111/j.1751-1097.1970.tb06044.x.
[225] R-phycoerythrin and C-phycocyanin, Photochem. Photobiol. 25 (1977) 565–569, https://doi.org/10.1111/j.1751-1097.1977.tb09129.x.
[226] J. Grabowski, E. Gantt, Photophysical properties of phycobiliproteins from phycobilisomes: fluorescence lifetimes, quantum yields, and polarization spectra, Photochem. Photobiol. 28 (1978) 39–45, https://doi.org/10.1111/j.1751-1097.1978.tb06927.x.
[227] R.R. Sonania, N.K. Singhb, J. Kumarc, D. Thakara, D. Madamwara, Concurrent purification and antioxidant activity of phycobiliproteins from *Lyngbya* sp. A09DM: an antioxidant and anti-aging potential of phycoerythrin in *Caenorhabditis elegans*, Process Biochem 49 (2014) 1757–1766, https://doi.org/10.1016/j.procbio.2014.06.022.
[228] R.R. Sonani, R.P. Rastogi, D. Madamwar, Natural antioxidants from algae: a therapeutic perspective, in: R.P. Rastogi, D. Madamwar, A. Pandey (Eds.), Algal Green Chemistry: Recent Progress in Biotechnology, Elsevier B.V, Amsterdam, Netherlands, 2017, pp. 91–120, https://doi.org/10.1016/B978-0-444-63784-0.00005-9.

Masahiko Taniguchi studied pharmacology at the Science University of Tokyo, Japan. He obtained his Ph.D. under the guidance of Prof. Shuntaro Mataka (2000) in the Department of Molecular Science and Technology at Kyushu University, Japan. In 2000, he joined North Carolina State University as postdoctoral fellow and is now Research Professor. His research interests concern hydroporphyrin chemistry, photochemistry, and scientific database development. In his spare time, he is an avid fisherman and devotee of all-things Americana.

Jonathan S. Lindsey (b. 1956) grew up in Rockport, Indiana, and did his undergraduate studies at Indiana University in Bloomington (1974–1978). His graduate and postdoctoral studies (1978–1984), at The Rockefeller University with Prof. David C. Mauzerall, encompassed tetrapyrrole-containing model systems relevant to the nascent field of artificial photosynthesis. A lifelong passion concerns the creation of tetrapyrrole macrocycles and understanding their roles in photosynthesis and diverse photochemical phenomena.